EFFECT OF T6 HEAT TREATMENT ON CORROSION OF Al-SiC$_p$ COMPOSITE & INHIBITION EVALUATION OF BENZIMIDAZOLE & ITS DERIVATIVES

Thesis

Submitted in partial fulfillment of the requirements for the degree of

DOCTOR OF PHILOSOPHY

By

MELBY CHACKO

DEPARTMENT OF METALLURGICAL AND MATERIALS ENGINEERING
NATIONAL INSTITUTE OF TECHNOLOGY KARNATAKA,
SURATHKAL, MANGALURU – 575025
October, 2017

DECLARATION

By the Ph.D Research Scholar

I hereby *declare* that the Research Thesis entitled "**Effect of T6 Heat Treatment on Corrosion of Al-SiC$_p$ Composite & Inhibition Evaluation of Benzimidazole & Its Derivatives"**, which is being submitted to the **National Institute of Technology Karnataka, Surathkal** in partial fulfillment of the requirements for the award of the Degree of **Doctor of Philosophy** in **Metallurgical and Materials Engineering** is a *bonafide report of the research work carried out by me*. The material contained in this Research Thesis has not been submitted to any University or Institution for the award of any degree.

MELBY CHACKO
Register number: 110672MT11F03
Department of Metallurgical and Materials Engineering
National Institute of Technology Karnataka, Surathkal

Place: NITK-Surathkal

Date:

CERTIFICATE

This is to *certify* that the Research Thesis entitled "**Effect of T6 Heat Treatment on Corrosion of Al-SiC$_p$ Composite & Inhibition Evaluation of Benzimidazole & Its Derivatives**", submitted by **Melby Chacko** (Register No: **110672MT11F03**) as the record of the research work carried out by her, is *accepted as the Research Thesis submission* in partial fulfillment of the requirements for the award of degree of **Doctor of Philosophy**.

Prof. Jagannatha Nayak
Research guide
(Signature with date and seal)

Dr. Uday Bhatt
Chairman-DRPC
(Signature with date and seal)

Dedicated to my beloved parents and my dear husband……

ACKNOWLEDGEMENT

I most sincerely place on record my heartfelt gratitude and deep sense of being indebted to my guide Prof. Jagannatha Nayak, Department of Metallurgical and Materials Engineering, NITK, for his invaluable guidance and support during my research work. I am immensely benefited by the inspiration and innovative viewpoints given to me from time to time. He has been kind enough and encouraged me all the time by giving scintillating ideas and motivating thoughts. He has taken lot of pain and strained himself to steer me to my safe destination.

I express my heartfelt thanks to the Research Progress Assessment Committee members Dr. Ramesh Kini M, Associate Professor, Department of Electronics and Communication Engineering and Prof. Kulkarni S M, Department of Mechanical Engineering for their overwhelming support, and also for making my presentations more constructive with their thoughtful comments and suggestions on my work. I would also like to thank Ministry of Human Resource Development, India for granting the scholarship.

I profusely thank Prof. K. N. Prabhu and Prof. A. O. Surendranathan, former Heads of Department of Metallurgical and Materials Engineering and Dr. Udaya Bhat K. current Head and Associate Professor, Department of Metallurgical and Materials Engineering, NITK, Surathkal for their valuable aid in the different stages of my research work.

It is my most cherished duty to heartily thank the technicians and non-teaching staff especially Mrs. Sharmila Dinesh and Ms. U. Rashmi of the Department of Metallurgical and Materials Engineering, NITK, Surathkal, for helping me throughout my PhD journey with a lasting smile, ever increasing enthusiasm and with a glow on their faces. Also, I wish to thank Dr. Sulochana Nayak, Medical Officer, Health Care Centre, NITK, who extended help by providing me the most needed medical support.

It is a privilege and great pleasure to acknowledge the efforts and support of my pals Dr. Akshata G. Patil, Dr. T. Senthil, Mr. Kamal Babu, Dr. Kripa M. Suvarna,

Mr. Vishwanath Hiremath, Dr. M. Selvakumar, Ms. Shourie Ranjana, Dr. Lekha B. M., Ms. Haritha P. Haridas, Mr. B. Sachin Kumar, Ms. Shamitha C., Mr. Siby Thomas and Ms. Vajreshwari U., who took care of me like kith and kin and helped me to keep my spirits high during my research work.

I am humbled when I think of extending my thanks to my family members because of whom I exist and because of whom I am what in my life today. My wholehearted respect and gratitude to my mother Mrs. Thankamma Chacko, father Mr. P. D. Chacko, husband Mr. Thomas George M, sister Mrs. Rose Merin Chacko and brother-in-law Mr. Binesh Jose. Finally I thank all my friends and colleagues for their kind assistance, comments and suggestions directly and indirectly for completing my research work.

MELBY CHACKO

ABSTRACT

Aluminium alloys, particularly 6061, reinforced with SiC have been the focus of the attention because of their application potential in an extensive range of demanding applications, such as automobiles, aerospace, and defense. There are many other applications which involve exposure of the composites to the potential corrosive environment. Because of the duplex nature of the composites, they are prone to accelerated corrosion compared to their monolithic counterpart. Corrosion of these composites not only limit their service life but also lead to deterioration of their unique mechanical properties for which they are designed. Studies reveal the role of micro structural changes and processing routes on the corrosion behaviour. Also, aging treatment was found to have an influence on the corrosion rate as the heat treated samples showed higher corrosion rates as compared to the non-treated samples.

Corrosion studies in organic acid solutions are rare in comparison with similar studies in mineral acids. Acetic acid is a frequently used organic acid in many industrial processes. At high temperatures, these acids dissociate, generating new aggressive ions which cause faster corrosion and they can provide sufficient protons to act as true acids. Adding inhibitors to the corrosion medium is a general practice for the corrosion protection. Heterocyclic organic compounds which contain oxygen, sulphur, phosphorous, nitrogen and aromatic rings are considered to be the most active and resourceful inhibitors in the acidic corrosive medium for the metals, alloys, and composites. Latterly, benzimidazole and its derivatives have established a considerable reputation on their corrosion inhibition properties for metals and alloys, owing to the existence of aromatic rings and nitrogen atom. In the present study benzimidazole (BI), 2-methylbenzimidazole (2-CH_3-BI), and 2-mercaptobenzimidazole (2-SH-BI) are used as inhibitors.

Aging profile of T4 and T6 treated Al-SiC_p was obtained using Rockwell B hardness. Under-aging, peak-aging, and over-aging temperatures and time were found out. Samples were corrosion tested and found to be susceptible to corrosion in acetic acid where peak-aged samples exhibited higher corrosion and over-aged samples showed minimum corrosion. Three inhibitors were tested for their efficiency. Results proved that they are excellent inhibitors. The maximum inhibition efficiency obtained using BI was 66%, 69% offered by 2-CH_3-BI and 75% was achieved in the presence of 2-SH-BI. Inhibition efficiency of inhibitors followed the order of 2-SH-BI > 2-CH_3-BI > BI. Activation energy, enthalpy, entropy, and free energy of adsorption were calculated for all experimental conditions. Results suggest that inhibitors get adsorbed on the composite surface by mixed adsorption, where chemisorption is predominant.

Keywords: Al-SiCp, Aging, Electrochemical corrosion, inhibition, benzimidazole, and derivatives.

CONTENTS

LIST OF FIGURES

LIST OF TABLES

NOMENCLATURE

6061 Al-SiCp	Aluminium metal matrix composite with magnesium and silicon as alloying elements and which has silicon carbide particles dispersed in the Aluminium matrix
MMC	Metal Matrix Composite
PRMMC	Particle reinforced metal matrix composites
$W.m^{-1}.K^{-1}$	Watts per meter-Kelvin
°C	Degree Celsius
K^{-1}	Per Kelvin
GPa	Giga Pascal
mV	Millivolt
EIS	Electrochemical Impedance spectroscopy
mm	Millimeter
Vol%	Volume percentage
Weight%	Weight percentage
HR_B	Rockwell B Hardness
SEM	Scanning electron microscopy
GP	Guinier-Preston
mpy	Milli-inches per year

BI	Benzimidazole
2-CH3-BI	2-Methylbenzimidazole
2-SH-BI	2-Mercaptobenzimidazole
g/mol	Gram/mole
ppm	Parts per million
SCE	Saturated calomel electrode
EW	Equivalent weight
$\mu A/\ cm^2$	Micro amperes per meter square
gm/cm^3	Gram per centimeter cube
D	Density
IGC	Intergranular corrosion
θ	Surface coverage
IE	Inhibition efficiency
Ea	Activation energy
CR	Corrosion rate
R	The universal gas constant
T	Temperature
ΔH#	Enthalpy of activation
ΔS#	Entropy of activation
ΔGads	Free energy of adsorption
h	Planck’s constant
N	Avogadro’s number

KJ/mol	Kilo Joule per mole
mol/dm^3	Mole per decimeter cube
ΔG#	Standard free energy
C	Concentration
mol/L	Mole per liter
R	Linear correlation coefficients
N	Nitrogen
O	Oxygen

CHAPTER 1

INTRODUCTION

Metal matrix composite (MMC) is a material which comprises of metal alloys reinforced with continuous or discontinuous fibers, whiskers or particulates, the end properties of which are intermediate between the alloy and reinforcement. These materials have remained the centre of attention of aerospace, automobile, and mineral processing industry because of the several advantages they extend which include high strength to weight ratio, elevated temperature toughness, low density, high stiffness and high strength compared to its original alloy. The particle reinforced metal matrix composites (PRMMC) satisfy many demands for performance driven applications in aerospace, automobile, and electrical industry. The particle reinforced composites can be tailored and engineered with specific required properties for the specific application. The commonly used reinforcement materials are silicon carbide, aluminium oxide, and graphite in the form of particles and whiskers.

Al- SiC is a metal matrix composite consisting of Silicon carbide particles dispersed in a matrix of aluminium alloy. It combines the benefits of high thermal conductivity of metal and low coefficient of thermal expansion of ceramic. The Silicon carbide improves its stiffness and wear resistance. The toughness and ductility are reduced by the ceramic. Its density ranges from 2.7- 3.00 g/cm^3 and thermal conductivity from 170-200 $W.m^{-1}.K^{-1}$. It has thermal expansion coefficient ranging from 6.5- 9.5 x $10^{-6}.K^{-1}$ and elastic modulus from 200-300 GPa. These alloys have established applications in various fields such as advanced printed circuit board, microelectronic packaging, bicycle frames, shoes and formula one racing car brakes etc. Al- SiC is an advanced packaging material for high technology thermal management. Al-SiC is compatible with a wide range of metallic and ceramic substrate and plating materials used in microelectronic packaging for aerospace, military, automobile and microwave applications.

The ultimate goal of an engineer is to design metal matrix composites to have good mechanical properties and inherent corrosion resistance. But, one of the main draw backs of aluminium matrix composite is the drop-off in corrosion resistance when compared to the base alloy. Corrosion can be defined as destruction or deterioration of a material because of reaction with its environment. It has been established that Al-SiC composites suffer more localized corrosion than their similitudes. Improved mechanical properties of composites are achieved by sacrificing corrosion resistance of it. Base alloys inherently develop a protective oxide surface film which bestows corrosion resistance; but, the addition of reinforcing phase leads to inhomogeneities and can induce discontinuities in the surface film, enhancing the number of sites where corrosion can be initiated thus devising the composite more vulnerable to corrosion attack. The preferential localized attack has been based on factors, such as reactive silicon carbide matrix, the presence of crevices and pores, processing routes, the presence of secondary phases and the volume percentage of reinforcement. So a detailed study on the corrosion behaviour of this composite is relevant.

Corrosion of structural elements is a major issue for any industry because of the wide use of acid solutions for industrial cleaning, pickling, descaling, acidizing, in petrochemical processes and in oil well acidification. Most organic acids are well resisted by aluminum alloys at room temperature. However, at high temperatures, the acids can dissociate, forming more aggressive ions that can cause faster corrosion. Acetic acid is most frequently used as reactants or solvents in many industrial processes. Also, equipment made of aluminum alloys, are widely and successfully used for handling these acids. Corrosion studies on metals in organic acid solutions like acetic acid and formic acid are scarce in comparison with similar studies in mineral acids.

The aging history has an effect on the mechanical and corrosion resistance. Aging time seems to strongly govern the corrosion response of metal alloys. The aging treatment of the composite has a crucial impact on the grain structure of the matrix by influencing the precipitation of the secondary phase alloying elements. Aging treatment has an effect on the corrosion behavior of the composite. Heat treatment temperature affects the microstructure which in turn affects the corrosion behaviour. Aging time strongly influences the corrosion behaviour as well. Studies established that the corrosion rate of the aluminium alloys and composites was struck by the nature of heat treatment given to the samples. Hence the investigation on the effect of aging on the corrosion behavior of 6061Al-SiC will lead to better utilization of the composite in various fields.

Corrosion of metallic surfaces can be reduced or controlled by the addition of chemical compounds to the corrodent. This form of corrosion control is called inhibition and the compounds added are known as corrosion inhibitors. A large number of corrosion inhibitors have been developed and used for the application to various systems. Among them, heterocyclic organic compounds containing sulfur, oxygen, nitrogen and aromatic rings are the most effective and efficient inhibitors for the metals in acidic medium. In recent years, benzimidazole and its derivatives have received considerable attention on their inhibition properties for metallic corrosion. Their effectiveness is related to the chemical composition, spatial molecular structure, surface charge density and their affinity for the metal surface. Although sufficient knowledge on the inhibition properties of benzimidazole and its derivatives on different types of steel, such as mild steel particularly, has accumulated over several years, existing knowledge on their inhibition behavior on aluminium composites is meager. Hence benzimidazole and its derivatives are chosen as the inhibitors for the present work.

CHAPTER 2

LITERATURE REVIEW

2.1. Fundamentals of Corrosion

Corrosion can be defined as destruction or deterioration of a material because of reaction with its environment. Most metals are found in nature in the form of chemical compounds such as oxides, sulphides, carbonates, chlorides etc. In the refining process energy is summated to the ore to extract the metal. The same amount of energy needed to extract metals from their ores is released during the chemical reactions that produce corrosion. Corrosion makes the metal return to its combined state in chemical compounds alike the ores from which metals were extracted. Corrosion is theoretically equivalent to the reverse of extractive metallurgy if the material getting deteriorated is a metal. It must be noted that the deterioration by physical cause is not corrosion, but it is termed as erosion, galling, wear etc. [Fontanna 1978].

2.1.1. Classification of Corrosion

Table 2.1: Corrosion categorisation

Sl.No	Factor	Types	Characteristics
1.	Nature of corrosion	1. Wet Corrosion	The electrochemical attack in the presence of moisture.
		2. Dry Corrosion	The direct chemical attack in the absence of moisture.
2.	Mechanism of corrosion	1. Electrochemical corrosion	Destruction by electrolytes.
		2. Chemical corrosion	Direct chemical attack.

2.1.2. Forms of Corrosion

This classification is based on the visual aspect of corroded metal. The eight forms of corrosion are briefly explained below.

a. **Uniform corrosion**

Uniform attack is a virtually common form of corrosion. It is more often characterized by a chemical or electrochemical reaction that carries on uniformly over the entire exhibited surface. The metal becomes thinner and eventually fails. Example: corrosion of steel in acid solution.

b. **Galvanic corrosion**

A potential difference normally exists between two dissimilar metals when they are plunged in a corrosive or conductive solution. If these metals are placed in contact this potential difference produces electron flow between them. Corrosion of active metal is increased while that of noble metal is decreased as compared with the behavior of these metals when they are not in contact. Example: steel screws in copper sheet.

c. **Crevice corrosion**

Intensive localized corrosion frequently occurs within crevices and other shielded areas on the metal surface exposed to corrosives. The material within the crevice acts as the anode and the exterior material becomes the cathode. Example: corrosion of steel in an industrial environment resulting from the wetted area within the crevice.

d. **Pitting corrosion**

Pitting is a class of extremely localized attack that results in holes in the metal. It is one of the most destructive and insidious forms of corrosion. It is difficult to detect and it causes equipment to fail. Example: Al in chloride containing environment.

e. **Inter granular corrosion**

Localized attack at and adjacent to grain boundaries with relatively little corrosion of the grains is inter granular corrosion. This takes place due to the segregation of impurities at the grain boundaries, enrichment of one of the alloying element or depletion of one of these elements in the grain boundary areas. Example: Small amount of iron in aluminium segregate in the grain boundaries and cause inter granular corrosion.

f. **Selective leaching**

Selective leaching is the removal of one element form a solid alloy by corrosion process. Example: Selective removal of zinc form brass alloy.

g. **Erosion corrosion**

Acceleration or increase in the rate of deterioration or attack on a metal because of relative movement between a corrosion fluid and the meal surface. All equipment exposed to moving fluid are subject to erosion corrosion. Example: Piping systems, valves, pumps, etc.

h. **Stress corrosion**

Stress corrosion cracking refers to cracking caused by the simultaneous presence of tensile stress and a specific corrosion medium. During cracking, the metal or alloy virtually unattacked over most of its surface and a fine crack is formed normal to the direction of stress. Example: Cracking of stainless steel in hydrochloric acid.

2.1.3. Electrochemical theory of corrosion

The corrosion of metal is an electrochemical process and consists of at least one oxidation and one reduction reaction. The electrochemical nature of corrosion can be illustrated by the corrosion of iron in HCl. When iron is placed in dilute HCl, a vigorous reaction occurs, as a result of which hydrogen gas is evolved and iron dissolves.

$Fe + 2HCl \longrightarrow FeCl_2 + H_2$

Noting that the chloride ion is not involved in the reaction, the above equation can be written as,

$Fe + 2H^+ \longrightarrow Fe^{2+} + H_2$

The above reaction can be divided into two reactions, oxidation of iron and reduction of hydrogen ion.

Oxidation (anodic reaction) : $Fe \longrightarrow Fe^{2+} + 2e^-$

Reduction (cathodic reaction): $2H^+ + 2e^- \longrightarrow H_2$

Both reactions occur simultaneously and with the same rate on the metal surface. During metallic corrosion, the rate of oxidation is equal to the rate of reduction.

All corrosion reactions can be classified into a few generalized reactions when viewed from a stand point of partial processes of oxidation and reduction. The anodic reaction in every corrosion reactions is the oxidation of the metal.

$$M \longrightarrow M^{n+} + ne^-$$

There are several cathodic reactions. The most common are,

Hydrogen evolution : $2H^+ + 2e^- \longrightarrow H_2$

Oxygen reduction : $O_2 + 4H^+ + 4e^- \longrightarrow 2H_2O$

(Acid solution)

Oxygen reduction : $O_2 + 2H_2O + 4e^- \longrightarrow 4OH^-$

(Basic or neutral)

Metal ion reduction : $M^{3+} + e^- \longrightarrow M^{2+}$

Metal deposition : $M^+ + e^- \longrightarrow M$

During corrosion, more than one oxidation and one reduction reaction may occur. Since the anodic and cathodic reactions occurring during corrosion are mutually dependent, it is possible to reduce the corrosion rate by reducing the rate of either of the reactions.

2.1.4. Polarization

The deviation from equilibrium potential is called polarization. It is divided into two types; activation polarization and concentration polarization.

a. **Activation polarization**

Activation polarization refers to an electrochemical process that is controlled by the reaction taking place at the metal-electrolyte interface. Activation polarization usually is the controlling factor during corrosion in concentrated acids i.e. which contain a high concentration of active species. A reaction for which an activation polarization dominates is referred as ‘activation controlled’.

b. **Concentration polarization**

Concentration polarization is observed when the reaction rates are controlled by the diffusion in the electrolyte. The reduction rate is controlled by diffusion occurring within the bulk solution. It dominates when the concentration of reducible species is small. A reaction for which concentration polarization dominates is referred to as ‘diffusion controlled’. Only the cathodic reaction can be under diffusion control.

2.1.5. Effect of environmental variables

a. **Effect of temperature**

The increase in temperature increases the rate of almost all chemical reactions. The increase in temperature may also change the pH of the medium which has a direct effect on corrosion rate.

b. **Effect of pH**

The corrosion rate for iron is high at low pH, becomes almost independent of pH in the nearly neutral range and decreases with increase in pH.

c. **Effect of velocity**

For corrosion processes that are controlled by activation polarization, agitation and velocity have no effect on the corrosion rate. If the corrosion process is under cathodic diffusion control, then agitation increases the corrosion rate. Some metals owe their corrosion resistance in certain mediums to the formation of massive bulk protective films on their surface. When these materials are exposed to extremely high corrosive velocity, mechanical damage or removal of these films occurs resulting in an accelerated attack.

d. Effect of corrosive concentration

The increase in the concentration of corrosive ions in the medium increases the corrosion rate to a larger extent. The addition of chlorides to HCl increases the corrosion rate of iron [Fontanna 1978].

2.2. Corrosion Measurement Techniques

The corrosion measurement techniques are classified into two types:

DC Electrochemical monitoring techniques and

AC Electrochemical monitoring techniques

2.2.1. DC Electrochemical monitoring techniques

a. Tafel extrapolation method

This technique uses data obtained from cathodic or anodic polarization measurements. The metal sample is termed the working electrode and is polarized by -250mV anodically and +250mV cathodically from the rest potential. Cathodic current is supplied to it by means of an auxiliary electrode, such as platinum. Current is measured by means of an ammeter, and the potential of the working electrode is measured with respect to a reference electrode by a potentiometer-electrometer circuit.

In a Tafel plot potential (E) versus log current density, is plotted and it is observed that curve is nonlinear at low current, but at higher current it becomes linear at approximately 50mV more active than the corrosion potential. This region of linearity is referred to as the ‘Tafel Region’. The schematic picture is shown in Fig 2.1. The applied cathode current is equal to the difference between the current corresponding to the reduction process and that corresponding to the oxidation or dissolution process. To determine the corrosion rate from such polarization measurements, the Tafel region is extrapolated to the corrosion potential. At the corrosion potential, the rate of hydrogen evolution is equal to the rate of metal dissolution, and this point corresponds to the corrosion rate of the system expressed in terms of current density i_{corr} [Stansbury 2000].

The anodic and cathodic Tafel plots are described by the equations.

$\eta_a = \alpha_a + \beta_a \log i_{(anodic)}$

$\eta_c = \alpha_c + \beta_c \log i_{(cathodic)}$

where, η_a = anodic polarization potential

η_c = cathodic polarization potential

Logi =logarithm of the current

$\alpha_a, \beta_a, \alpha_c, \beta_c$ = anodic and cathodic Tafel constants.

The corrosion rate can be expressed as,

Corrosion Rate (mpy) = $0.129 \times EW \times i_{corr} / D$

where, EW=Electro chemical equivalent weight of the corroding material

i_{corr}= Corrosion current density ($\mu A/cm^2$).

D=Density of corroding sample (g/ cm^3)

Advantages of Tafel extrapolation method:

1. The technique is very rapid compared to weight loss method.
2. With this technique, it is possible to measure extremely low corrosion rate.
3. It can be used for continuously monitoring the corrosion rate of the system.

Disadvantage of Tafel extrapolation method:

1. The method can be applied only to systems containing one reduction process since the Tafel region is usually distorted if more than one process occurs.
2. To ensure reasonable accuracy, Tafel region must extend over a current range of at least one order of magnitude but this cannot be achieved because of

interferences from concentration polarization in determining Tafel region [Zaki 2006 and Fontanna 1978].

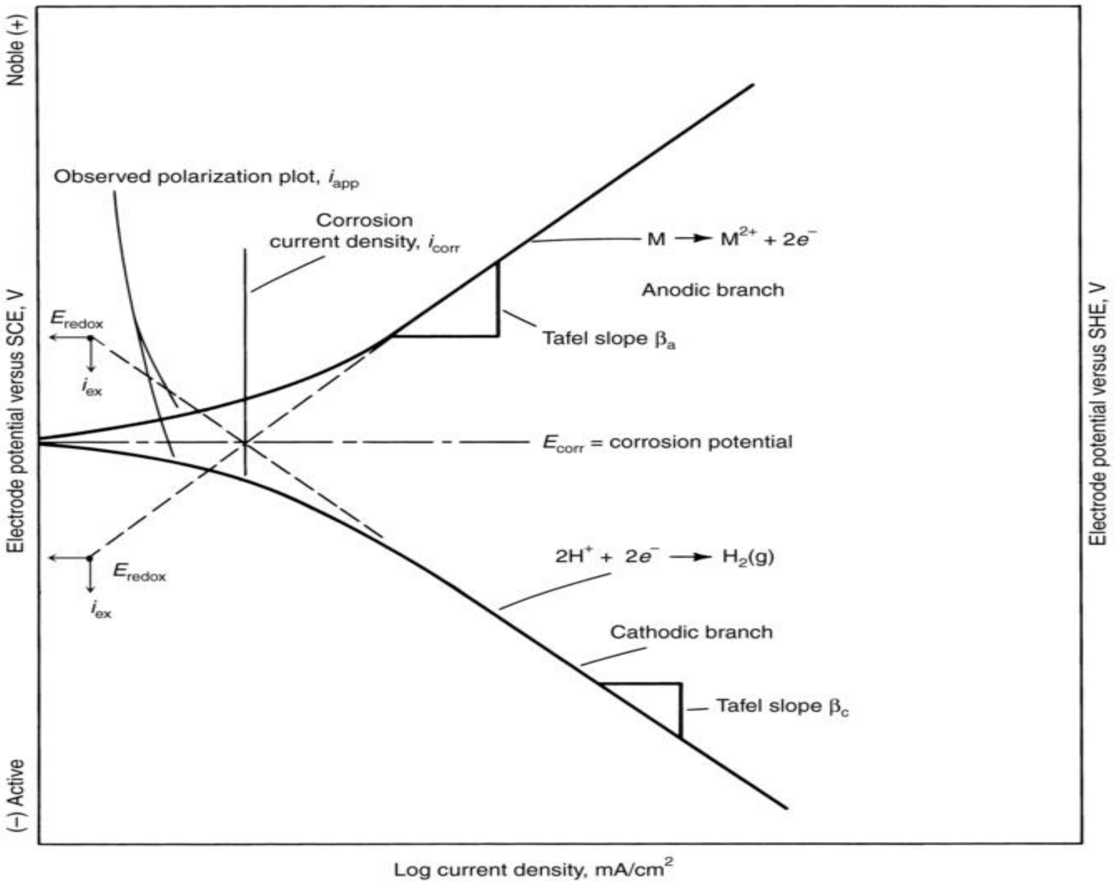

Fig 2.1: Schematic diagram of cathodic and anodic polarization curves.

b. Linear polarization method

A Linear polarization technique is another method that utilizes polarization behavior to determine the corrosion rate of metals. The disadvantages of the Tafel extrapolation can be largely overcome by using a linear polarization analysis. Within ±20 mV of the corrosion potential, it is observed that the applied current density is a linear function of the electrode potential. Electrode potentials that are more positive than the corrosion potential results in anodic current, whereas potentials that are more negative than the corrosion potential result in cathodic current to the specimen. The usefulness of this measurement is that the slope of potential Vs current plot i.e, $\Delta E / \Delta i_{app}$ can be used to measure the corrosion rate. The relationship of the slope of the linear polarization curve to the corrosion current, the anodic and the cathodic Tafel slope are,

$\Delta E/\Delta i_{app} = \beta_a\beta_c/2.303\ i_{corr}\ (\beta a+\beta c)$

where, $\Delta E/\Delta i_{app}$ is the slope of the linear portion of the curve, β_a and β_c are the anodic and cathodic slope respectively, and i_{corr} is the corrosion current density. Linear polarization curve is shown in Fig 2.2.

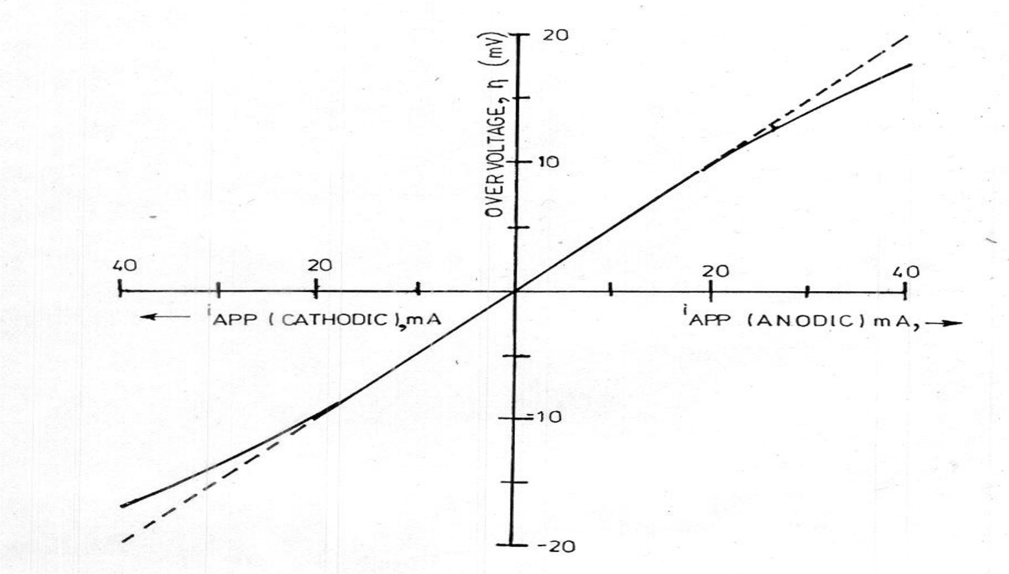

Fig 2.2: Schematic Linear Polarization Curve.

The slope of the linear polarization curves is determined experimentally, and the values of the anodic and cathodic slopes are determined either experimentally or estimated. After these values are obtained, the corrosion rate can be calculated from the calculated value of the corrosion current i_{corr} . For example, for systems where anodic and cathodic slopes are equal to 0.12 per decade, the relationship between the slopes of linear polarisation curve and corrosion rate is,

$\Delta E/\Delta i_{app}= 0.026/\ i_{corr}$

Advantages of linear polarisation technique

1. They permit rapid corrosion rate measurement and can be used to monitor corrosion rate in various process streams.

2. These are used for measuring very low corrosion rates in nuclear, pharmaceutical and food processing industries, which are difficult and tedious to perform by conventional methods.
3. Electrochemical corrosion rate measurements may be used to measure the corrosion rate of structures that cannot be visually inspected or subjected to weight loss tests, like underground pipes tanks and large chemical plant components [Zaki 2006].

2.2.2. AC Electrochemical monitoring technique (Electrochemical impedance spectroscopy)

Electrochemical methods based on alternating currents can be used to obtain insights into corrosion mechanisms and to establish the effectiveness of corrosion control methods, such as inhibition and coatings. In an alternating-current circuit, impedance determines the amplitude of current for a given voltage. Impedance is the proportionality factor between voltage and current. In electrochemical impedance spectroscopy (EIS), the response of an electrode to alternating potential signals of varying frequency is interpreted on the basis of circuit models of the electrode/electrolyte interface. Fig 2.3 (a) and (b) shows two circuit models that can be used for analyzing EIS spectra.

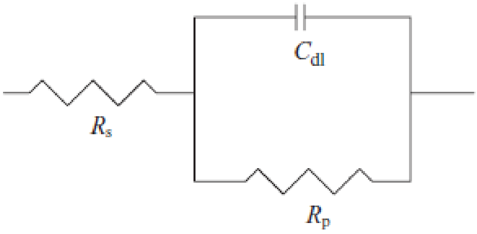

Fig 2.3(a)

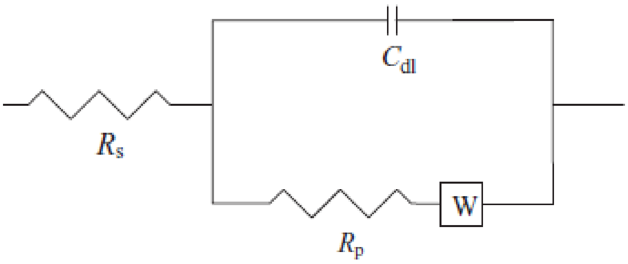

Fig 2.3(b)

The simplest model for characterizing the metal – solution interface, Fig 2.3(a) includes the three essential parameters, R_s (the solution resistance), C_{dl} (the capacitance of the double layer), and R_p (the polarization resistance). When direct - current measurements are carried out (i.e., the frequency is zero), the impedance of the capacitor approaches infinity. In parallel electrical circuits, the circuit with the smallest impedance dominates, with the result that, under these conditions, the sum of R_s and R_p is measured. If R_s if significant, the corrosion rate is underestimated.

When diffusion control is important, another element, Z_d, sometimes called the Warburg impedance, is added in series with R_p, as shown in Fig 2.3(b). In electrochemical impedance spectroscopy, the impedance of the corroding metal is analyzed as a function of frequency. A sinusoidal potential change is applied to the corroding electrode at a number of frequencies, ω. At each frequency, the resulting sinusoidal current waveform is out of phase with the applied potential signal by an amount, the phase angle, θ, that depends on the circuit parameters. The current amplitude is inversely proportional to the impedance of the interface. The electrochemical impedance, Z(ω), is the frequency–dependent proportionality factor in the relationship between the voltage signal and the current response, $Z(\omega) = E(\omega) / i(\omega)$ where E is the voltage signal, $E= E_0\sin(\omega t)$; i is the current density, $i= i_0 \sin(\omega t + \theta)$; Z is the impedance (ohm- cm^2); and t is the time (seconds). Impedance is a complex number that is described by the frequency-dependent modulus, |Z|, and the phase angle, θ, or, alternatively, by the real component, Z′, and the imaginary component, Z″. The mathematical convention for separating the real and imaginary components is to multiply the magnitude of the imaginary component by j [=$\sqrt{-1}$] and report the real and imaginary values as a complex number. The equations for electrochemical impedance are

$$E = E_{real} + E_{imaginary} = E' + jE''$$

$$I = I_{real} + I_{imaginary} = I' + jI''$$

$$Z= Z'+ jZ''= (E' + jE'') / (I' + jI'')$$

$$\tan \theta = Z'/ Z''$$

$$|Z|= |Z'|^2 + |Z''|^2$$

In electrochemical impedance analysis, Nyquist plots are commonly used. A plot of Z′ Vs Z″ at various frequencies gives a semicircle which cuts the real axis at higher and lower frequencies which are shown in Nyquist plot Fig 2.4. At high frequency, the impedance Z corresponds to solution resistance R_s and low frequency Z corresponds to R_s+ R_p, the difference between the two values gives polarization resistance R_p. The polarization resistance R_p is inversely proportional to the corrosion rate. The corrosion rates are calculated by using the relationship,

i_{corr}= B / R_p, where, B is assumed to be 0.025. (B= $\beta_a\beta_c/2.303\ I_{corr}\ (\beta a+\beta c)$).

Advantages of EIS

1) Applicable to low conductivity systems.

2) They provide mechanistic information.

3) Estimation of corrosion rates in low conductivity media.

4) Estimation of extremely low corrosion rate and metal contamination rate.

5) Rapid assessment of corrosion inhibitor performance in aqueous and nonaqeous media [Uhlig 2008].

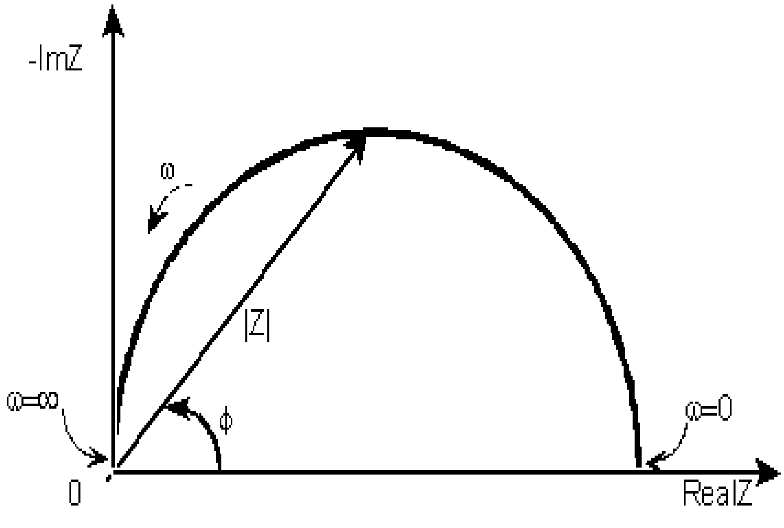

Fig 2.4: Nyquist plot.

2.3. Corrosion Inhibitors

An inhibitor is a chemical substance that, when added in small concentration to an environment, effectively decreases the corrosion rate. Most inhibitors function by forming an adsorbed layer on the metal surface, probably not more than a monolayer in thickness, which essentially blocks discharge of H^+ and dissolution of metal ions [Uhlig 2008].

Corrosion of metallic surfaces can be reduced or controlled by the addition of chemical compounds to the corrodent. This form of corrosion control is called inhibition and the compounds added are known as corrosion inhibitors. These inhibitors will reduce the rate of either anodic oxidation or cathodic reduction, or both. The inhibitors themselves form a protective film on the surface of the metal. It has been postulated that the inhibitors are adsorbed into the metal surface either by physical (electrostatic) adsorption or chemisorption. Physical adsorption is the result of electrostatic attractive forces between the organic ions and the electrically charged metal surface. Chemisorption is the transfer, or sharing of the inhibitor molecule’s charge to the metal surface, forming a coordinate-type bond. The adsorbed inhibitor reduces the corrosion rate of the metal surface either by retarding the anodic dissolution reaction of the metal or by retarding the cathodic evolution of hydrogen, or both. The most common and widely known use of inhibitors is their application in automobile cooling systems and boiler feed waters [Philip 2007].

2.3.1. Classification of inhibitors

One of the main classification is into inorganic and organic inhibitors depending on whether the inhibitor is organic or inorganic in nature. It can also be classified as anodic and cathodic inhibitors.

a. Anodic Inhibitors

Oxidation of metal is the reaction that occurs at anodic sites during corrosion. For example, in rusting of iron, Fe^{+2} ions are formed at the anodic region. If the formation of Fe^{+2} is prevented the cathodic reaction also stops and thereby corrosion process is retarded. This is achieved by the addition of anions such as chromate, tungstate, molybdate, phosphate etc.

These anions combine with metal ions formed at the anode region, forming the sparingly soluble respective salts. These complexes deposit on the anodic sites forming protective films, which act as a barrier between the fresh metal surface and the corrosion medium thereby preventing any further anodic reaction. Anodic inhibitors are found to be effective only when sufficient amount of the inhibitor is added into corrosion medium. When the insufficient amount is added the situation is more disastrous than not adding at all. This is because of the fact that insufficient amount of the inhibitor cannot cover the entire anodic surface with the protective film. The small uncovered anodic region exposed to the corrosive medium undergoes accelerated corrosion due to the area effect i.e. the ratio of cathodic to the anodic site.

b. Cathodic Inhibitor

The two types of cathodic reactions are the liberation of hydrogen or absorption of oxygen. Therefore there are two distinct approaches in achieving inhibition of cathodic reactions. That is either by preventing the liberation of hydrogen or by preventing/retarding the absorption of oxygen.

Inhibition of hydrogen liberation: The liberation of hydrogen at the cathode can be prevented either by preventing/retarding the diffusion of H^+ ions the cathode or by increasing the hydrogen over voltage on the metal surface. The diffusion of hydrogen ions to the cathode is prevented by the addition of certain organic compounds which contain nitrogen or sulfur. Urea, thiourea, aliphatic amines, mercaptans and heterocyclic compounds are widely used. Such substances, when added to the corroding environment, are adsorbed on the cathodic surface. The evolution of hydrogen at the cathode can be prevented by increasing hydrogen over voltage. This is achieved by oxides of arsenic, antimony or salts like sodium meta arsenide. They deposit as adherent metallic films on the cathode region and thereby prevent the liberation of hydrogen, as the hydrogen over voltage on these metals is very high.

Inhibition of oxygen absorption: The absorption of oxygen can be stifled either by removing the oxygen from the corrosive media or by simply decreasing the diffusion rate of oxygen to the cathode. The first objective is achieved by adding reducing agents or oxygen scavengers such as hydrazine, sodium sulphite. These substances remove oxygen from the corroding environment by reducing it. It can be achieved by adding salts such as $ZnSO_4$, $NiSO_4$, etc. into the corrosion medium. The cations of salts migrate towards the cathode surface and react with catholically formed alkali to deposit their hydroxide on the cathodic sites. The protective film being impermeable to oxygen prevents its diffusion to the cathode.

c. **Mixed Inhibitor**

Mixed inhibitors work by reducing both the cathodic and anodic reactions. They are generally film forming compounds that cause the formation of precipitates on the surface, blocking both anodic and cathodic sites indirectly. The most common inhibitors of this category are the silicates and phosphates. The protection depends heavily on pH. Phosphate requires oxygen for effective inhibition. Silicates and phosphates do not afford the degree of protection provided by chromates and nitrites. However, they are very useful in a situation where nontoxic additives are required. The effectiveness of these Inhibitors is related to the extent to which they adsorb and cover the metal surface [Zaki 2006].

2.3.2. Inhibitor Evaluation

Because there may be more than one inhibitor suitable for a specific application, it is necessary to have a means of comparing the performance of each. This can be done by determining the inhibitor efficiency according to the following correlation:

$$IE = \theta * 100$$

$$\text{And } \theta = \{icorr - icorr\ (inh)\} / icorr$$

where IE is the inhibitor efficiency in %, θ is the surface coverage of an inhibitor, icorr is the corrosion current density in the absence of inhibitor and icorr (inh) is the corrosion current density in the presence of inhibitor. The corrosion rate can be measured in any unit, as long as units are consistent across both tests [Philp 2007].

2.3.3. Examples of corrosion inhibitors

The active part of organic inhibitors contains one or more functional groups containing one or more hetero atoms N, O, S, P, or Se through which the inhibitor anchor on to the metal surface. These groups are attached to a parent chain, which increases the ability of the inhibitor molecule to cover a large surface area. Some of the organic inhibitors are shown in Table 2.1 [Winston 2011].

Table 2.2: Examples of organic inhibitors

Structure	Name	Structure	Name
-OH	hydroxy	$-CONH_2$	Amide
-C≡C-	-yne	-SH	Thiol
-C-O-C-	epoxy	-S-	sulfide
-COOH	carboxy	-S=O	sulfoxide
-C-N-C	amine	-C=S-	Thio
$-NH_2$	amino	-P=O	phosphonium
-NH	imino	-P-	phospho
$-NO_2$	nitro	-As-	Arsano
-N=N-N-	triazole	-Se-	Seleno

2.4. Aluminium Alloys

Aluminium alloys are characterized by their low specific gravity that can vary slightly above and below the specific gravity of pure aluminium depending on the major alloying elements. In addition to their lightweight, other advantages of aluminium casting alloys include relatively low melting temperatures, negligible gas solubility with the exception of hydrogen, excellent castability, good machinability and surface finish, good corrosion resistance and good electrical and thermal conductivity [Chawla 1998].

2.4.1. Alloy Designation System

Aluminium alloys are of two types. Wrought alloys and cast alloys. The Aluminium Association standardized the designation of wrought aluminium and wrought aluminium alloys in 1954. A four- digit numerical system is used to identify wrought Al and Al alloys. As shown below, the first digit of the four- digit designation indicates the group.

a. **Wrought alloy designation**

Aluminium, > 99%	1xxx
Copper	2xxx
Manganese	3xxx
Silicon	4xxx
Magnesium	5xxx
Magnesium and silicon	6xxx
Zinc	7xxx
Other element	8xxx
Unused series	9xxx

For the 2xxx through 7xxx series, the alloy group is determined by the alloying element present in the greatest mean%.

Al: In the 1xxx group, the series 10xx is used to designate unalloyed compositions that have natural impurity limits. The last two of the four digits in the designation indicate the minimum Al%.

Al Alloys: In the 2xxx through 8xxx alloy groups, the second digit in the designation indicates alloy modification. If the second digit is zero, it indicates the original alloy; integer through 9, assigned consecutively, indicates modifications of original alloy. The last two of four digits in the 2xxx through 8xxx groups give the amount of alloying additions and thus serve to identify the different Al alloys in the group.

b. Cast alloy designation

Controlled unalloyed compositions	1xx.x
Copper	2xx.x
Silicon	3xx.x
Binary Al-Si alloys	4xx.x
Magnesium	5xx.x
Currently unused	6xx.x
Zinc	7xx.x
Tin	8xx.x
Currently unused	9xx.x

For 2xx.x through 8xx.x alloys, the alloy group is determined by the alloying element present in the greatest mean%. The second two digits identify the specific Al alloy or for the Al (1xx.x) series indicate purity. The last digit, which is separated from the others by decimal point, indicates a product form, whether casting or ingot.

Al Castings and ingot: For the 1xx.x group, the second two of the four digits in the designation indicate the minimum Al%. The last digit indicates the product form: 1xx.0 indicates casings and 1xx.1 indicate ingot.

Al Alloy Castings: For the 2xx.x through 9xx.x alloy groups, the second two of the four digits in the designation give the amount of alloying additions and thus serve to identify the different Al alloys in the group [Davis 1993].

2.4.2. Heat- Treatable and Non- Heat- Treatable Alloys

Many alloys respond to thermal treatment based on phase solubilities. These treatments include solution heat treatment, quenching and precipitation, or age hardening. For either casting or wrought alloys, such alloys are described as heat treatable. A large number of other wrought compositions rely instead on work hardening through mechanical reduction, usually in combination with various annealing procedures for property development. These alloys are referred to as nonheat- treatable or work- hardening alloys. Some casting alloys are essentially not heat treatable and cannot be work hardened because of their brittleness. They are used only in as- cast or in thermally modified conditions unrelated to solution or precipitation effects [Davis 1993].

2.4.3. System for Heat- Treatable Alloys

The temper designation system for wrought and cast products that are strengthened by heat treatment employs the W and T designations. The W designation denotes as unstable temper, whereas the T designation denotes a stable temper other than F, O or H. It is based on the sequence of basic treatments used to produce the various tempers. They are as follows:-

F: As Fabricated

O: Annealed, Recrystallized

H: Strain hardened

W: Solution Heat-treated

T: Thermally Treated [Winkler2004].

The T is followed by a numerical form 1 to 10 each numeral indicating a specific sequence of basic treatments.

T1: Cooled from an elevated temperature shaping process and naturally aged to a substantially stable condition.

T2: Cooled from an elevated temperature shaping process, cold- worked and naturally aged to a substantially stable condition.

T3: Solution heat- treated, cold- worked and naturally aged to a substantially stable condition.

T4: Solution heat- treated and naturally aged to a substantially stable condition.

T5: Cooled from an elevated temperature shaping process and artificially aged.

T6: Solution heat- treated and artificially aged.

T7: Solution heat- treated and overaged or stabilized.

T8: Solution heat- treated, cold- worked and artificially aged.

T9: Solution heat –treated, artificially aged and cold- worked.

T10: Cooled from an elevated temperature shaping process, cold- worked and artificially aged [Davis 1993].

2.5. Metal Matrix Composites

Metal matrix composites (MMCs), like all composites; consist of at least two chemically and physically distinct phases, suitably distributed to provide properties not obtainable with either of the individual phases. Generally, there are two phases, e.g., a fibrous or particulate phase, distributed in a metallic matrix. MMCs offer the following advantages:

- Higher strength-to-weight ratio.
- Exceptional dimensional stability.
- Higher elevated temperature stability.
- Higher strength and stiffness.
- Higher service temperatures.
- Higher electrical conductivity.
- Higher thermal conductivity.

2.5.1. Classification of MMCs

In general, there are three kinds of metal matrix composites (MMCs):

- Particle reinforced MMCs.
- Short fiber or whisker reinforced MMCs.
- Continuous fiber or sheet reinforced MMCs [Chawla 2006].

2.5.2. Aluminium Matrix Composites

The recent worldwide interest shown in the metal matrix composite (MMC) materials has been fuelled by the fact that mechanical properties of light alloys can be enhanced by incorporating reinforcing fibers (usually ceramic). Several manufacturers are marketing a range of particulate reinforced MMC products with different compositions, for example, 12% alumina, 9% carbon fiber, reinforced Al-12% SiC, and particulate SiC-Al ingots. The major reinforcements used in aluminium-based MMCs are boron, graphite, silicon carbide, and alumina [Winston 2011].

Depending on the intended use, the reinforcement is either a whisker, a particle, or in a few cases monofilaments. SiC whiskers are discontinuous, rod- or needle-shaped fibers in the size range of 0.1-1 mm in diameter and 5-100 mm in length. Because they are nearly single crystals, the whiskers typically have very high tensile strengths (up to 7 GPa) and elastic modulus (up to 550 GPa). SiC particles have a lower cost, and since they have an irregular shape the composites produced show isotropic properties. Duralcan^{TM} is an example of a readily available Al-SiC$_p$ (p for the particle) composite; examples of applications include brake disks, drums, calipers, and backplate, stabilizer bars, train brake rotors, and bike and golf components [Ghali 2010].

2.5.3. Corrosion behaviour of Aluminium, Its Alloys, and Composites

Corrosion resistance of aluminium is dependent upon a protective oxide film. This film is stable in aqueous media when the pH is between about 4.0 and 8.5. The oxide film is naturally self-renewing and accidental abrasion or other mechanical damage of the surface film is rapidly repaired. The conditions that promote corrosion of aluminium and its alloys, therefore, must be those that continuously abrade the film mechanically or promote conditions that locally degrade the protective oxide film and minimize the availability of oxygen to rebuild it. When aluminium is exposed to alkaline conditions, corrosion may occur, and when the oxide film is perforated locally, the accelerated attack occurs because aluminium is attacked more rapidly than its oxide under alkaline conditions. The result is pitting. In acidic conditions, the oxide is more rapidly attacked than aluminium, and more general attack should result. Aluminium alloys, particularly the 2xxx series, are less corrosion resistant than the commercial purity metal. Some aluminium alloys, for example, are susceptible to intergranular corrosion as a result of low-temperature aging reactions and the subsequent precipitation in the grain boundaries. Susceptibility to intergranular attack in these alloys shows up as exfoliation and stress-corrosion cracking [Roberge 2000].

Pourbaix (E-pH) diagrams represent the stability of a metal as a function of potential and pH. At a particular combination of pH and potential, a stable phase can be determined from the Pourbaix diagram. In such diagrams, the redox potential of the corroding system is plotted on a vertical axis and the pH on a horizontal axis. These diagrams are constructed from calculations based on Nernst equations and solubility data for metal and its species, such as Fe, Fe_2O_3, $Fe(OH)_2$, Fe_3O_4, etc in equilibrium. And we can identify the stability region (immunity, corrosion, and passivity), however these are only indications; actual rates cannot be derived from the diagrams. The information in the diagrams can be beneficially used to control corrosion of pure metals in the aqueous environment. By altering the pH and potential to the regions of immunity and passivation, corrosion can be controlled. The E-pH diagram of aluminum is one of the simplest E-pH diagrams.

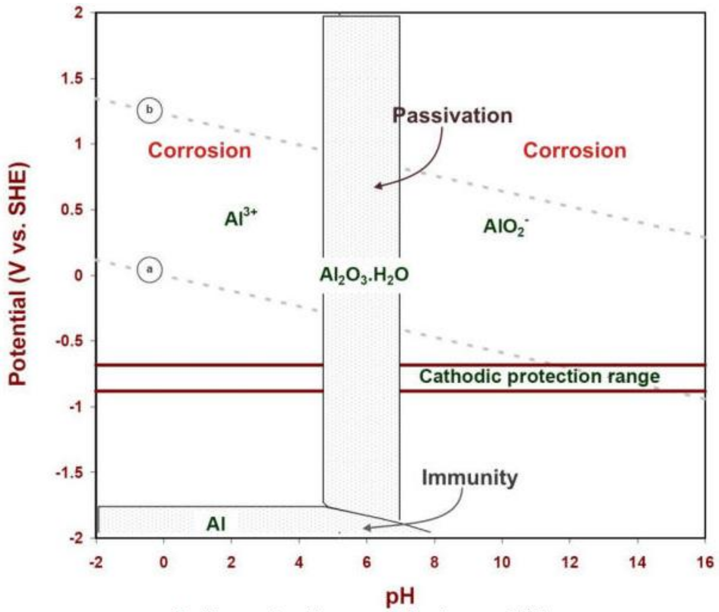

E-pH corrosion diagram of aluminum at 25°C

Fig 2.5: Pourbaix diagram of Aluminium

The usefulness of this graphical representation of thermodynamic data for corrosion studies was discussed by Pourbaix who showed three possible states of a metallic material:

Immunity region: In the conditions of potential and pH of that region a metal is considered to be totally immune from corrosion attack and safe to use.

Passive region: In such region a metal tends to become coated with an oxide or hydroxide that may form on the metal either as a compact and adherent film practically preventing all direct contact between the metal itself and the environment, or as a porous deposit which only partially prevents contact between the metal and the environment;

Corrosion region: Thermodynamic calculations indicate that, in such region of an E-pH diagram, a metal is stable as an ionic (soluble) product and therefore susceptible to corrosion attack [Hsin-Hsiung Huang 2016].

Aluminium alloys of the 1xxx, 3xxx, 5xxx, and 6xxx series are resistant to corrosion by many natural waters. The more important factors controlling the corrosiveness of fresh waters on aluminium include water temperature, pH, and conductivity; availability of cathodic reactant; presence or absence of heavy metals; and the corrosion potentials of the specific alloys [ASM 2005]. Corrosion of aluminium alloys in seawater is mainly of the pitting type, as would be expected from its salinity and enough dissolved oxygen to act as a cathodic reactant to polarize the alloys to their pitting potentials. The corrosion rate of the copper-containing 2xxx and 7xxx series alloys in moist low resistivity soils are several times greater than the corrosion rate of the more resistant 1xxx, 3xxx, 5xxx, and 6xxx series alloys. Most aluminium alloys are inert to strong nitric or acetic acid solutions but are readily attacked in dilute nitric, sulfuric, or hydrochloric acid solutions [Ghali 2010].

The corrosion behaviour of cast and heat-treated Al-6%Zn-1%Mg and Al-6%Zn-1%Mg-1%Ag alloys and metal matrix composites (MMCs) were investigated using dynamic polarization techniques, The materials studied are heat-treated cast Al-6%Z-1%Mg (Al-6-1) and Al-6%Zn-1%Mg-1%Ag (Al-6-1-1) alloys and metal matrix composites (MMCs) reinforced with 50 vol% of continuous, 15 μm diameter Altex (15%SiO_2-Al_2O_3) fibers. It was observed that due to the presence of second phase particles and micro segregation, pitting occurs preferentially at the grain boundary and fiber/matrix interface regions in the cast alloys and composites, respectively [Flower et al. 2004]. Using continuous immersion techniques, the stress corrosion cracking (SCC) behaviour of the cast and heat-treated Al-6%Zn-1%Mg (Al-6-1) and Al-6%Zn-1%Mg-1%Ag (Al-6-1-1) metal matrix composites were evaluated. It was found that the Al-6-1-1 composites exhibit longer lifetimes compared to the Al-6-1when tested under various SCC conditions [Winkler 2004].

Aluminium alloy 6061, 2024 and 7075 reinforced with SiC have been the focus of attention because of their application potential in a wide range of demanding applications; such as automotive, aerospace and defense. There are many other applications, which involve exposure of the composites to the potential corrosive environment. Despite the great risk of corrosion, most of the work on composites is concerned on its mechanical properties and processing routes, and there are several investigative studies addressing the corrosion behavior of aluminium metal matrix composites but they are not conclusive since corrosion behavior varies with respect to processing and type of reinforcement [Lloyd 1994 and Paciej 1986].

It has been observed that localized corrosion degrades physical and mechanical properties. 50% degradation in the transverse strength of composite was observed after it was immersed in 3.5 wt% NaCl for six hours. The magnitude of pitting corrosion observed on Al 6061-SiC was greater compared to corresponding unreinforced alloys [Bhat et al. 1991]. The pits on Al 6061 reinforced with SiC reinforcement were observed to be shallower and more numerous than on the unreinforced alloy. The silicon carbide/Al interface has been suggested to be the preferred sites for pits initiation. Corrosion damage in extruded composite was observed to be lesser due to the absence of defects like gas pores, and a more homogenous distribution of particles compared to the unreinforced alloys. The presence of SiC is reported to alter the growth of corrosion pits [Sun et al.1991].

A Large number of pits is formed in the composite compared to the wrought alloys. Composites corrode faster than the base alloy even though the attack is confined to the interface. The pits are, however, shallower on the composite. It has been established by studies on 6061 Al-SiC. The effect of SiC reinforcement of localized corrosion is not clearly understood. Some investigators suggest that pits initiate at SiC particles, whereas others suggest that SiC is not a preferred site for pit nucleation. There is also evidence to suggest that SiC introduces micro structural changes in the matrix, which affect the corrosion process [Trzaskoma et al. 1983].

The microstructure plays a pivotal role in the corrosion behavior of Al-SiC composites. Corrosion resistance is also affected by processing conditions that have an influence on micro structural features, void content, dislocation density around SiC particles and the precipitation of active phases around SiC particles are affected by processing conditions. In certain solution heat treatments and high extrusion ratios improved the corrosion resistance of a 6061 Al-15 vol% SiC MMC [Hollingsworth et al. 1984].

2.5.4. Heat treatment and Corrosion of Aluminium Alloys

The heat treatment and corrosion of Aluminium 6063 alloy was investigated. The effect of heat treatment on the microstructure and the corrosion of Aluminium 6063 were also studied. The sample conditions were; as- cast, solution treated, supersaturated and age hardened condition. The result showed that the corrosion rate of the alloy was increased and it was due to the nature of heat treatment given to the samples. Similarly, it was also found that the corrosion rate of the Al 6063 alloy was higher in the as- cast sample compared to the heat treated alloy. The corrosion behaviour of the as- cast sample is quite different from the solutionized sample. There was a steady and progressive drop in the corrosion rate of the solutionized sample implying that there was the stability of passive film formation [Ovat 2012].

Alloys 6061 in T6 temper exhibits shallow intergranular corrosion whereas in T4 temper 6013 Al exhibits only pitting [Burleigh 1993], which shows the role of micro structural changes and processing routes on the corrosion behaviour. Aging time appears strongly influence the corrosion behaviour as indicated by preliminary investigations on 2124 Al-SiC. The degree of corrosion of Al/ SiC composites increases with increasing SiC_p contents [Sun 1991].

The effect of temper on seawater corrosion of an Al/ SiC composite was studied. It was found that T4 temper alloy has higher corrosion resistance than F and O temper alloy. This was attributed to the formation of finer and more homogeneously distributed precipitates in T4 temper alloy [Ahmad 1996]. The corrosion behaviour of T6 heat-treated Al-Mg based MMCs reinforced with carbon (C) fibres, alumina (Al_2O_3) fibers and silicon carbide (SiC) whiskers have been investigated [Shimizu et al. 2000].

The aging treatment was found to have an influence on the corrosion rate as the T6 treated samples showed higher corrosion rates as compared to the non-treated samples under similar experimental conditions. These higher corrosion rates of aged samples are attributed to two parameters; (i) presence of intermetallic precipitates which are anodic to the matrix causing galvanic effect and (ii) the matrix strain arising due to age- hardening effect. Among the aged specimens, the peak- aged samples show the highest corrosion as the above effects are maximum in these samples. Over-aging causes coarsening of precipitates thereby reducing the interfacial area between the matrix and the precipitate. It also reduces the matrix strain due to incoherency. Thus, these samples show lower corrosion rates [Nayak 2008].

In another study, the peak aged composites have a higher corrosion current and a lower corrosion potential. It can be stated that the peak aged is morphologically unstable in corrosion media since pitting corrosion dominates. This effect may arise due to the uniform distribution of precipitates of alloying elements during peak aging. Among the artificially aged composites (T6 treatment), the peak aged composite is more prone to pitting corrosion [Rajasekaran 2012].

2.6. Corrosion by Acids

Many aluminium-based alloys are resistant to nitric acid in concentrations of about 80-99%. Alloys such as 1100, 3003, and 6061 have received the widest use for handling nitric acid at these concentrations. Dilute sulfuric acid solutions, up to about 10% in concentration cause some attack on aluminium-based alloys. The action on aluminium (1100) of solutions containing sulfuric acid, nitric acid, and water was studied. Aluminium is most resistant to solutions dilute in both acids or high in nitric acid concentration (above 82%), or in 100% sulfuric acid. Hydrofluoric, hydrochloric, and hydrobromic acid solutions, except at concentrations below about 0.1%, are definitely corrosive to aluminium alloys. The rate of attack is greatly influenced by temperature. Both perchloric and phosphoric acid solutions in intermediate concentrations definitely attack aluminium. Dilute (below 1%) phosphoric acid solutions have a relatively mild, uniform etching action that makes them useful for cleaning aluminium surfaces. Boric acid solutions in all concentrations up to saturation have negligible action on aluminium alloys. Chromic acid solutions in concentrations up to 10% have a mild, uniform etching action [Ghali 2010].

Most organic acids are well resisted by aluminium alloys at room temperature. In general, rates of attack are highest for solutions containing about 1% or 2% of the acid. Formic acid, acetic acid, oxalic acid, and some organic acids containing chlorine (such as trichloroacetic acid) are exceptions and are definitely corrosive. Equipment made of aluminium alloys, such as 1100 or 3003, is widely and successfully used for handling acetic, butyric, citric, gluconic, malic, propionic, and tartaric acid solutions [Lifka 2005].

2.6.1. Corrosion by Acetic Acid

Corrosion studies on metals and alloys in organic acid solutions are scarce in comparison with similar studies in mineral acids. The presence of reactive carboxyl group -COOH in organic acids makes them a basic unit for lots of compounds such as drugs, pharmaceuticals, plastics, and fibers. Acetic acid is utilized as chemical intermediates. This acid is used in textile, leather, dye, rubber, nylon, plastic, paint, pharmaceuticals and medicines, food, pesticide, herbicide, bactericide, fungicide, agriculture, poultry, oil, pulp and paper, flavor and perfume, chemical manufacturing and metal industries. Also, acetic acid is more frequently used as reactants or solvents in many industrial processes [Singh 2011]. Acetic acid is by far the most important organic acid among the lower carbon acids in the aliphatic series. The anodic behaviour of mild steel in deareated carboxylic acid solutions and corrosion behaviour of steel in acetic, oxalic and citric acids was studied. Corrosion behavior of 316L stainless steel in acetic acid solution over the concentration range 70%-90% has been also studied. All these studies show that acetic acid is highly corrosive [Mukherjee 2010].

Few corrosion studies of this acid have been made. Nevertheless, at high temperatures, this acid dissociates forming more aggressive ions that can cause faster corrosion rather than what it is expected. [Rafiquee et al. 2007]. Though organic acids are weakly acidic they render adequate protons to act as true acids towards most metals [Singh 1995]. Acetic acid is slightly less corrosive in its pure form but has been found to act an essential role in some corrosion systems.

There were certain investigations which gave strong and complimentary evidence about the major role played by acetic and formic acid in the growth mechanism of localized corrosion attack [Singh 2011]. Acetic acid occupies exactly the same position in the field of organic chemistry, as sulphuric acid in the heavy chemical industry as an important reagent. Depending on the method of manufacture, acetic acid may contain traces of other compounds in the form of impurities such as formic acid and minor amounts of oxidizing and reducing agents. Formic acid present in acetic acid, as a result of being more highly ionized than other organic contaminants, shows potent reactivity towards corrosion [Mukherjee 2008].

2.7. Corrosion Inhibition by Benzimidazole (BI) and Its Derivatives

Corrosion inhibitors are chemical compounds supplied to the corrosive medium to slow down or reduce the rate of acidic attack on metal, alloy or composite. The addition of inhibitors is one of the most practical methods of corrosion protection. The chemicals which can act as corrosion inhibitors may be organic or inorganic. Inhibitors adsorb on the metal surface forming a barrier between the sample and the corrosive environment [Viswanathan 2010]. Amongst them, heterocyclic organic compounds containing sulphur, phosphorous, oxygen, nitrogen, and aromatic rings are the most effective and efficient inhibitors for the metals in the acidic medium due to their special molecular structure. In many factors for the inhibiting effects, the planarity of heterocycles and the presence of a lone pair of electrons on hetero-cyclic atoms are particularly important structure characteristics because they mainly determine the adsorption of inhibitor molecules on the metal surface [Wang 2002]. Generally the tendency to form a stronger coordination bond, and consequently resulting in the high inhibition efficiency, increases in the following order $O < N < S < P$ [Sankarap 1991].

However, the application of these compounds as inhibitors have been questioned latterly, on account of negative effects they have produced in the environment. Hence, the development of the new corrosion inhibitors of natural basis and non-toxic has been considered to be necessary and important. As of their natural origin, non-toxic properties and minor negative impacts on the aquatic atmosphere, drugs (chemical medicines) seem to be perfect candidates to substitute traditional noxious corrosion inhibitors. Drugs and corrosion inhibitors have so many similarities. Carboxylic and heterocyclic units are abundant in drugs. Five- and six-membered rings are more common, but small ring systems come about with reasonable frequency. Out of five- and six-membered systems, the common ones are aromatic or pseudo aromatic. Henceforth, replaced benzene rings are common and heterocycles such as pyridines, furans, thiophenes, imidazoles, isoxazols and others occur generally in drug structure. Because of the above stated structural similarities, corrosion protection properties of many drugs have attracted too much attention latterly [Gece 2011].

In recent years, BI and its derivatives have received considerable attention on their inhibition properties for metallic corrosion [Xiumei 2011]. BI is a heterocyclic aromatic compound. This bicyclic compound consists of the fusion of benzene and imidazole. Of all the benzimidazole derivatives, 2-substituted BI derivatives such as 2-methylbenzimidazole (2-CH_3-BI) and 2- mercaptobenzimidazole (2-SH-BI), have been found to be biologically most potent [Obot 2010]. BI and its derivatives have been demonstrated that they are excellent inhibitors in acidic solution since the nitrogen atom and the aromatic ring in molecular structure are likely to facilitate the adsorption of compounds on the metallic surface [Xiumei 2011].

2.8. Proposed Work

The literature survey indicates that there is a need of systematic study of the effect of aging treatments on the corrosion behavior of 6061Al-SiC_p composite. Hence aging treatments are to be carried out and the investigations on the effect of aging on the corrosion behaviour of Al-SiC are to be done. Corrosion studies are to be executed in acetic acid which is a strong corrosive medium and which frequently comes in contact with the sample in industries and daily use. A perusal of literature reveals that the inhibition effect of BI and its derivatives on corrosion of 6061Al-SiCp composite has not been reported yet, and there is only scanty information available to profoundly understand their inhibition mechanism as an acidic inhibitor. Therefore these three inhibitors such as benzimidazole, 2-methylbenzimidazole, and 2-mercaptobenzimidazole have been chosen for inhibition analysis and mechanism of inhibition is also to be examined.

2.9. Objectives

- To study age hardening response of Al-SiC samples and to obtain aging curves.
- To study the corrosion behaviour of T6 treated Al-SiC in acetic acid at three different concentrations and five different temperatures.
- To understand the effect of aging treatment on corrosion behaviour.
- To choose suitable inhibitors for the corrosive medium from the literature review and to study corrosion inhibition using the chosen inhibitors.
- To elucidate the inhibition mechanism of the selected inhibitors.

CHAPTER 3

T4 AND T6 TREATMENT OF 6061 Al-SiC COMPOSITE

3.1. Experimental Work

3.1.1. Specimens

6061 Al-SiC composite material with 15 vol% SiC particles of size 23 µm and 99.9% purity is used in this study. The 6061 Al-SiC composites were cast in the form of cylinders each of 90 mm diameter and 240 mm length by stir casting technique at NIIST, Trivandrum, Kerala. These cylinders were extruded at 430^0C-480^0C with an extrusion ratio of 30:1 at serval engineers, Mangaluru, Karnataka. The experiments were performed with composite in extruded rod form. The extruded samples were cut in cylinders of 2 cm length and diameter of 1.15 cm. The composition of the base metal alloy is given in Table 3.1.

Table 3.1: Composition of 6061 Al alloy (matrix) used in the study

Element	Cu	Mg	Si	Mn	Cr	Others	Al
Weight %	0.15- 0.2	0.8-1.2	0.4-0.6	0.15	0.04-0.35	1.25 max	Balance

The microstructure of the 6061 Al-15 vol% SiC composite was obtained using JEOL made JSM 6380LA SEM and is shown in Figure 3.1. It's clearly seen in the image that the reinforced SiC particles are distributed uniformly.

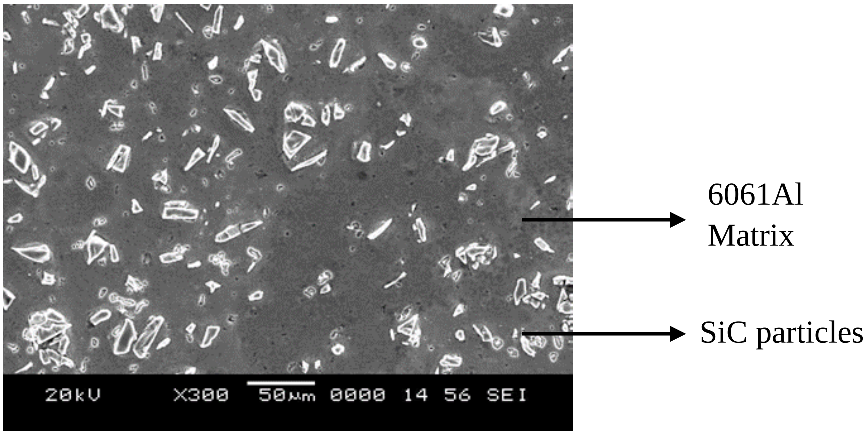

Fig. 3.1: SEM image of 6061 Al-SiCp composite.

3.1.2. Method

The composite samples were polished and solution treated at a temperature of 350ºC for 30 minutes. They were then water quenched at room temperature. This was followed by aging the quenched composites at room temperature (T4 treatment) and at 140ºC, 160ºC, 180ºC, 200 ºC and 220ºC (T6 treatment) for various durations of time. The aging behaviour of the composite was studied using Rockwell hardness measurement. Rockwell B Hardness (HR_B) tests were performed immediately after aging. Each hardness value was the average of at least three measurements in two samples.

3.2. Results and Discussion

The hardness measurements for T4 treatment showed a sharp rise after the solution treatment for the first few hours. It then increased gradually up to around 720 hours. Peak hardness was observed at 720 hours and hardness decreased gradually after that. Table 3.2 shows the Rockwell B hardness values of natural aging and the aging curve is depicted in Fig. 3.2. The Rockwell B hardness values of T6 treated 6061 Al-SiC composite at various temperatures of aging are given in Table 3. Fig. 3.3, 3.4, 3.5, 3.6 and 3.7 depicts hardness variation with time in T6 treatment. Fig. 3.8 shows the peak hardness variation with aging temperature in T6 treatment. Fig. 3.9 shows the variation of peak-aging time with different aging temperatures.

Table 3.2: Rockwell B hardness values of T4-treated 6061Al-SiC composite.

Time of Aging (Hours)	Hardness (Rockwell B)	Time of Aging (hours)	Hardness (Rockwell B)
0	62	48	83
2	64	120	86
4	65	240	87
6	67	480	89
8	71	720	90
24	77	960	88

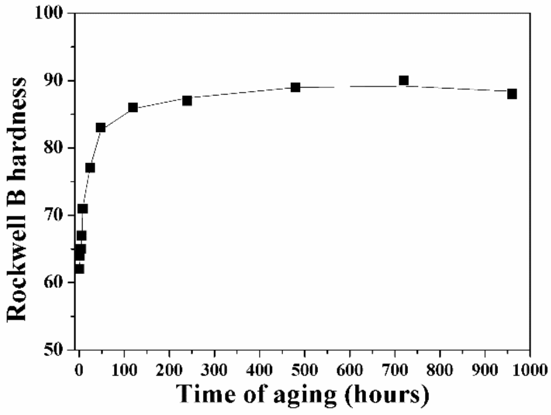

Fig. 3.2: Hardness variation with time in T4 treatment.

In 6061 Al alloy, Mg and Si are the major alloying elements. When this alloy is solutionized both these alloying elements are taken into solid solution as a single α phase. Quenching the alloy results in super saturated solid solution α as the solubility for these elements at room temperature is very less. Given an opportunity, the excess solutes diffuse out of α lattice and forms intermetallic precipitates of Mg_2Si (β phase). However, the formation of these precipitates occurs in successive stages. The aging sequence for 6061 Al alloy and its composite are as follows: Super-saturated solid solution → clusters of solute atoms and vacancies (Primitive Guinier-Preston [GP] zones)→ needle-shaped GP zones (β'')→ rod-shaped, metastable, semi-coherent β' phase → stable, semi-coherent, Mg_2Si precipitate (β phase) [Appendino et al. 1991].

Table 3.3: Rockwell B hardness values of T6-treated 6061 Al-SiC composite.

Time of Aging (Hours)	Rockwell B hardness of the composite aged at				
	140°C	160°C	180°C	200°C	220 °C
0	62	62	62	62	62
1	68	79	86	70	66
2	73	84	91	78	71
3	78	87	98	85	69
4	88	94	93	75	64
5	79	85	82	72	60

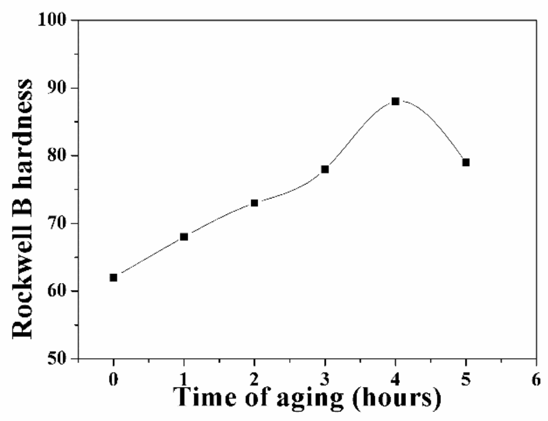

Fig. 3.3: Hardness variation with time in T6 treatment at 140°C.

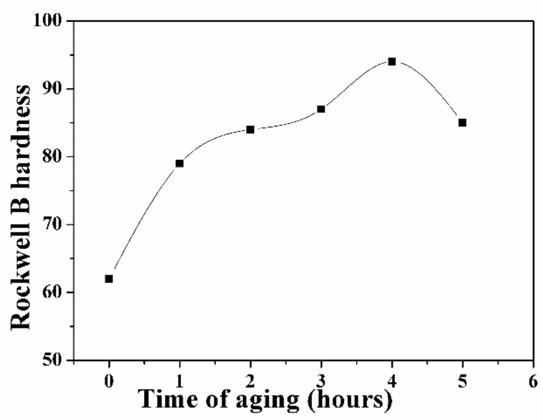

Fig. 3.4: Hardness variation with time in T6 treatment at 160°C.

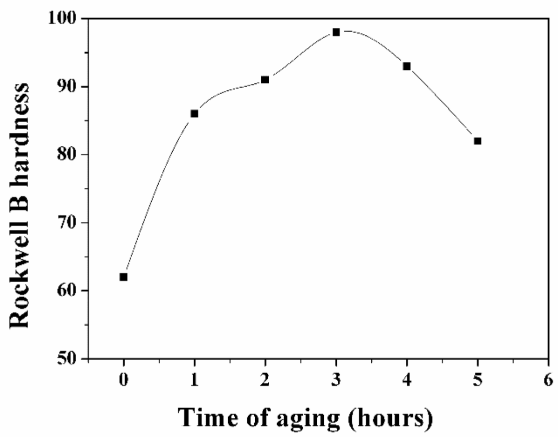

Fig. 3.5: Hardness variation with time in T6 treatment at 180°C.

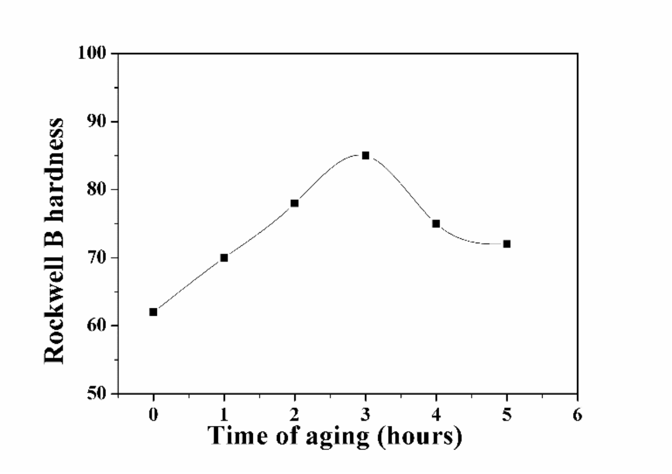

Fig. 3.6: Hardness variation with time in T6 treatment at 200°C.

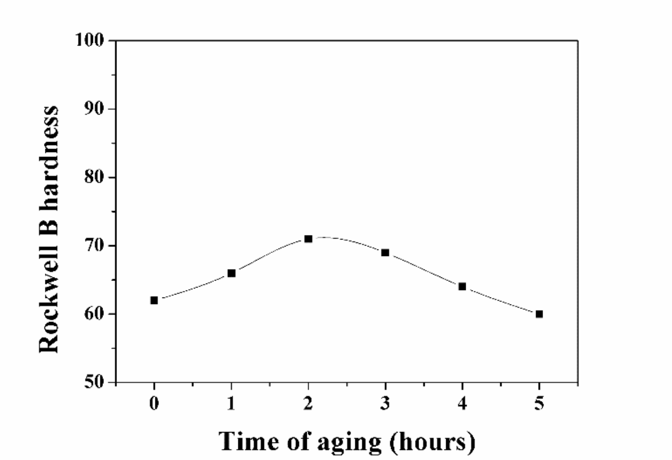

Fig. 3.7: Hardness variation with time in T6 treatment at 220°C.

If aging is done at room temperature, it is called natural aging (T4 treatment) and if it occurs at higher temperatures it is called artificial aging (T6 Treatment). Guinier Preston or GP zones have been recognized as microstructural elements in age hardenable Al alloys. These zones are formed by natural aging at room temperature and in the early stages of the industrially important artificial aging at temperatures in a range of 100-180°C [Berg et al 2001]. Since natural aging is carried out at room temperature, the diffusion rate is very low and therefore it is expected that the alloy takes very long period to get aged. In artificial aging, we can expect higher rates of diffusion resulting in faster attainment of aging effect. Since the aging phenomenon is diffusion controlled, both time and temperature play vital roles in the process.

In the case of aluminium composites, the effects of reinforcements on the age-hardening behaviour have not been reported consistently. But it was found that the age-hardening is accelerated since the times to reach the peak hardnesses were shortened by the presence of reinforcements in these composites. For this reason, the diffusion of alloy elements is required in order to produce precipitation during the artificial aging, and many dislocations were introduced by thermal mismatch betweem matrix and reinforcement. These high density dislocations offer a high diffusivity path for the diffusion of alloying elements; accelerating the age-hardening of composites [Ahn 2001, Christman 1998 and Yu 1993]. On the contrary, the driving force for natural aging mainly depends on the concentration of alloying elements in the super-saturated solid solution [Appendino 1991 and Borrego 2003].

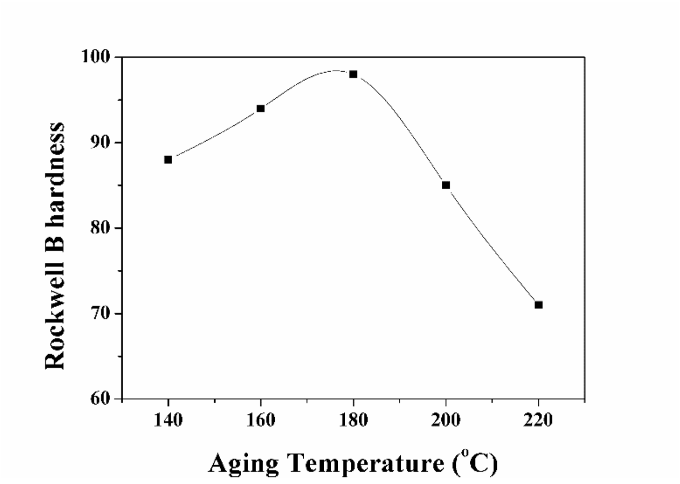

Fig. 3.8: Peak hardness variation with aging temperature in T6 treatment.

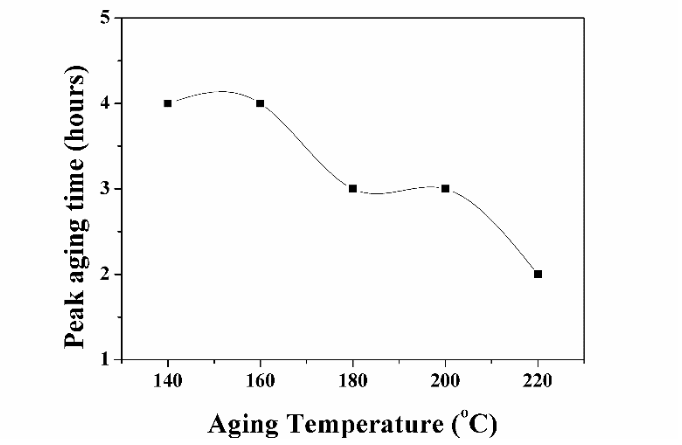

Fig. 3.9: Peak aging time variation with aging temperature in T6 treatment.

From the hardness profile of fig. 3.3, 3.4, 3.5,3.6 and 3.7, the aged specimens were categorized into three groups namely a) under-aged b) peak-aged and c) over-aged. The variation in hardness is associated with the microstructural evolution. The formation of Mg and Si clusters takes place initially. These contribute marginally to the increase in hardness. Peak-aging is associated with a dense population of β'' needle-shaped precipitates. Since these precipitates are coherent precipitates; a large amount of lattice strain is developed because of lattice mismatch. This results in high hardness. Only a part of these precipitates remain in the microstructure during over-aging as the metastable phases like β' is formed. These precipitates are semi-coherent and there by the lattice strain involved is less, which results in the lowering of hardness values [Ozturk et al. 2010 and Marioara 2007]. In natural aging treatment, the peak hardness of 90 HR_B was observed after 720 hours and in artificial aging treatment peak hardness of 98 HR_B was achieved after 3 hours at 180°C. The peak-aging time decreased with the increase of aging temperature as shown in Fig. 3.9, which suggests age- hardening kinetics became faster as the aging temperature was increased [Min 2004].

From the results obtained for the aging treatments, we can conclude that the peak hardness in T4 treatment is 90 HR_B which was obtained at 720 hours of aging at room temperature. In T6 treatments, the temperature for under-aging, peak-aging and over-aging was determined using aging curves. Refering to Fig. 3.8 it can be concluded that the composite was under- aged at 140°C and 160°C, peak-aged at 180°C and over-aged at 200°C and 220°C. Maximum peak hardness value of 98 HR_B was obtained when the composite was aged at 180°C for 3 hours. The peak-aging time was decreased from 4 to 2 hours when the aging temperature was increased.

3.3 Conclusions

- The peak hardness in T4 treatment is 90 HR_B which was obtained at 720 hours of aging at room temperature.
- In T6 treatments, the temperature for under-aging, peak-aging and over-aging was determined using aging curves.
- The composite was under- aged at 140 and 160°C, peak-aged at 180°C and over-aged at 200°C.
- Maximum Peak hardness value of 98 HR_B was obtained when the composite was aged at 180°C for 3 hours.

- The peak-aging time was decreased from 4 to 2 hours when the aging temperature was increased.

CHAPTER 4

CORROSION STUDIES ON T6 TREATED Al-SiC COMPOSITE

4.1. Experimental work

4.1.1. Specimens

For corrosion tests, 6061 Al-SiCp cylindrical coupons of 5 cm length and 1 cm diameter were first solutionized, quenched and aged (T6 treatment) at 140°C, 180 °C and 220°C. At each aging temperatures under-aged, peak-aged and over-aged samples were obtained. Samples aged at 140°C for 1 hour were considered as under-aged, those that were aged for 4 hours as peak-aged and samples aged for 6 hours as over-aged. Similarly, samples aged at 180°C for 1 hour were considered as under-aged, those that were aged for 3 hours as peak-aged and samples aged for 6 hours as over-aged. Samples aged at 220°C for 1 hour were considered as under-aged, those that were aged for 2 hours as peak-aged and samples aged for 4 hours as over-aged. These samples were then mounted in an epoxy material. The surface preparation of the specimens was carried out using emery papers of different grades up to 4/0 grit and wet polished with diamond paste, rinsed with double distilled water, degreased with acetone and dried at room temperature before use.

4.1.2. Electrolyte

Analytical grade acetic acid and distilled water were used for preparing test solutions for all the experiments. The range of concentrations of acetic acid used for the corrosion study was determined by conducting corrosion tests in 10 %, 30 %, 50 %, and 70 % acetic acid at different temperatures. Corrosion rates obtained for different concentration by Tafel extrapolation method are shown in Table 4.1.

As seen in Table 4.1, corrosion rates increase as the temperature was increased. The increase in corrosion rate with temperature may be attributed to the increase in the conductivity of the acetic acid solution. It was observed that there is a rapid increase in the corrosion rate with increase in the concentration of acetic acid till it reached a maximum at 30 %. Any further increase in the concentration of acetic acid resulted in the decrease in the corrosion rate at each temperature.

Table 4.1: Corrosion rates of underaged (at 140°C) 6061 Al-SiC composite for various concentrations of acetic acid at different temperatures.

Concentrations of Acetic acid (vol %)	Corrosion rates (mpy)				
	30°C	35°C	40°C	45°C	50°C
10 %	4.5	6.0	10.2	14.7	24.1
30 %	6.2	8.4	17.8	18.9	30.6
50 %	5.6	7.9	16.1	17.3	23.6
70 %	4.7	7.1	10.1	11.0	12.5

The marked decrease in corrosion rate at higher concentrations of acetic acid is assumed to be a consequence of the increase in the viscosity of the solutions due to the formation of a dimer, resulting in a decrease in the mobility of the ions. Acetic acid is generally associated to form a dimer and polymer at higher concentrations. Besides this, an increased concentration leads to an increase in electro-static ion-ion interactions and a decrease in the degree of acetic acid dissociation. The decrease in corrosion rate must have occurred due to precipitation of the corrosion product. Since acetic acid is a weak acid, it is feebly dissociated at higher concentrations. Thus, a decrease in dissociation and increase in viscosity reduce its conduction. With the increase in the acid concentration, the concentration of undissociated acetic acid molecules increases, thereby decreasing free hydrogen ion concentration which in turn decreases corrosion rate [Singh 2010].

So, it was decided to carry out experiments in 10 %, 20 %, and 30 % acetic acid as it is more corrosive towards the sample.

4.1.3. Inhibitors

As obvious from the literature review, benzimidazole and its derivatives have received considerable attention on their inhibition properties. So, for the present study benzimidazole and its two derivatives such as 2-methylbenzimidazole and 2-

mercaptobenzimidazole are chosen as inhibitors. The details of the above-mentioned inhibitors such as molecular structures, abbreviations, and molar masses are given in Table 4.2. Optimized structure of these inhibitors is shown in Fig. 4.1.

Table 4.2: Molecular structure, abbreviation and molar mass of inhibitors

Inhibitor	Structure	Abbreviation	Molar mass (g/mol)
Benzimidazole	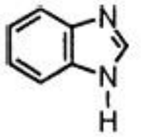	BI	118.14
2-Methylbenzimidazole	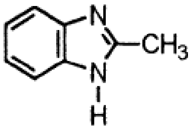	2-CH_3-BI	132.10
2-Mercaptobenzimidazole	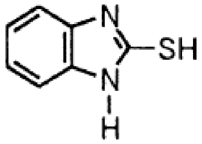	2-SH-BI	150.20

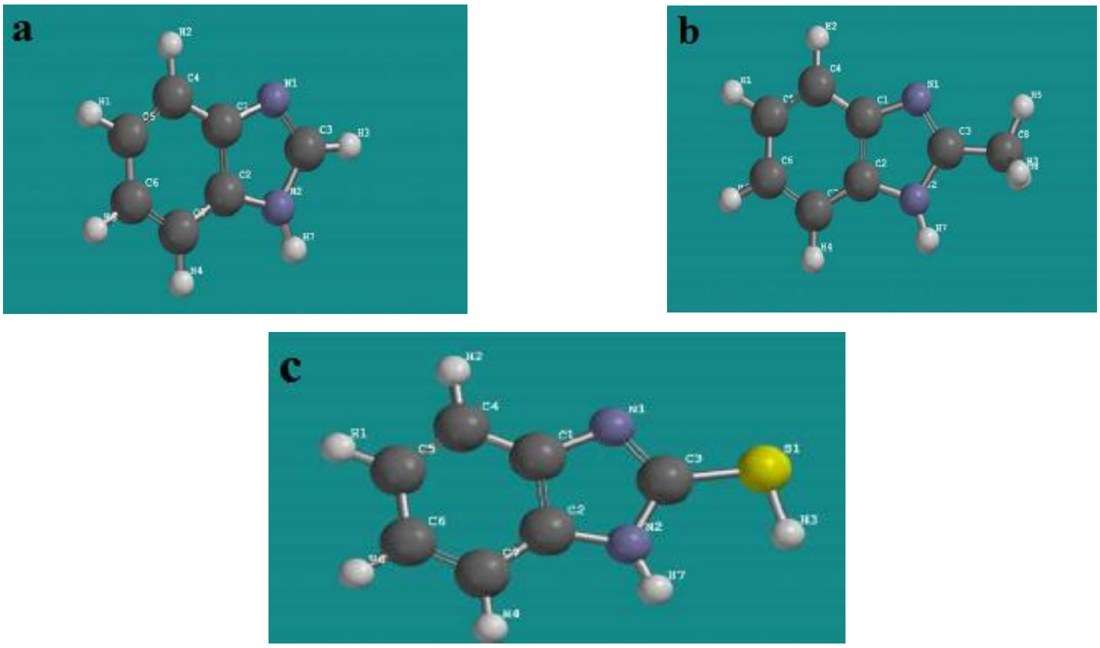

Fig. 4.1: Optimized structures of the compounds (a) BI; (b) 2-CH_3-BI; (c) 2-SH-BI [Obot 2010]

4.1.4. Corrosion testing method

An area of 1 cm^2 of the polished 6061 Al- SiC specimens were exposed to 150ml of acetic acid solution (10 %, 20 % and 30 %) at 30°C, 35°C, 40°C, 45°C and 50°C with and without inhibitors (50, 100 and 200ppm). Electrochemical measurements were performed with a potentiostat under software control (BIOLOGIC, SP-150 {Fig 4.2}).

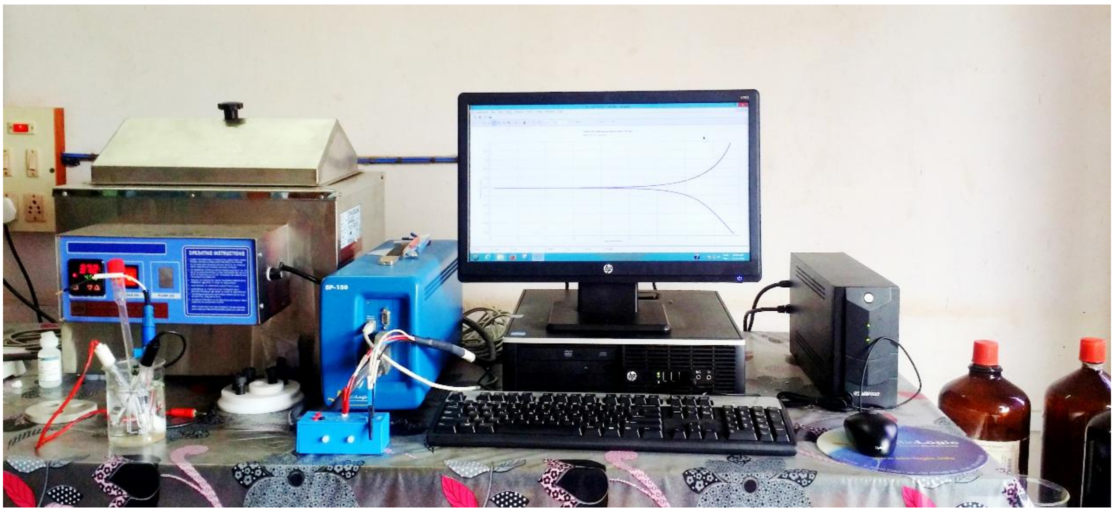

Fig. 4.2: BIOLOGIC (SP-150).

Polarization scans were initiated from -250 mV cathodically and scanned to approximately +250 mV anodically, all potentials being relative to the open-circuit corrosion potential. Polarization curves recorded over the range – 250 to +250 mV, from which corrosion rates were estimated. Potentiodynamic scan rates were 10 mV/s. A three electrode cell consisting of a large area platinum as a counter electrode, saturated calomel electrode (SCE) as a reference electrode and sample as working electrode was used. All potentials are referenced to the SCE. The corrosion rate is obtained from the expression, Corrosion Rate (mpy) = (0.129× EW× icorr)/D, where, i_{corr} is the corrosion current density in μA/ cm^2, Eq.Wt is the equivalent weight of the corroding specimen in gm and D is the density of the corroding species in gm/cm^3.

4.2. Results and Discussion

Corrosion rate measurements for different experimental parameters are given in the tables given below.

Table 4.3: Corrosion rates of under-aged (140 °C) samples with and without inhibitors at different temperatures.

Temperature	Acetic acid (vol %)	Corrosion rates (mpy) with and without inhibitors									
		0 ppm	BI			2-CH_3-BI			2-SH-BI		
			50 ppm	100 ppm	200 ppm	50 ppm	100 ppm	200 ppm	50 ppm	100 ppm	200 ppm
30 °C	10 %	4.5	3.9	3.5	3.2	3.5	3.1	2.7	3.1	2.6	2.1
	20 %	5.7	4.7	3.9	3.5	4.2	3.5	2.9	3.7	3.3	2.4
	30 %	6.2	5.5	4.8	4.0	5.1	4.4	3.6	4.5	4.0	3.1
35 °C	10 %	6.0	5.1	5.0	4.4	4.7	4.3	3.2	4.4	3.6	2.9
	20 %	7.2	5.9	5.6	5.0	5.3	4.9	3.9	4.8	4.2	3.3
	30 %	8.4	7.0	5.9	5.2	6.6	5.6	4.8	6.3	5.4	4.2
40 °C	10 %	10.2	6.7	5.2	4.6	6.2	4.9	4.4	5.9	4.7	4.3
	20 %	15.0	7.7	5.8	5.3	7.3	5.6	5.2	7.1	5.5	5.0
	30 %	17.8	12.9	8.8	8.0	11.3	8.7	7.9	9.9	8.7	7.8
45 °C	10 %	14.7	8.5	8.0	7.2	7.4	6.8	6.5	6.9	6.1	5.7
	20 %	17.8	9.7	8.4	7.9	8.8	8.0	6.9	8.4	7.7	6.2
	30 %	18.9	13.3	10.6	8.9	12.4	10.5	8.4	11.4	10.3	8.1
50 °C	10 %	24.1	13.5	11.8	10.0	12.1	9.8	7.7	10.6	8.4	6.8
	20 %	27.3	14.7	12.9	11.1	13.4	11.8	9.1	12.7	11.0	8.6
	30 %	30.6	21.3	17.8	13.7	19.6	14.9	12.0	16.8	13.6	11.5

Table 4.4: Corrosion rates of peak-aged (140 °C) sample with and without inhibitors at different temperatures.

Temperature	Acetic acid (vol %)	Corrosion rates (mpy) with and without inhibitors									
		0 ppm	BI			2-CH_3-BI			2-SH-BI		
			50 ppm	100 ppm	200 ppm	50 ppm	100 ppm	200 ppm	50 ppm	100 ppm	200 ppm
30 °C	10 %	5.8	4.6	3.9	3.5	3.9	3.5	3.2	3.4	3.0	2.5
	20 %	6.9	5.4	4.8	4.1	4.7	4.2	3.9	4.3	3.7	3.0
	30 %	7.6	6.3	5.6	4.9	5.6	5.0	4.3	5.0	4.5	3.6
35 °C	10 %	6.9	6.0	5.3	4.8	5.1	4.4	4.1	4.8	3.9	3.6
	20 %	8.1	7.4	6.5	5.6	6.2	5.3	4.7	5.4	4.6	4.0
	30 %	9.4	8.7	7.4	6.3	7.3	6.4	5.5	6.3	5.8	4.6
40 °C	10 %	12.9	9.3	7.6	5.9	8.1	6.3	5.1	6.9	5.4	4.7
	20 %	17.4	12.5	11.2	7.1	10.1	7.8	6.0	7.8	6.5	5.3
	30 %	18.9	14.6	12.6	9.3	11.7	10.2	8.3	10.3	9.4	8.0
45 °C	10 %	17.3	12.4	10.2	7.9	10.3	7.6	7.0	7.8	6.9	6.4
	20 %	19.9	15.1	11.8	9.2	12.3	8.8	8.1	9.2	8.1	7.5
	30 %	22.6	18.3	14.7	12.5	14.1	11.5	9.6	12.3	10.8	8.9
50 °C	10 %	26.6	21.7	16.5	13.1	17.6	13.7	11.6	15.8	12.3	9.1
	20 %	30.1	24.8	19.4	15.5	20.1	15.9	13.4	18.2	13.8	10.8
	30 %	34.4	27.4	22.9	18.7	23.9	18.3	16.3	20.4	15.6	13.2

Table 4.5: Corrosion rates of over-aged (140 °C) sample with and without inhibitors at different temperatures.

Temperature	Acetic acid (vol %)	Corrosion rates (mpy) with and without inhibitors									
		0 ppm	BI			2-CH_3-BI			2-SH-BI		
			50 ppm	100 ppm	200 ppm	50 ppm	100 ppm	200 ppm	50 ppm	100 ppm	200 ppm
30 °C	10 %	4.0	3.5	3.2	2.8	3.1	2.9	2.1	2.8	2.3	1.8
	20 %	5.2	4.4	3.6	3.1	3.9	3.1	2.6	3.4	2.8	2.1
	30 %	5.8	5.1	4.4	3.6	4.7	4.0	3.5	4.0	3.4	3.0
35 °C	10 %	5.7	4.8	4.3	3.8	4.2	3.6	2.7	3.6	3.1	2.3
	20 %	6.6	5.4	5.0	4.4	4.9	4.3	3.4	4.2	3.7	2.9
	30 %	7.7	6.7	5.4	4.9	6.0	4.9	4.3	5.5	4.3	3.6
40 °C	10 %	9.1	5.7	4.8	4.3	5.1	4.2	3.8	4.4	3.7	3.2
	20 %	11.9	7.0	5.5	5.0	6.2	5.0	4.7	5.3	4.2	3.8
	30 %	14.5	11.3	7.2	6.4	9.9	6.4	5.8	7.4	5.6	4.6
45 °C	10 %	12.2	7.6	6.7	6.1	6.9	5.9	5.6	6.1	5.0	4.4
	20 %	14.9	9.0	7.8	6.9	8.1	7.0	6.3	7.4	6.1	5.5
	30 %	16.3	11.8	9.6	8.4	10.3	8.2	7.4	9.2	7.3	6.7
50 °C	10 %	20.6	10.9	9.0	7.8	8.9	7.6	6.4	7.1	6.2	5.2
	20 %	22.8	12.5	10.3	9.1	10.8	8.8	7.3	8.6	7.4	6.3
	30 %	26.4	18.7	15.3	12.5	16.5	12.4	10.2	13.8	10.7	8.6

Table 4.6: Corrosion rates of under-aged (180 °C) sample with and without inhibitors at different temperatures.

Temperature	Acetic acid (vol %)	Corrosion rates (mpy) with and without inhibitors									
		0 ppm	BI			2-CH_3-BI			2-SH-BI		
			50 ppm	100 ppm	200 ppm	50 ppm	100 ppm	200 ppm	50 ppm	100 ppm	200 ppm
30 °C	10 %	6.4	5.6	4.8	4.5	5.0	4.6	4.2	4.7	4.4	3.9
	20 %	6.7	5.8	5.0	4.6	5.5	5.1	4.7	5.2	4.9	4.3
	30 %	7.1	6.3	5.5	5.0	5.7	5.3	4.9	5.4	5.1	4.5
35 °C	10 %	6.6	6.1	5.8	5.3	5.8	5.6	5.0	5.5	5.0	4.8
	20 %	8.0	7.2	6.8	6.3	7.0	6.7	5.9	6.7	6.3	5.4
	30 %	9.2	8.6	8.1	7.5	8.1	7.6	7.1	7.7	7.4	6.7
40 °C	10 %	11.6	9.2	8.7	8.1	8.8	8.3	7.7	8.4	8.1	7.2
	20 %	15.9	12.2	11.8	10.0	10.8	10.2	9.7	10.3	9.9	9.3
	30 %	19.3	17.0	16.0	13.7	14.9	14.1	11.1	14.2	13.7	10.4
45 °C	10 %	15.3	14.1	13.3	11.9	12.7	12.2	11.6	12.2	11.9	11.0
	20 %	19.7	17.5	16.8	12.4	13.4	12.8	11.8	12.7	12.1	11.3
	30 %	21.0	18.0	17.2	13.1	14.0	13.6	12.2	13.1	12.4	11.8
50 °C	10 %	25.0	20.2	19.8	15.7	17.4	16.5	13.9	16.7	15.9	12.6
	20 %	27.1	21.7	21.0	16.1	18.2	17.9	16.7	17.7	17.1	15.4
	30 %	32.1	24.6	23.5	18.3	21.7	20.7	18.3	20.1	19.8	17.2

Table 4.7: Corrosion rates of peak-aged (180 °C) sample with and without inhibitors at different temperatures.

Temperature	Acetic acid (vol %)	Corrosion rates (mpy) with and without inhibitors									
		0 ppm	BI			2-CH_3-BI			2-SH-BI		
			50 ppm	100 ppm	200 ppm	50 ppm	100 ppm	200 ppm	50 ppm	100 ppm	200 ppm
30 °C	10 %	7.8	6.5	5.7	5.0	6.1	5.4	4.9	5.3	4.9	4.2
	20 %	9.1	7.9	6.8	5.9	7.0	6.2	5.6	6.2	5.6	4.8
	30 %	10.7	9.2	8.0	6.8	8.4	7.4	6.6	7.1	6.5	5.7
35 °C	10 %	9.2	7.8	6.7	6.0	7.0	6.1	5.6	6.2	5.7	5.2
	20 %	10.7	9.1	8.0	7.1	8.3	7.5	6.4	7.5	6.9	6.0
	30 %	12.4	10.4	8.9	7.8	9.1	8.2	7.6	8.3	7.7	7.1
40 °C	10 %	13.7	10.8	9.4	8.8	9.6	8.9	8.2	9.0	8.5	7.9
	20 %	17.8	15.5	13.4	11.9	12.7	11.5	10.6	11.4	10.7	9.9
	30 %	23.1	19.8	18.1	14.6	16.6	15.2	13.2	15.9	14.3	11.3
45 °C	10 %	18.1	16.3	14.7	12.9	14.5	13.4	12.1	13.2	12.5	11.7
	20 %	22.9	19.8	17.5	14.7	16.1	14.9	13.0	14.8	13.6	12.2
	30 %	24.5	21.7	19.3	16.1	18.3	17.1	14.6	16.7	15.4	13.4
50 °C	10 %	28.7	24.7	21.4	17.3	20.3	18.9	14.7	18.3	17.0	13.2
	20 %	31.2	27.8	23.8	19.5	23.4	20.3	17.5	20.5	18.7	16.2
	30 %	35.6	30.2	26.7	21.4	25.9	23.9	20.1	22.7	20.4	18.6

Table 4.8: Corrosion rates of over-aged (180 °C) sample with and without inhibitors at different temperatures.

Temperature	Acetic acid (vol %)	Corrosion rates (mpy) with and without inhibitors									
		0 ppm	BI			2-CH_3-BI			2-SH-BI		
			50 ppm	100 ppm	200 ppm	50 ppm	100 ppm	200 ppm	50 ppm	100 ppm	200 ppm
30 °C	10 %	5.7	5.1	4.4	3.8	4.6	4.1	3.7	4.1	3.6	3.2
	20 %	6.2	5.5	4.8	4.1	5.0	4.6	4.2	4.6	4.2	3.8
	30 %	6.8	6.0	5.1	4.7	5.4	5.0	4.5	5.0	4.8	4.1
35 °C	10 %	6.0	5.6	5.0	4.6	5.3	4.9	4.5	4.8	4.4	4.0
	20 %	7.4	6.7	6.2	5.6	6.4	6.0	5.5	6.1	5.7	4.9
	30 %	8.6	7.8	7.2	6.8	7.1	6.8	6.1	6.8	6.4	5.7
40 °C	10 %	10.8	8.7	8.1	7.5	8.2	7.6	7.0	7.6	6.9	6.1
	20 %	14.6	11.5	10.7	9.4	9.9	8.7	7.8	9.0	8.6	7.5
	30 %	18.7	16.8	15.2	12.6	13.4	12.8	10.4	12.6	11.7	9.7
45 °C	10 %	14.1	12.6	11.9	10.7	11.8	10.6	9.7	10.9	10.1	9.3
	20 %	17.4	15.9	14.7	11.2	12.4	11.5	10.3	11.7	10.9	10.0
	30 %	19.7	17.3	16.2	12.4	13.7	12.9	11.6	12.4	11.6	10.9
50 °C	10 %	23.2	19.1	18.3	14.1	16.1	15.3	12.3	15.3	13.8	11.6
	20 %	25.4	20.7	19.8	15.6	17.6	16.3	14.9	16.2	15.1	14.2
	30 %	29.3	23.4	22.4	17.1	20.1	19.1	16.8	18.9	16.8	14.7

Table 4.9: Corrosion rates of under-aged (220 °C) sample with and without inhibitors at different temperatures.

Temperature	Acetic acid (vol %)	Corrosion rates (mpy) with and without inhibitors									
		0 ppm	BI			2-CH_3-BI			2-SH-BI		
			50 ppm	100 ppm	200 ppm	50 ppm	100 ppm	200 ppm	50 ppm	100 ppm	200 ppm
30 °C	10 %	3.9	3.5	3.1	2.5	3.2	2.6	2.3	2.9	2.5	2.0
	20 %	4.2	3.6	3.2	2.6	3.5	2.9	2.4	3.1	2.7	2.1
	30 %	4.7	4.4	3.8	2.9	4.0	3.1	2.7	3.6	2.8	2.4
35 °C	10 %	5.8	5.2	4.1	3.0	4.9	3.6	2.9	4.0	3.2	2.6
	20 %	6.6	5.8	4.5	3.3	5.7	4.2	3.1	4.9	3.9	2.9
	30 %	7.7	6.9	5.8	4.7	6.1	5.0	4.1	5.6	4.6	3.6
40 °C	10 %	8.7	6.0	4.9	4.3	5.4	4.3	3.8	5.0	4.5	3.8
	20 %	14.2	7.2	5.3	4.9	6.8	4.9	4.3	6.1	5.2	4.6
	30 %	15.1	11.7	8.0	7.7	10.2	7.5	6.9	9.3	8.1	7.2
45 °C	10 %	12.7	7.9	7.3	6.5	6.9	6.1	5.6	6.2	5.4	5.0
	20 %	15.8	9.0	8.0	7.2	8.0	7.4	6.1	7.8	7.0	5.8
	30 %	17.1	12.6	9.8	8.3	11.7	9.8	7.7	10.6	9.7	7.6
50 °C	10 %	21.8	12.7	11.2	9.4	11.7	9.2	7.1	9.9	7.8	5.9
	20 %	24.3	14.2	12.1	10.5	12.6	11.0	8.7	11.8	10.3	7.9
	30 %	26.6	20.8	16.8	12.3	18.4	13.5	11.2	15.1	12.6	10.7

Table 4.10: Corrosion rates of peak-aged (220 °C) sample with and without inhibitors at different temperatures.

Temperature	Acetic acid (vol %)	Corrosion rates (mpy) with and without inhibitors									
		0 ppm	BI			2-CH$_3$-BI			2-SH-BI		
			50 ppm	100 ppm	200 ppm	50 ppm	100 ppm	200 ppm	50 ppm	100 ppm	200 ppm
30 °C	10 %	5.3	4.3	3.6	2.9	3.7	3.2	2.6	3.3	3.0	2.4
	20 %	6.4	5.0	4.5	3.7	4.5	3.9	3.5	3.9	3.4	2.8
	30 %	7.0	5.9	5.2	4.5	5.1	4.6	4.0	4.7	4.1	3.3
35 °C	10 %	6.3	5.9	4.9	4.1	5.2	4.2	3.7	4.6	3.7	3.3
	20 %	7.6	7.1	6.0	5.2	6.0	5.0	4.9	5.3	4.3	3.9
	30 %	8.9	7.9	6.8	5.9	6.9	5.8	5.5	6.1	5.4	4.3
40 °C	10 %	10.1	8.7	6.1	5.2	7.3	5.8	4.8	6.3	5.1	4.1
	20 %	16.5	10.1	7.9	6.4	8.9	7.0	5.7	7.2	6.2	5.0
	30 %	18.2	13.5	10.2	8.7	11.2	8.6	7.6	10.0	8.8	7.9
45 °C	10 %	14.7	10.2	8.6	7.0	9.4	6.7	6.2	7.0	6.4	5.9
	20 %	17.8	13.8	10.9	8.6	11.3	8.2	7.5	8.5	7.8	6.7
	30 %	19.7	15.4	12.4	10.8	12.9	10.3	8.9	10.7	10.0	8.4
50 °C	10 %	23.5	16.7	14.6	11.9	14.6	10.8	9.6	11.7	9.2	7.3
	20 %	27.9	19.4	16.3	14.6	16.9	13.9	11.0	15.2	12.9	8.7
	30 %	30.5	24.1	19.4	17.2	20.1	16.3	13.7	18.4	14.1	11.9

Table 4.11: Corrosion rates of over-aged (220 °C) sample with and without inhibitors at different temperatures.

Temperature	Acetic acid (vol %)	Corrosion rates (mpy) with and without inhibitors									
		0 ppm	BI			2-CH_3-BI			2-SH-BI		
			50 ppm	100 ppm	200 ppm	50 ppm	100 ppm	200 ppm	50 ppm	100 ppm	200 ppm
30 °C	10 %	3.2	2.8	2.5	2.2	2.6	2.4	2.0	2.5	2.1	1.7
	20 %	3.9	3.4	3.0	2.4	3.1	2.7	2.2	2.9	2.5	2.0
	30 %	4.3	4.0	3.8	2.7	3.8	3.0	2.5	3.4	2.6	2.3
35 °C	10 %	5.4	5.0	3.9	2.8	4.0	3.2	2.4	3.1	2.7	2.0
	20 %	6.2	5.3	4.2	3.0	4.7	3.9	2.8	3.9	3.3	2.6
	30 %	7.3	6.0	4.9	4.3	5.5	4.5	3.7	5.0	4.0	3.3
40 °C	10 %	8.5	5.3	4.6	3.9	4.1	3.7	3.2	3.9	3.4	3.0
	20 %	10.7	6.8	5.3	4.5	5.7	4.3	4.0	5.0	4.1	3.8
	30 %	13.6	10.7	7.0	6.1	8.2	5.8	5.4	6.9	5.5	4.5
45 °C	10 %	11.5	7.3	6.5	5.8	6.2	5.6	5.2	5.8	5.2	4.3
	20 %	13.8	8.6	7.4	6.6	7.5	6.4	5.9	6.5	6.2	5.1
	30 %	15.1	11.4	9.1	7.8	10.0	8.1	7.1	8.9	6.9	6.2
50 °C	10 %	18.3	9.6	8.7	7.3	8.2	7.0	5.7	7.0	6.1	5.0
	20 %	21.3	12.8	10.1	9.7	10.6	8.2	7.1	8.2	7.3	6.5
	30 %	24.9	16.9	13.6	11.8	15.1	11.8	9.8	13.4	10.2	8.2

Tafel plots obtained for varying acid concentration in the absence of inhibitors are displayed in Fig. 4.3- 4.20. Fig. 4.21- 4.29 represent Tafel plots for varying acid concentration in the presence of inhibitors. Similar plots were obtained for all experimental conditions from which corrosion rates were calculated.

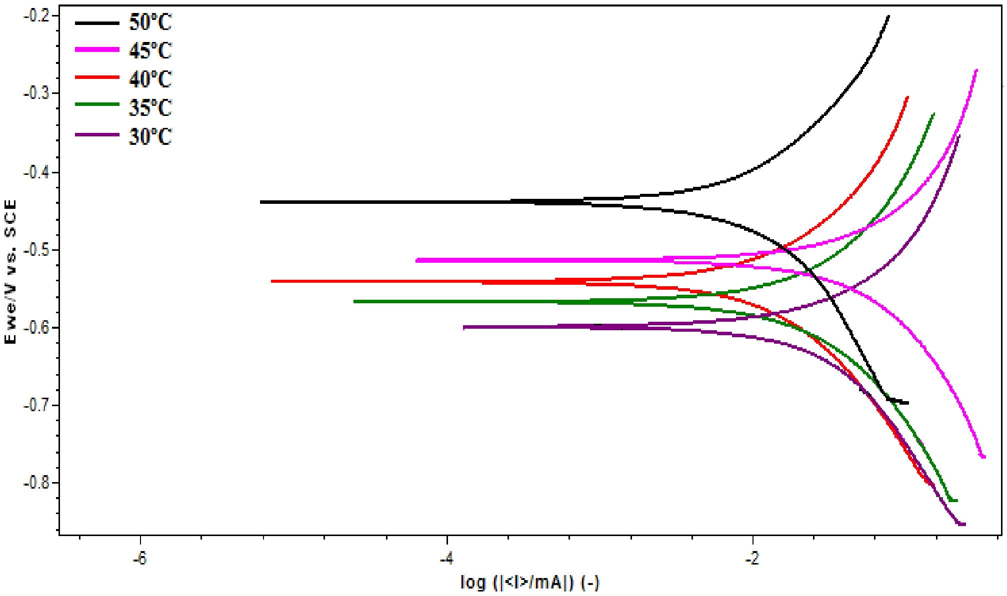

Fig.4.3: Tafel plots for under-aged (140 °C) samples in 10 % acetic acid

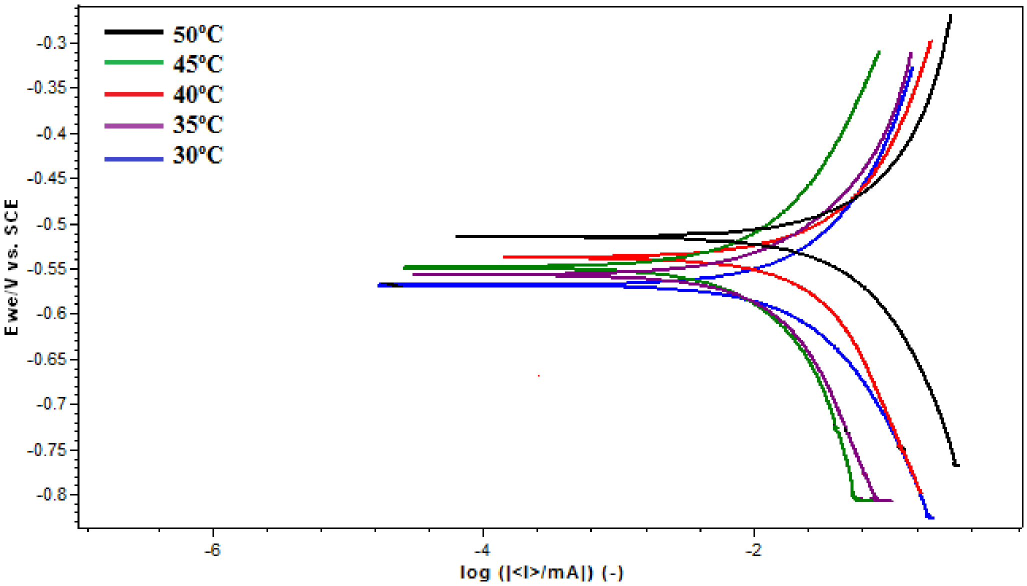

Fig.4.4: Tafel plots for under-aged (140 °C) samples in 30 % acetic acid

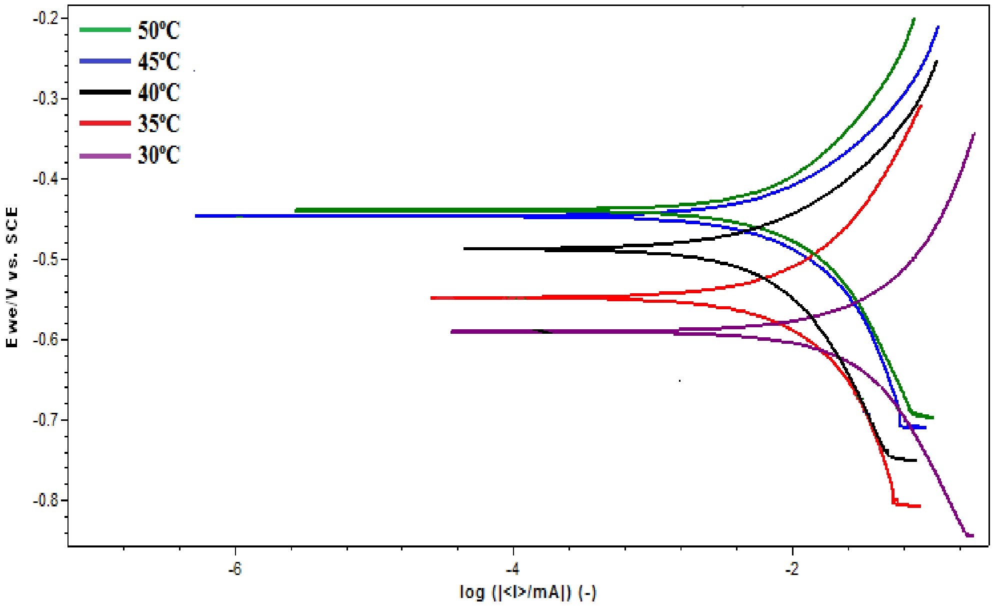

Fig.4.5: Tafel plots for peak-aged (140 °C) samples in 10 % acetic acid

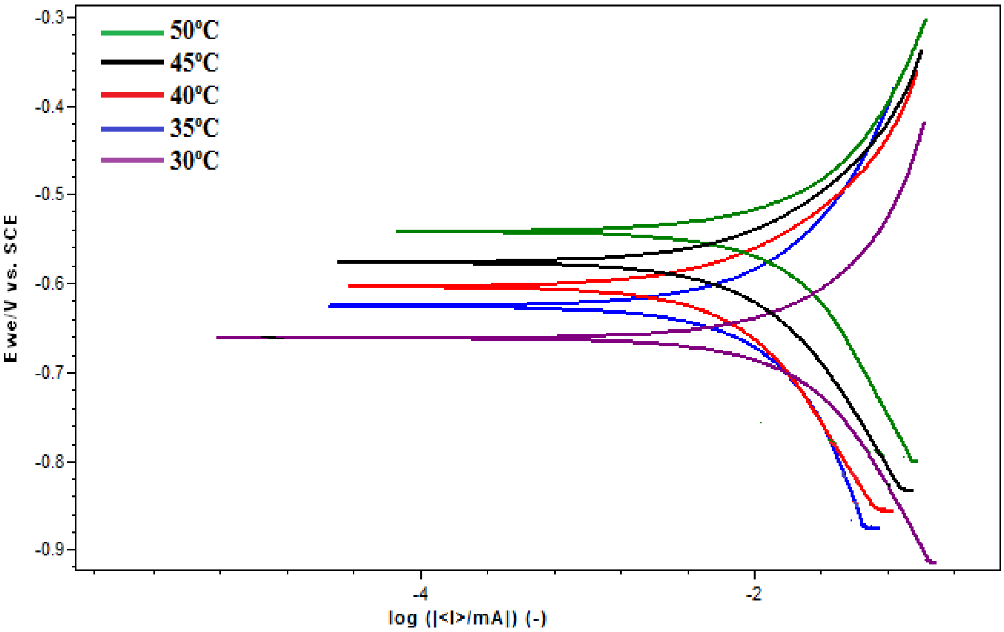

Fig.4.6: Tafel plots for peak-aged (140 °C) samples in 30 % acetic acid

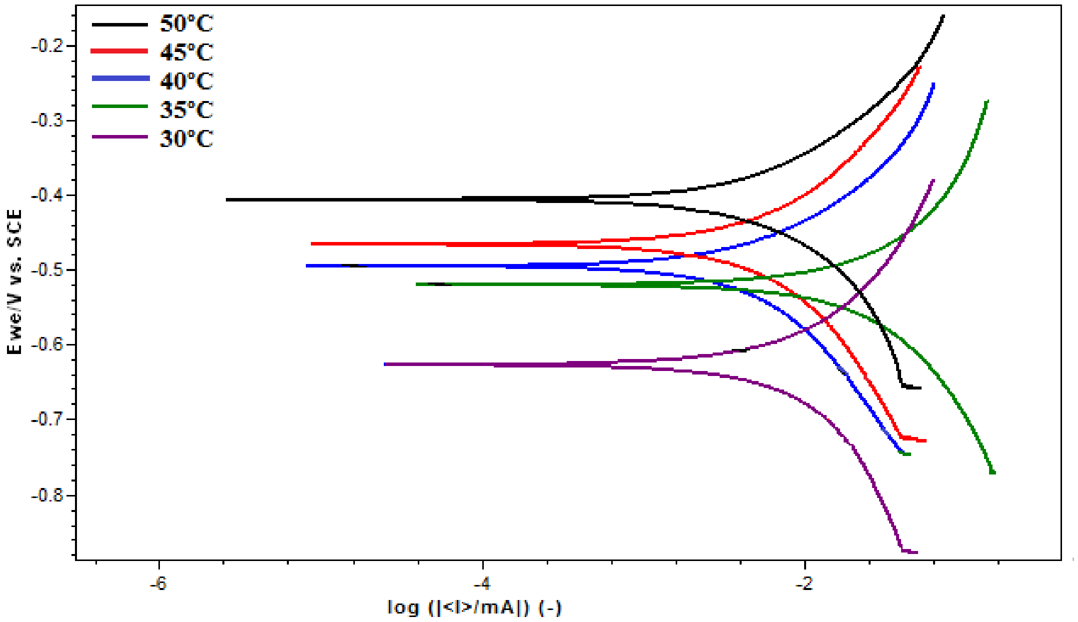

Fig.4.7: Tafel plots for over-aged (140 °C) samples in 10 % acetic acid

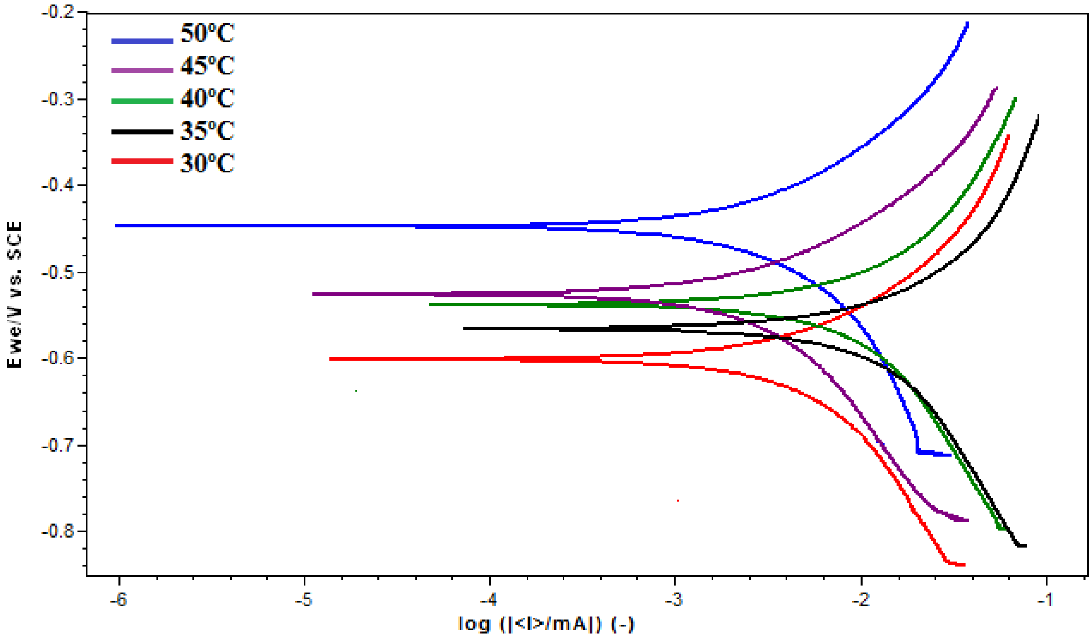

Fig.4.8: Tafel plots for over-aged (140 °C) samples in 30 % acetic acid

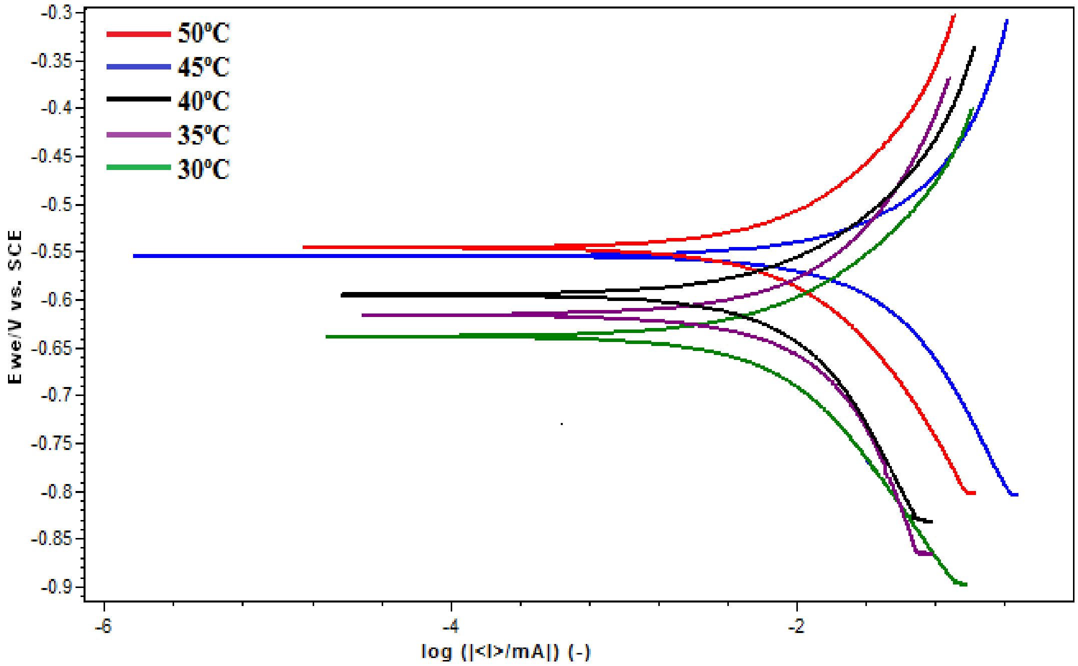

Fig.4.9: Tafel plots for under-aged (180 °C) samples in 10 % acetic acid

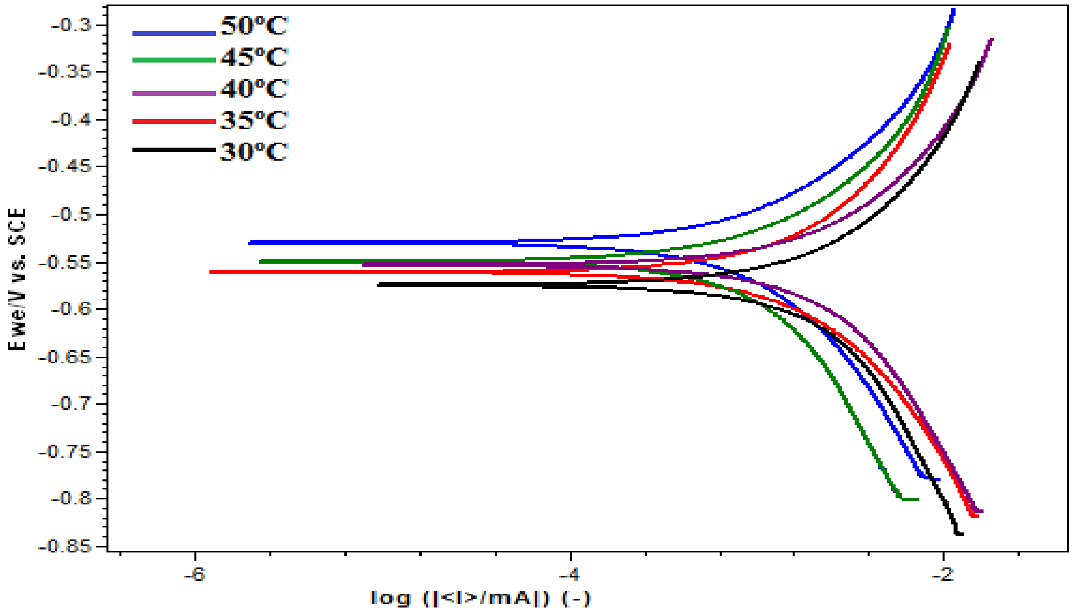

Fig.4.10: Tafel plots for under-aged (180 °C) samples in 30 % acetic acid

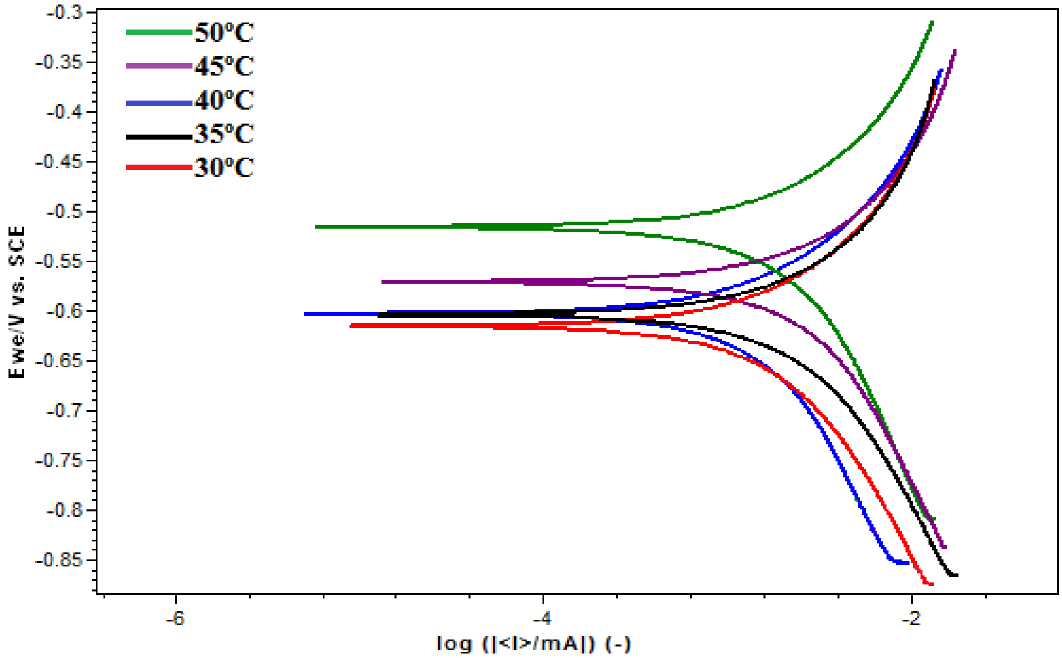

Fig.4.11: Tafel plots for peak-aged (180 °C) samples in 10 % acetic acid

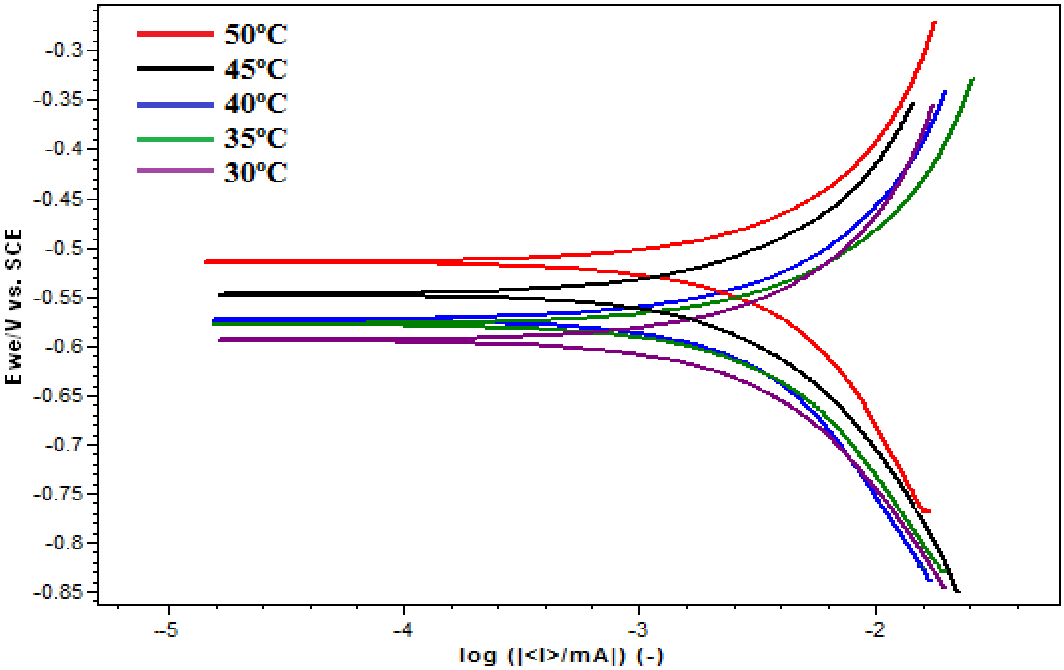

Fig.4.12: Tafel plots for peak-aged (180 °C) samples in 30 % acetic acid

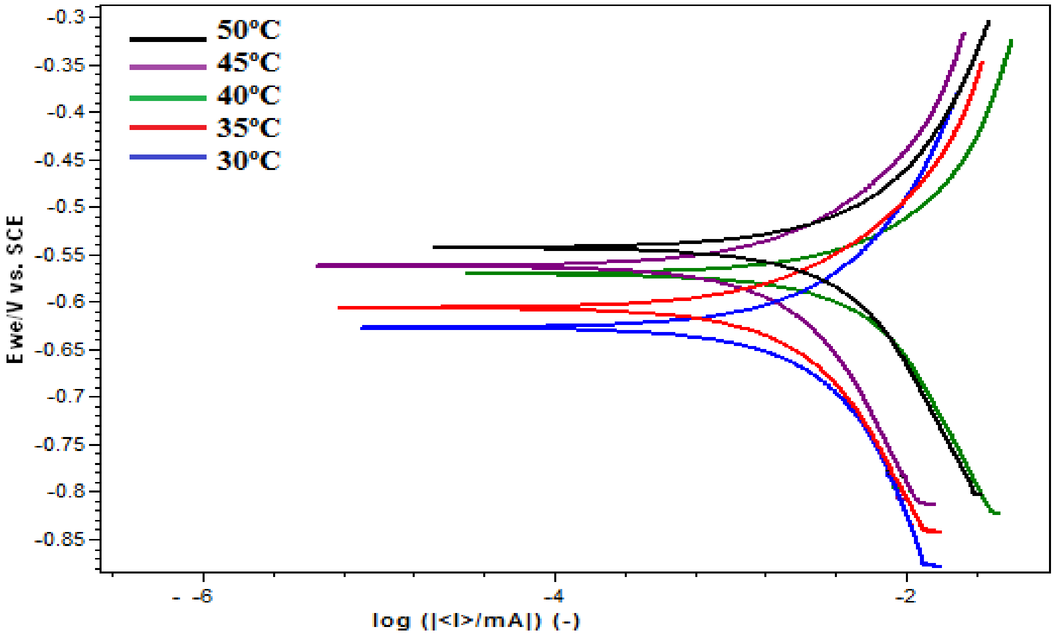

Fig.4.13: Tafel plots for over-aged (180 °C) samples in 10 % acetic acid

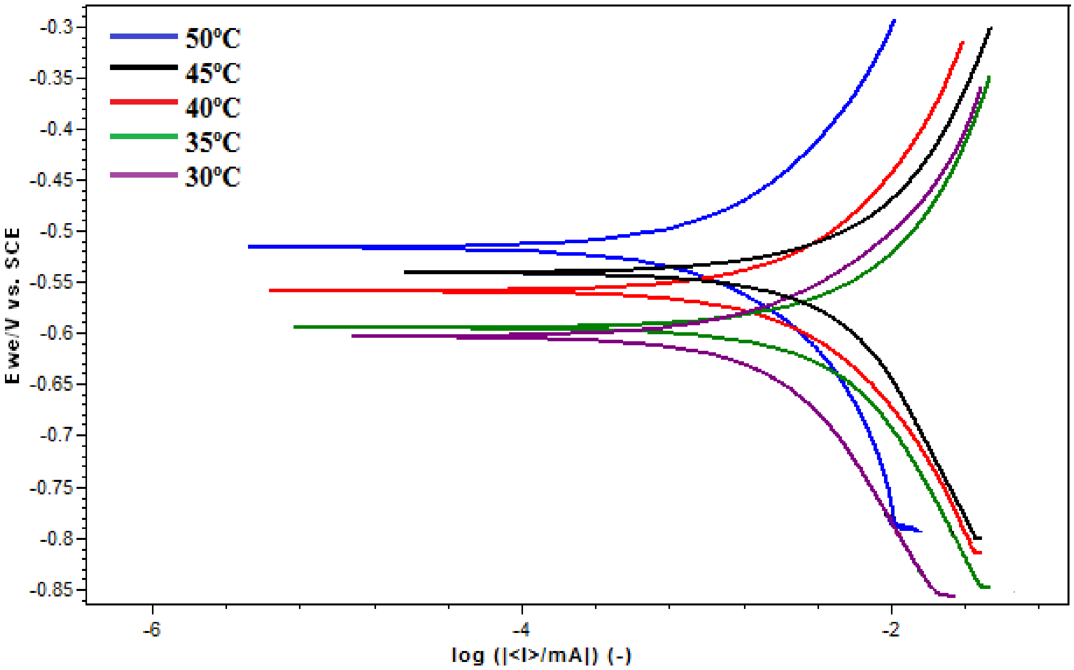

Fig.4.14: Tafel plots for over-aged (180 °C) samples in 30 % acetic acid

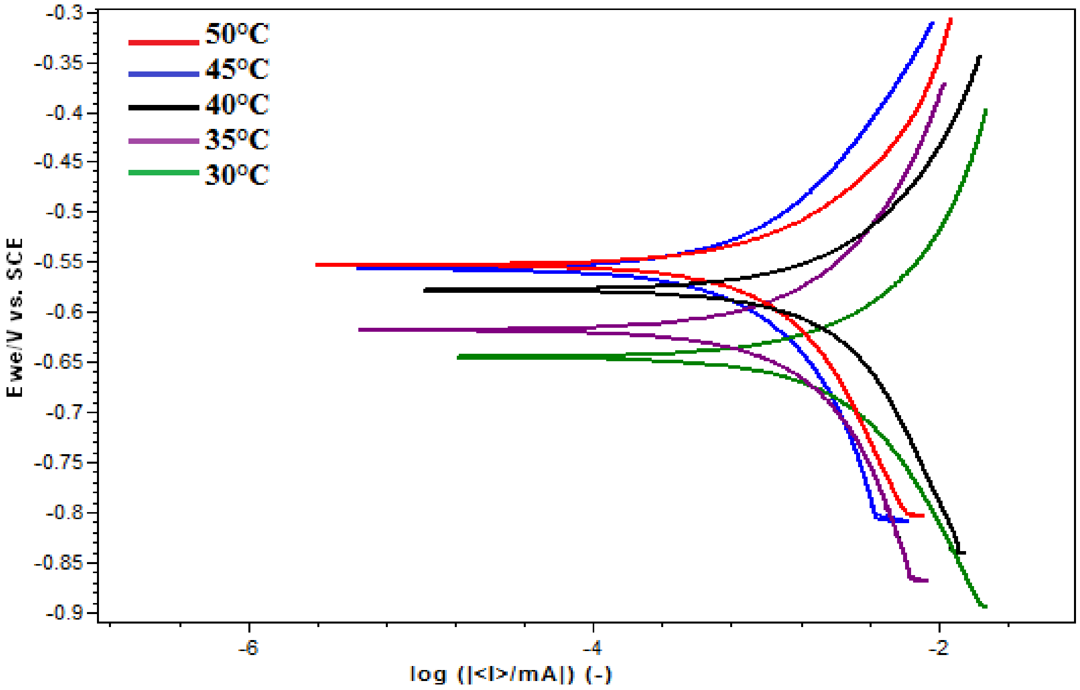

Fig.4.15: Tafel plots for under-aged (220 °C) samples in 10 % acetic acid

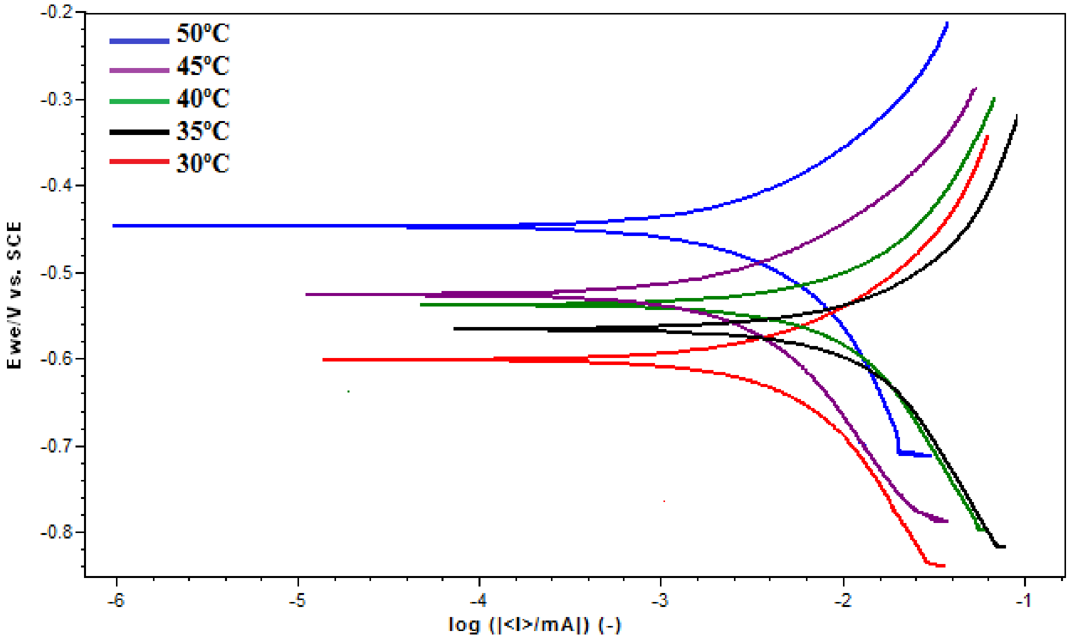

Fig.4.16: Tafel plots for under-aged (220 °C) samples in 30 % acetic acid

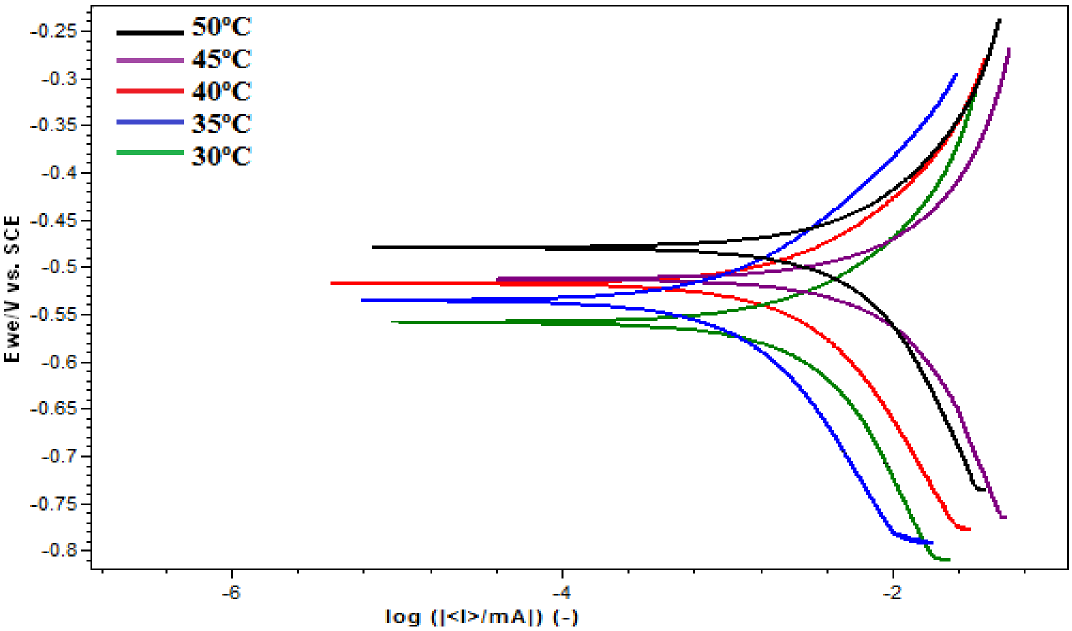

Fig.4.17: Tafel plots for peak-aged (220 °C) samples in 10 % acetic acid

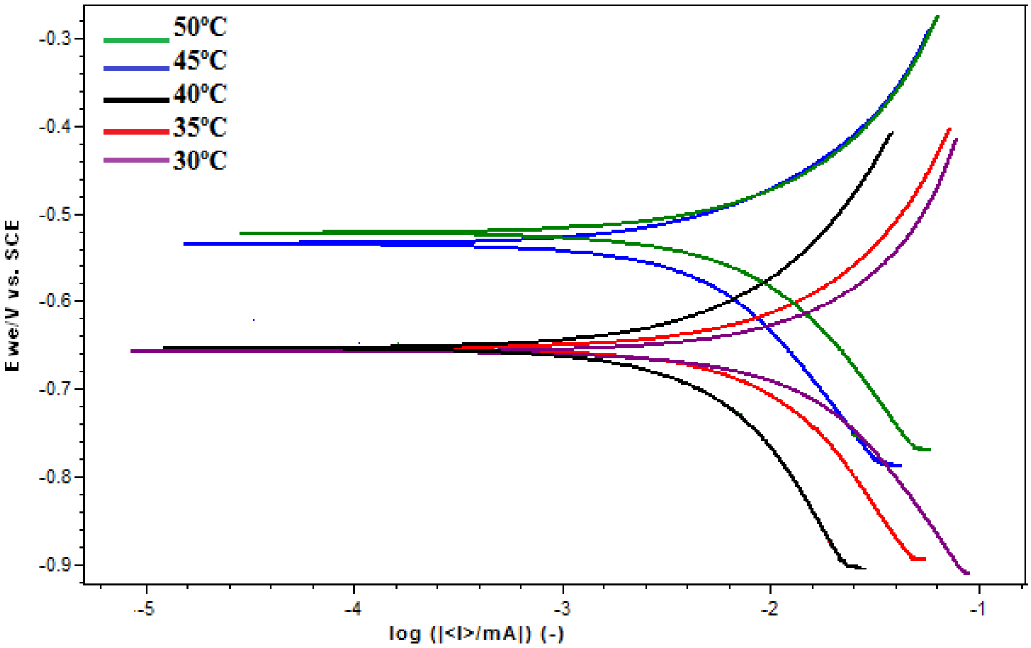

Fig.4.18: Tafel plots for peak-aged (220 °C) samples in 30 % acetic acid

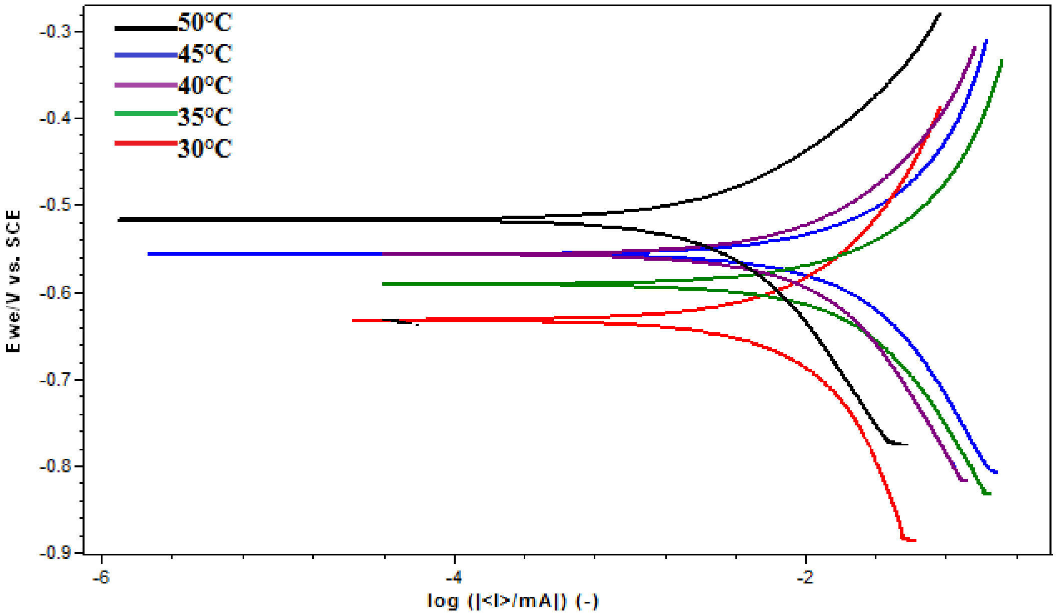

Fig.4.19: Tafel plots for over-aged (220 °C) samples in 10 % acetic acid

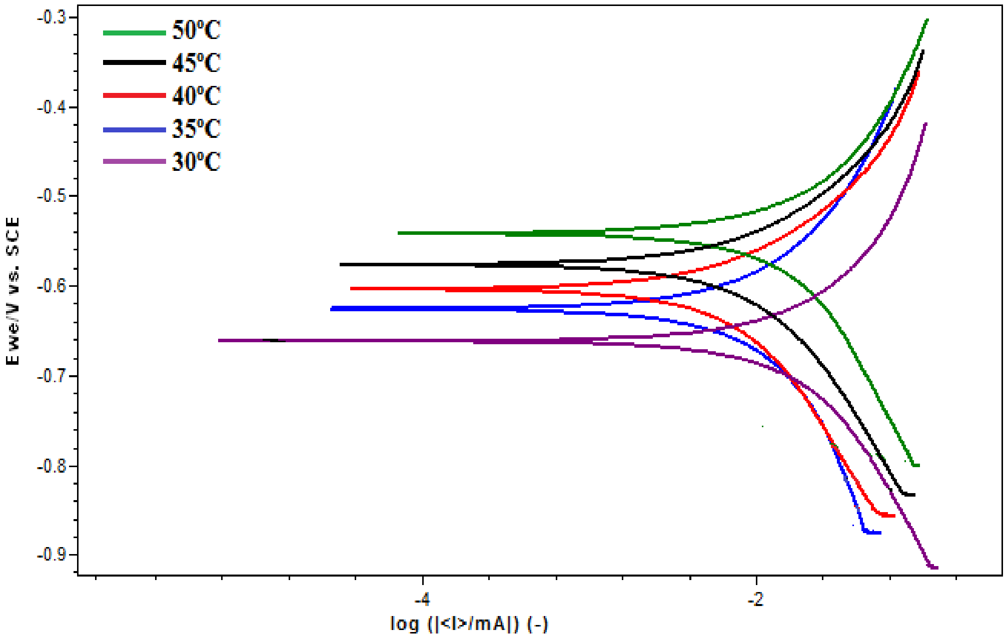

Fig.4.20: Tafel plots for over-aged (220 °C) samples in 30 % acetic acid

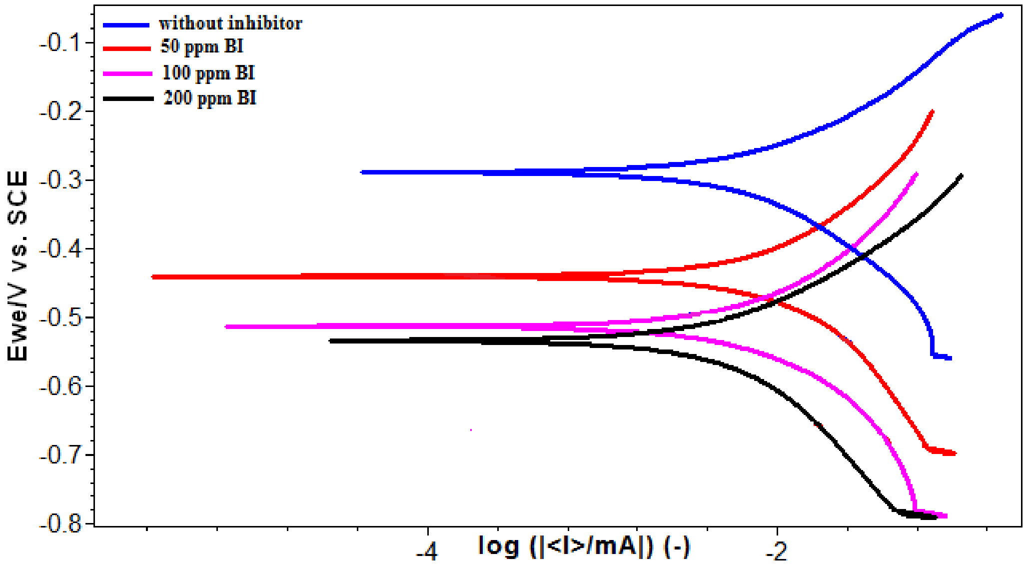

Fig.4.21: Tafel plots for under-aged (140 °C) samples in 10 % acetic acid at 30°C

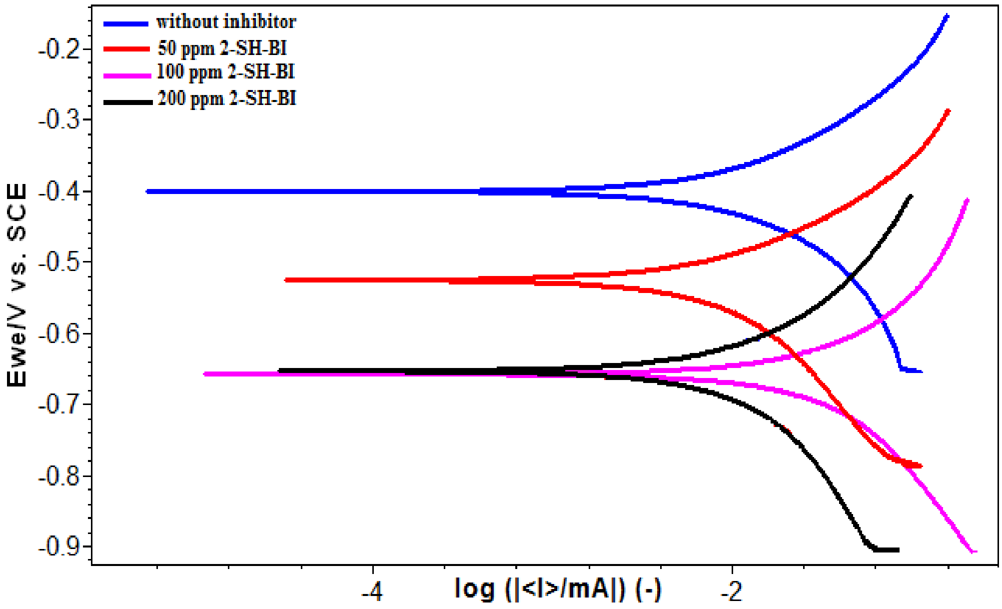

Fig.4.22: Tafel plots for under-aged (180 °C) samples in 10 % acetic acid at 30°C

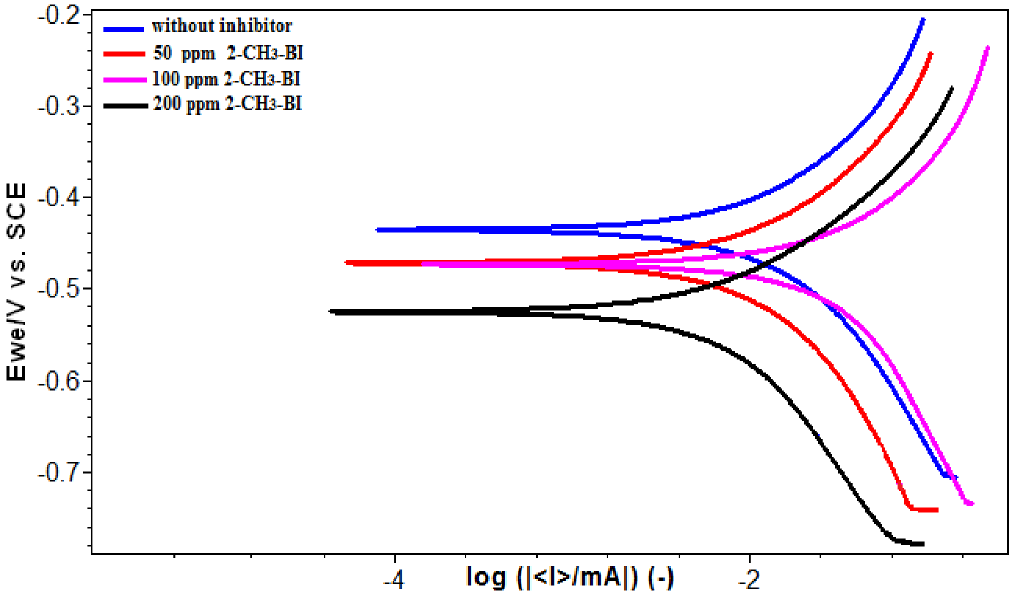

Fig.4.23: Tafel plots for under-aged (220 °C) samples in 10 % acetic acid at 30°C

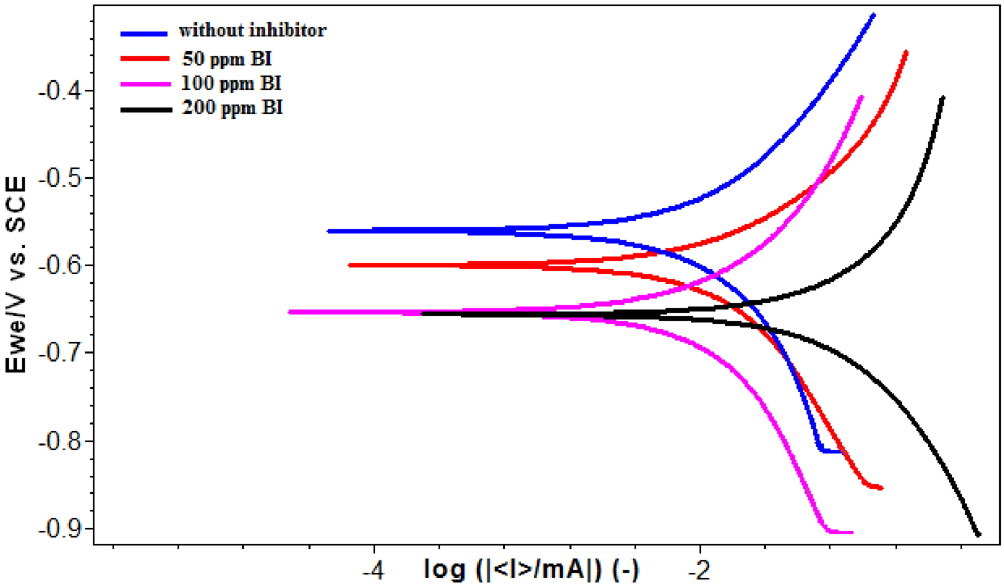

Fig.4.24: Tafel plots for peak-aged (140 °C) samples in 10 % acetic acid at 30°C

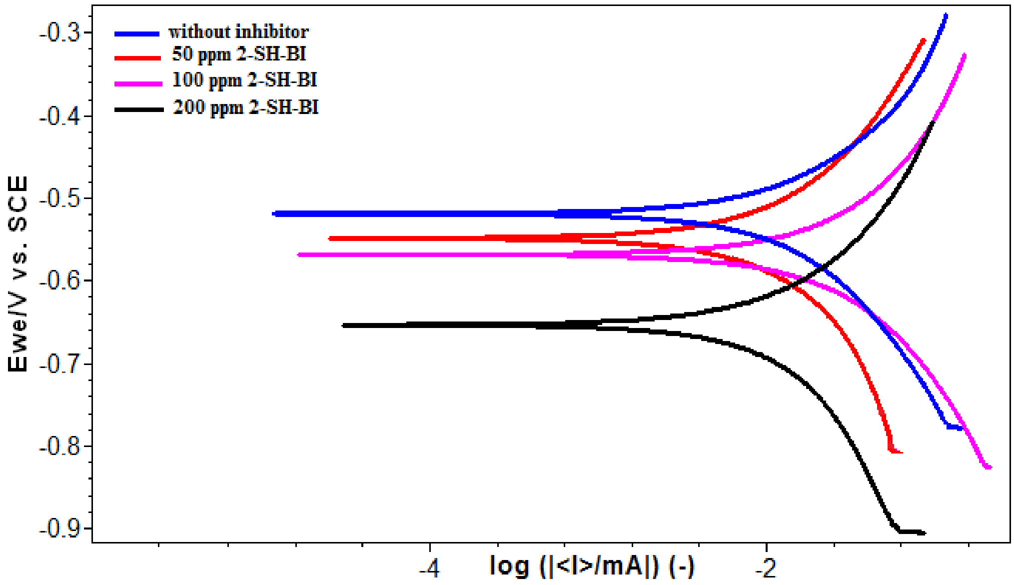

Fig.4.25: Tafel plots for peak-aged (180 °C) samples in 10 % acetic acid at 30°C

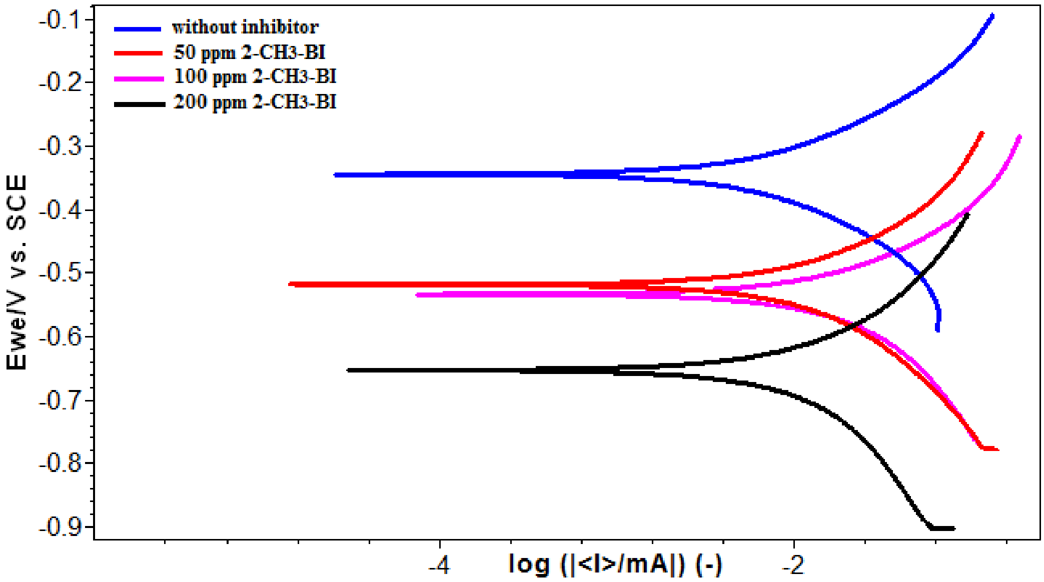

Fig.4.26: Tafel plots for peak-aged (220 °C) samples in 10 % acetic acid at 30°C

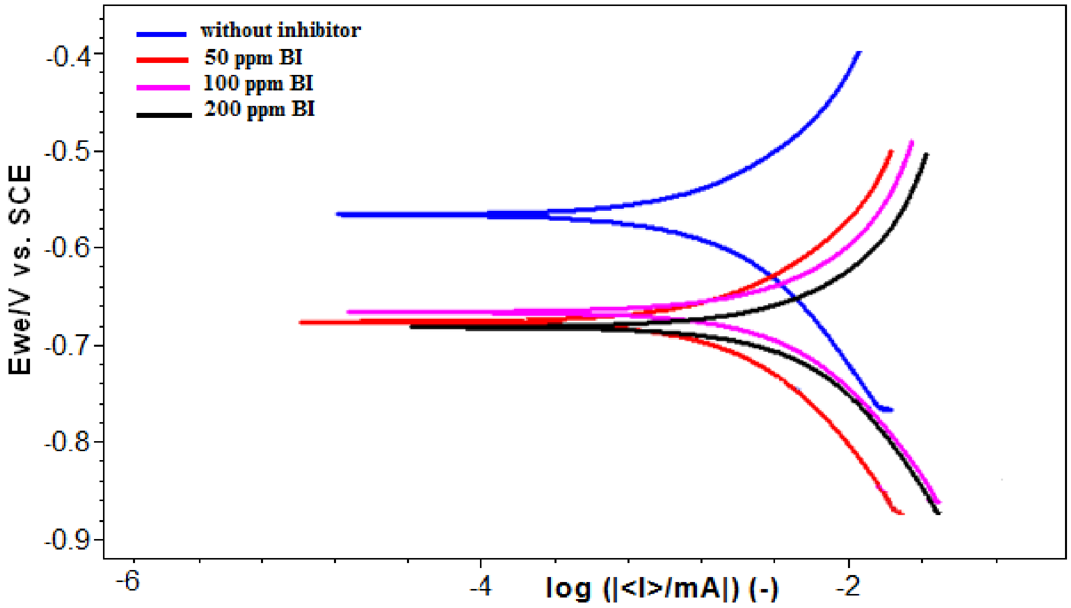

Fig.4.27: Tafel plots for over-aged (140 °C) samples in 10 % acetic acid at 30°C

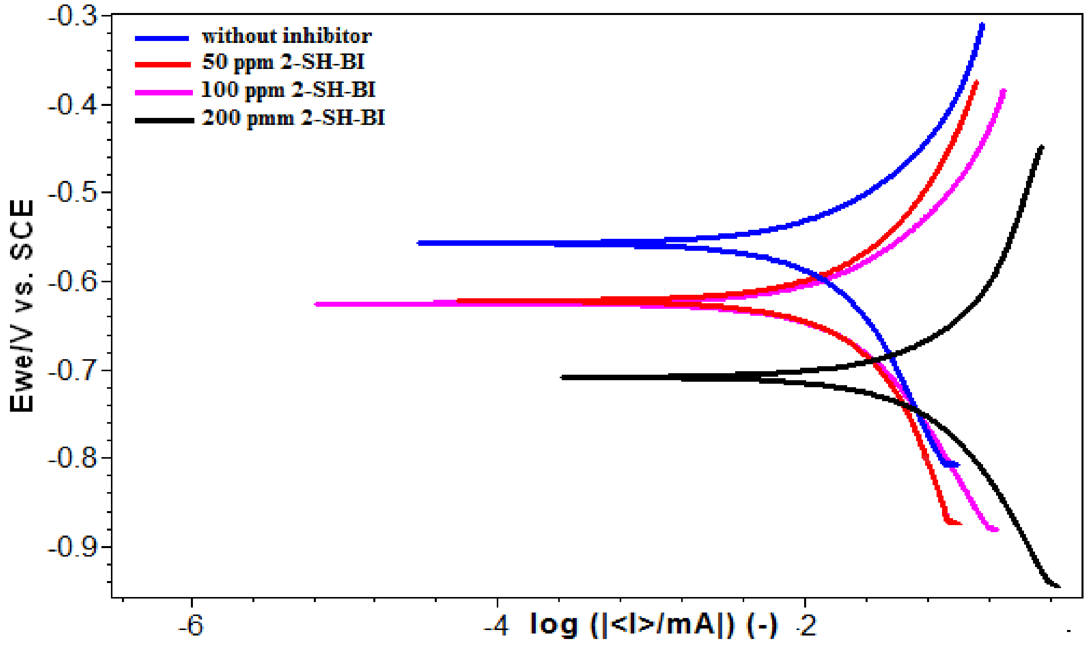

Fig.4.28: Tafel plots for over-aged (180 °C) samples in 10 % acetic acid at 30°C

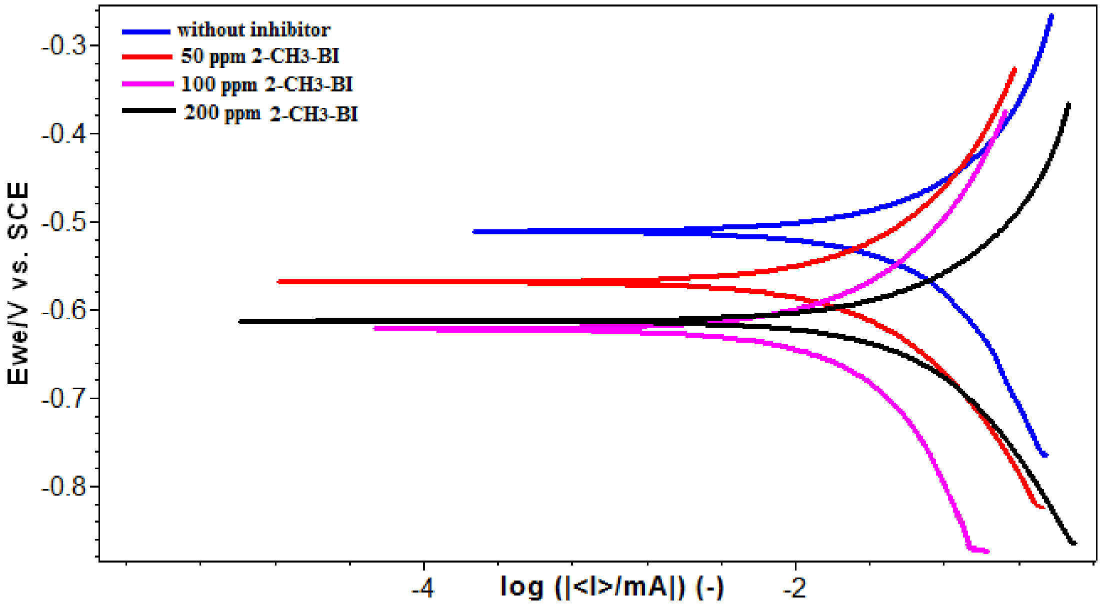

Fig.4.29: Tafel plots for over-aged (220 °C) samples in 10 % acetic acid at 30°C

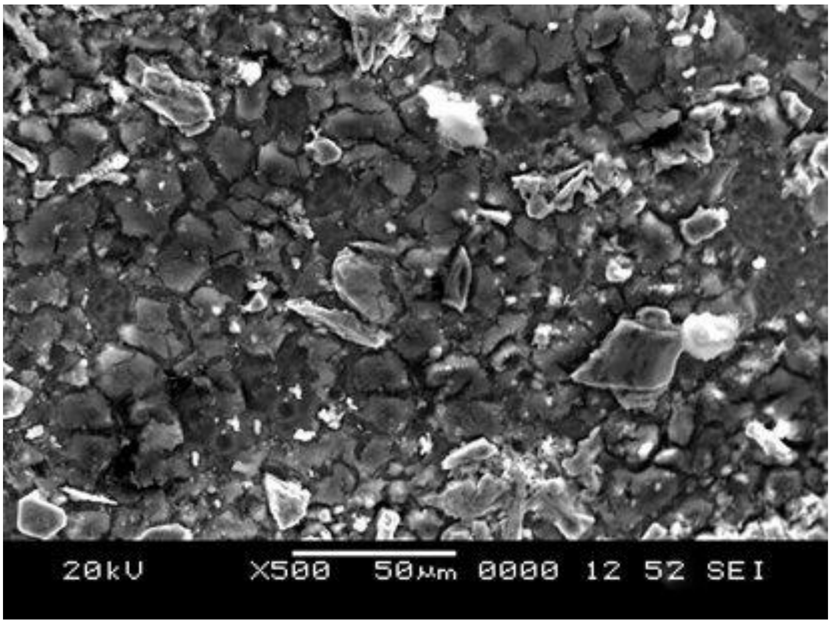

Fig.4.30: SEM image of corroded peak-aged (180 °C) sample in 30 % acetic acid at 50°C

Results indicate that 6061 Al-SiC composite testers are reasonably susceptible to corrosion even in lower concentrations of acetic acid. But its corrosion rate is comparatively higher at higher temperatures like 45°C and 50°C and in all three selected concentrations of acetic acid. The corrosion rate of the 6061 Al-SiC increased with increase in temperature. It is possibly because of the increased kinetics of the reaction. As the acid concentration increased from 10 % to 30 %, corrosion rate showed an escalation, as more acidic ions were present and so, more number of metal ion dissolution took place which led to an increase in the corrosion rate. The increase in corrosion rate with temperature may be attributed to the increase in the conductivity of acetic acid solution at all concentrations tested [Singh and Gupta, 2000]. The severity of corrosion can be realised from Fig. 4.30.

Corrosion proneness of 6061 Al-SiC composite can be attributed to various reasons. A perusal of literature on the corrosion behaviour of MMCs have revealed that the occurrence of reinforcement may or may not affect corrosion resistance, depending not only on the metal-reinforcement combination but also on manufacturing process parameters. Studies also reveal that difference in coefficients of thermal expansion of reinforcement and the matrix, promote the generation of dislocations in the matrix near the interface during heating and cooling cycles, and a high dislocation density can lead to a higher corrosion rate [Arsenault R. J, 1991 and Shimizu et al. 1995]. The interfacial attack on the sample peak-aged at 180°C, when exposed to 20 % acetic acid at 40°C, is displayed in Fig. 4.31. The difference in the thermal expansion coefficient of the aluminium matrix and SiC particle and the interfacial reaction during aging treatment might have led to an increase in dislocation density in the interfacial region between the matrix and the reinforcement and hence the corrosion attack occurred. Also, as SiC is cathodic to Al alloy matrix, there is vast possibility for galvanic corrosion attack.

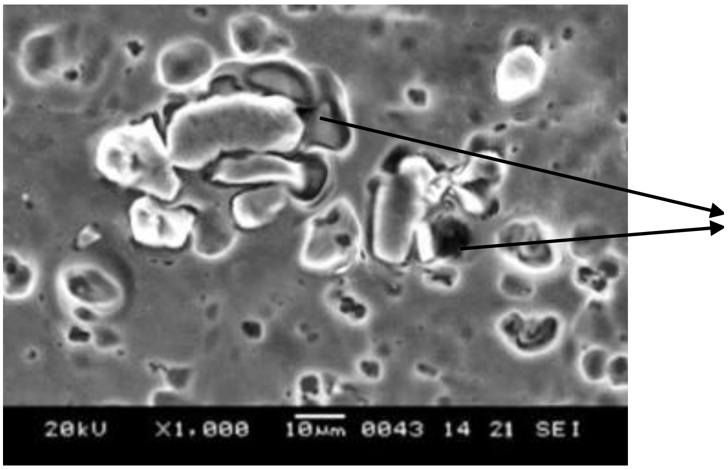

Fig.4.31: SEM image of interfacial attack on peak-aged (180 °C) sample in 20 % acetic acid at 40°C

But, the corrosion resistance of the composite is adversely affected by the existence of second phase particles. Corrosion feature of the matrix, i.e. Al 6061 alloy, is influenced by the chemistry, dimension and distribution of intermetallic precipitates formed during heat treatments. So it is essential to concentrate on the second phase particles than reinforcement to understand the corrosion characteristic of the composite [Shimizu et al. 1995].

Studies on corrosion behaviour of aluminium alloys have shown that intermetallic particles present in microstructure would significantly increase the corrosion proneness. The corrosion performance of these intermetallic and second phase particles are determined mainly by their redox potential with respect to the matrix. Research on particle-induced corrosion points out that, particles can either be nobler or more active with respect to the alloy matrix. Particles that are nobler than the matrix act as cathodes. Cathodic particles support matrix dissolution, whereas anodic particles are likely to dissolve and consequently localized corrosion would advance. During corrosion, because of the dissolution of a particular constituent element from the anodic particles and redeposition of cathodic elements on the surface of the alloy, the electrochemical nature of the precipitates may change during corrosion. Certain studies on the corrosion of aged 6061 Al alloy advocated that at the commencement of corrosion process, second phase particles like Mg_2Si as in the present work is anodic to Al base. However, during the continuation of corrosion process, active Mg is favorably dissolved and hence enrichment of Si occurs which makes Mg_2Si potential, change to a positive direction. As a result of which the corroded Mg_2Si turn out to be cathodic to Al matrix, causing the anodic dissolution and corrosion of Al at a later stage. Hence most precipitates are likely to act cathodically.

It was also reported that 6xxx series Al alloys are susceptible to intergranular corrosion (IGC) when these were subjected to aging treatments. IGC of 6xxx Al alloys is the consequence of microgalvanic cell action at the grain boundary, associated with second phase particles, which are either more active or noble than the adjacent aluminium matrix. The susceptibility of 6061 Al alloy is purely centered on the mole ratio of Mg to Si and presence of Cu. 6061 Al alloy with Mg/Si ratio higher than 1.73 are not sensitive to intergranular corrosion as the Mg_2Si precipitates are dispersed discontinuously at the grain boundary and so there would be no continuous corrosion network. 6061 Al alloy with Cu content < 0.12 wt% is slightly prone to IGC, but water quenched samples with high Cu content were basically impervious to IGC. In this work, as the mole ratio of Mg/Si is greater than 1.73 for the sample and they are all water quenched, the possibility of the occurrence of IGC can be ruled out [Nikseresht et al. 2010, Zeng et al. 2011 and Menshawy et al. 2012]

In the current study, corrosion tests were conducted on samples which were aged at 140°C, 180°C, and 220 °C. It is clear from Table 3.3. that composites aged at 180 °C has high hardness and it can be considered as peak-aging temperature, 140 °C as under-aging temperature and 220 °C as over- aging temperature. The samples aged at these temperatures were again classified as under-aged, peak-aged and over-aged based on the time of aging at those particular temperatures. Based on this thought, the variation in the corrosion rates at these temperatures can be understood.

In under-aged samples, the formation of second phase particles like β'' (needle-shaped Mg_2Si) takes place initially, which will increase the volume fraction of cathodic particles within the specimen and as a result cathodic reaction rate will be enhanced which make composite prone to corrosion. Successively, the anodic reaction will be derived at a higher rate leading to higher Icorr values with aging time. At peak aging temperature, it is expected that more and more fresh cathodic particles are swiftly reached by the corroding zone around these particles and this will contribute to the more rapid dissolution rate of the matrix. This is the reason why peak-aged samples have higher corrosion rates than the other two. During over-aging, coarsening of those precipitates happens, thus reducing the electrochemical potential difference between the matrix and depleted zone. The coarsening process will decrease the cathodic reaction sites and so Icorr value decreases than that obtained for under-aged samples. This justification is examined true from the values shown in Table 4.3 to Tables 4.11 where corrosion rates are higher for peak-aged samples and much lower for over-aged samples. Thus, the corrosion of the sample used in the present study is due to various reasons of which the presence of second phase particles are more significant, even though interfacial attack and presence of acetic acid ions also contribute to the corrosion rate of the samples. Its also to be noted that corrosion rates were drastically reduced after the addition of three different inhibitors such as benzimidazole, 2-methylbenzimidazole, and 2-mercaptobenzimidazole. The inhibition mechanism of these inhibitors is discussed in the next chapter.

4.3. Conclusions

- A rapid increase in the corrosion rate with increase in the concentration of acetic acid was observed till it reached a maximum at 30 %. Further increase in the concentration of acetic acid resulted in the reduction of the corrosion rate.
- Corrosion rate of the 6061 Al-SiC increased with increase in temperature
- The interfacial attack between the Al matrix and silicon carbide particles was prominent.
- Peak-aged samples were more corrosion prone while over- aged samples were minimally corroded.
- The addition of inhibitors showed a marked reduction in corrosion rates.

CHAPTER 5

INHIBITION EVALUATION OF BI, 2−CH_3−BI AND 2−SH−BI

5.1. Experimental work

As discussed in chapter four, inhibitors selected for this study are benzimidazole (BI), 2-methylbenzimidazole (2-CH_3-BI) and 2-mercaptobenzimidazole (2-SH-BI). In Tables 4.3-4.11, corrosion rates showed a noticeable drop after the addition of inhibitors to the experimental environment. To evaluate the potentiality of these inhibitors, there are certain factors which are to be taken into account for. The ability of the inhibitor molecule to get adsorbed on to the sample surface and its surface coverage on the sample are a few among significant factors. The surface coverage (θ) of an inhibitor is calculated as, $\theta = \{icorr - icorr\ (inh)\}/\ icorr$ where, icorr is the corrosion current density in the absence of inhibitor and icorr (inh) is the corrosion current density in the presence of inhibitor. The effectiveness of inhibitors is found out by calculating the percentage of inhibition. The percentage inhibition efficiency (IE) = $\theta \times 100$. Thermodynamical factors for inhibition reactions are crucial in understanding the mechanism of inhibition. Below given are the approaches for finding thermodynamic parameters.

Activation energy (Ea) for the corrosion processes of Al-SiC samples in varying concentrations of acetic acid at different temperatures was calculated from the Arrhenius equation, $\ln (CR)= B-(Ea/RT)$, CR being the corrosion rate for the process.

where, B is a constant which depends on the metal type, and R is the universal gas constant. The plot of ln (CR) vs. reciprocal of absolute temperature (1/T) gives a straight line whose slope is -Ea/R, from which the activation energy values for the corrosion process were calculated.

The enthalpy of activation ($\Delta H\#$) and entropy of activation ($\Delta S\#$) values for the corrosion process was calculated from transition state theory equation,

$CR = (RT/Nh) \exp (\Delta S\#/R) \exp (-\Delta H\#/RT)$ where h is Planck’s constant, and N is Avogadro’s number and R is the universal gas constant.

A plot of ln (CR/T) vs. (1/T) gives a straight line with slope is -ΔH#/R and intercept are ln (RT/Nh) + (ΔS#/R).

Free energy of adsorption of inhibitor was calculated using the following relation, $\Delta G_{ads} = -RT \ln [55.5 \times \theta/C\ (1-\theta)]$ where, ΔG_{ads} is the free energy of adsorption (KJ/mol), R is universal gas constant, T is temperature (K), C is concentration of inhibitor (mol/dm^3) and θ is surface coverage of inhibitor molecules.

5.2. Results and Discussion

Tables 5.1-5.9 display inhibition efficiency (%) of inhibitors BI, 2-CH_3-BI, and 2-SH-BI in all experimental conditions. Figures 5.1-5.9 depicts Arrhenius plots and figures 5.10-5.18 illustrate plots of ln (CR/T) vs. (1/T) for under-aged samples at different acetic acid concentrations. As the nature of graphs was same, plots for peak-aged and over-aged samples are not incorporated in this thesis. But values of activation energy, enthalpy, and entropy for all experimental factors were calculated from the plots and are exhibited in Tables 5.10-5.18. Standard free energy (ΔG#) values are presented in tables 5.19-5.27 and free energy of adsorption (ΔGads) values are showed in tables 5.28-5.36. Adsorption isotherms of three inhibitors for under-aged samples in 10% acetic acid at 30°C are portrayed in Fig. 5.19-5.21.

It is evident from tables 5.1-5.9 that selected inhibitors provide reasonable inhibition efficiency throughout all experiments. The lowest efficiency value obtained is 6.3% for under-aged (220°C) in the presence of 50 ppm of BI at 30°C in 30 (vol %)and the same value was obtained for peak-aged sample (220°C) in the presence of 50 ppm of BI at 35°C and 10 (vol %) respectively. The highest percentage of efficiency achieved is 74.8% for 200 ppm of 2-SH-BI for an over-aged (140°C) sample at 50°C in 10 vol % of acetic acid. It should be noted that as the acid concentration got increased to 30 vol %, inhibition efficiency was scaled down as large number of acid ions were present to accelerate the corrosion mechanism. No definite trend was observed in the change of inhibition efficiency of three inhibitors, suggesting that these compounds behave as mixed-type inhibitors. For further elucidating the inhibition mechanism, thermodynamical parameters are taken into consideration.

Table 5.1: % Inhibition efficiency (IE) of BI on under-aged samples

Under-aged at	Temperature	Acetic acid (vol %)	Inhibition Efficiency (%) of BI		
			50 ppm	100 ppm	200 ppm
140 °C	30 °C	10	13.3	22.2	28.8
		20	17.5	31.5	38.5
		30	11.3	22.6	35.5
	35 °C	10	15.0	16.7	26.7
		20	18.0	22.2	30.6
		30	16.7	29.8	38.1
	40 °C	10	34.3	49.0	55.0
		20	48.7	61.3	64.7
		30	27.5	50.6	55.1
	45 °C	10	42.2	45.6	51.0
		20	45.6	52.8	55.6
		30	29.6	43.9	52.9
	50 °C	10	43.9	51.0	58.5
		20	46.1	52.7	59.3
		30	30.4	41.8	55.2
180 °C	30 °C	10	12.5	25.0	29.6
		20	13.4	25.4	31.3
		30	11.3	20.8	29.6
	35 °C	10	7.60	12.1	19.7
		20	10.1	15.0	21.3
		30	6.50	12.0	18.5
	40 °C	10	20.7	25.0	30.2
		20	23.3	25.8	37.1
		30	11.9	17.1	29.0
	45 °C	10	7.80	13.1	22.2
		20	11.2	14.7	37.1
		30	14.3	18.1	37.6
	50 °C	10	19.2	20.8	37.2
		20	20.1	22.5	40.6
		30	23.4	26.8	43.1
220 °C	30 °C	10	10.3	20.5	35.9
		20	14.3	23.8	38.1
		30	6.30	19.1	38.3
	35 °C	10	10.3	29.3	48.2
		20	12.1	31.8	50.0
		30	10.4	24.7	39.1
	40 °C	10	31.0	43.7	50.6
		20	49.3	62.7	65.6
		30	22.5	47.0	49.0
	45 °C	10	37.8	42.5	48.8
		20	43.0	49.4	54.4
		30	26.3	42.7	51.5
	50 °C	10	41.7	48.6	56.9
		20	41.6	50.2	56.8
		30	21.8	36.8	53.8

Table 5.2: % Inhibition efficiency (IE) of BI on peak-aged samples

Peak-aged at	Temperature	Acetic acid (vol %)	Inhibition Efficiency (%) of BI		
			50 ppm	100 ppm	200 ppm
140 °C	30 °C	10	20.7	32.8	39.7
		20	21.7	30.4	40.6
		30	17.1	26.3	35.5
	35 °C	10	13.0	23.2	30.4
		20	8.60	19.8	30.9
		30	7.40	21.3	33.1
	40 °C	10	27.9	41.1	54.3
		20	28.2	35.6	59.2
		30	22.8	33.3	50.8
	45 °C	10	28.3	41.0	54.3
		20	24.1	40.7	53.8
		30	19.0	34.9	44.7
	50 °C	10	18.4	38.1	50.8
		20	17.6	35.5	48.5
		30	20.3	33.4	45.6
180 °C	30 °C	10	16.6	26.9	35.9
		20	13.2	25.3	35.2
		30	14.0	25.2	36.4
	35 °C	10	15.2	27.2	34.8
		20	14.9	25.2	33.6
		30	16.1	16.1	37.1
	40 °C	10	21.2	31.4	35.8
		20	12.9	24.7	33.1
		30	14.3	21.6	36.8
	45 °C	10	9.90	18.8	28.7
		20	13.5	23.5	35.8
		30	11.4	21.2	34.3
	50 °C	10	13.9	25.4	39.7
		20	10.9	23.7	37.5
		30	15.2	25.0	39.9
220 °C	30 °C	10	18.9	32.1	45.3
		20	21.9	29.7	42.2
		30	15.7	25.7	35.7
	35 °C	10	6.30	22.2	34.9
		20	6.60	21.1	31.6
		30	11.2	23.6	33.7
	40 °C	10	13.9	39.6	48.5
		20	38.8	52.1	61.2
		30	25.8	44.1	52.2
	45 °C	10	30.6	41.5	52.4
		20	22.5	38.8	51.7
		30	21.8	37.1	45.2
	50 °C	10	28.9	37.9	49.4
		20	30.5	41.6	47.7
		30	20.9	36.4	43.6

Table 5.3: % Inhibition efficiency (IE) of BI on over-aged samples

Over-aged at	Temperature	Acetic acid (vol %)	Inhibition Efficiency (%) of BI		
			50 ppm	100 ppm	200 ppm
140 °C	30 °C	10	12.5	20.0	30.0
		20	15.4	30.8	40.4
		30	12.1	24.1	38.0
	35 °C	10	15.8	24.6	33.3
		20	18.1	24.2	33.3
		30	13.1	30.1	36.4
	40 °C	10	37.4	47.3	52.7
		20	41.2	53.8	58.1
		30	22.1	50.3	55.9
	45 °C	10	37.7	45.1	50.0
		20	39.6	47.7	53.7
		30	27.6	41.1	48.5
	50 °C	10	47.1	56.3	62.1
		20	45.2	54.8	60.1
		30	29.2	42.0	52.7
180 °C	30 °C	10	10.5	22.8	33.3
		20	11.3	22.6	33.9
		30	11.8	25.0	30.8
	35 °C	10	6.70	16.7	23.3
		20	9.50	16.2	24.3
		30	9.30	16.3	20.9
	40 °C	10	19.4	25.0	30.6
		20	21.2	26.7	35.6
		30	10.2	18.7	32.6
	45 °C	10	10.6	15.6	24.1
		20	8.60	15.5	35.6
		30	12.2	17.8	37.1
	50 °C	10	17.7	21.1	39.2
		20	18.5	22.0	38.6
		30	20.1	23.5	41.6
220 °C	30 °C	10	12.5	21.9	31.2
		20	12.8	23.1	38.5
		30	7.00	11.6	37.2
	35 °C	10	7.40	27.7	48.1
		20	14.5	32.2	51.6
		30	17.8	32.9	41.1
	40 °C	10	37.6	45.9	54.1
		20	36.4	50.5	57.9
		30	21.3	48.5	55.1
	45 °C	10	36.5	43.5	49.6
		20	37.7	46.4	52.2
		30	24.5	39.7	48.3
	50 °C	10	47.5	52.5	60.1
		20	39.9	52.6	54.5
		30	32.1	45.4	52.6

Table 5.4: % Inhibition efficiency (IE) of 2-CH_3-BI on under-aged samples

Under-aged at	Temperature	Acetic acid (vol %)	Inhibition Efficiency (%) of 2-CH_3-BI		
			50 ppm	100 ppm	200 ppm
140 °C	30 °C	10	22.2	31.1	40.0
		20	26.3	38.6	49.1
		30	17.7	29.0	42.0
	35 °C	10	21.7	28.3	46.7
		20	26.4	32.0	45.8
		30	21.2	33.3	42.9
	40 °C	10	39.2	52.0	56.9
		20	51.3	62.7	65.3
		30	36.5	51.1	55.6
	45 °C	10	49.7	53.7	55.8
		20	50.6	55.1	61.2
		30	34.4	44.4	55.6
	50 °C	10	49.7	59.3	68.0
		20	50.9	56.8	66.6
		30	35.9	51.3	60.8
180 °C	30 °C	10	21.9	28.1	34.4
		20	17.9	23.9	29.9
		30	19.1	25.3	31.1
	35 °C	10	12.1	15.2	24.2
		20	12.5	16.3	26.3
		30	12.0	17.4	22.8
	40 °C	10	24.1	28.4	33.6
		20	32.1	35.8	39.1
		30	22.8	26.9	42.5
	45 °C	10	17.1	20.3	24.2
		20	32.1	35.0	40.1
		30	33.3	35.2	41.9
	50 °C	10	30.4	34.0	44.4
		20	32.8	33.9	38.3
		30	32.4	35.5	43.1
220 °C	30 °C	10	17.9	33.3	41.0
		20	16.7	30.9	42.9
		30	14.9	34.0	42.6
	35 °C	10	15.5	37.9	50.0
		20	13.6	36.4	53.0
		30	20.8	35.1	46.8
	40 °C	10	37.9	50.6	56.3
		20	52.1	65.5	69.7
		30	32.5	50.3	54.3
	45 °C	10	45.7	51.9	55.9
		20	49.4	53.2	61.4
		30	31.6	42.7	55.1
	50 °C	10	46.3	57.8	67.4
		20	48.1	54.7	64.2
		30	30.8	49.2	57.9

Table 5.5: % Inhibition efficiency (IE) of 2-CH_3-BI on peak-aged samples

Peak-aged at	Temperature	Acetic acid (vol %)	Inhibition Efficiency (%) of 2-CH_3-BI		
			50 ppm	100 ppm	200 ppm
140 °C	30 °C	10	32.8	39.7	44.8
		20	31.9	39.1	43.5
		30	26.3	34.2	43.4
	35 °C	10	26.1	36.2	40.6
		20	23.5	34.6	42.1
		30	22.3	31.9	41.5
	40 °C	10	37.2	51.2	60.5
		20	42.1	55.2	65.5
		30	38.1	46.0	56.1
	45 °C	10	40.4	56.0	59.5
		20	38.2	55.8	59.3
		30	37.6	49.1	57.5
	50 °C	10	33.8	48.5	56.4
		20	33.2	47.2	55.5
		30	30.5	46.8	52.6
180 °C	30 °C	10	21.8	30.8	37.2
		20	23.1	31.9	38.5
		30	21.5	30.8	38.3
	35 °C	10	23.9	33.7	39.1
		20	22.4	30.1	40.2
		30	26.6	33.9	38.7
	40 °C	10	29.9	35.0	40.1
		20	28.7	35.3	40.4
		30	28.1	34.2	42.9
	45 °C	10	19.9	29.0	33.1
		20	29.7	34.9	43.2
		30	25.3	30.2	40.4
	50 °C	10	29.3	34.1	48.8
		20	25.0	34.9	43.9
		30	27.2	32.9	43.5
220 °C	30 °C	10	30.2	39.6	50.9
		20	29.7	39.1	45.3
		30	27.1	34.3	42.9
	35 °C	10	17.5	33.3	41.3
		20	21.1	34.2	35.5
		30	22.5	34.8	38.2
	40 °C	10	27.7	42.6	52.5
		20	46.1	57.6	65.5
		30	38.5	52.7	58.2
	45 °C	10	36.1	54.4	57.8
		20	36.5	53.9	57.9
		30	34.6	47.7	54.8
	50 °C	10	37.9	46.6	59.1
		20	39.4	50.2	60.6
		30	34.1	46.6	55.1

Table 5.6: % Inhibition efficiency (IE) of 2-CH_3-BI on over-aged samples

Over-aged at	Temperature	Acetic acid (vol %)	Inhibition Efficiency (%) of 2-CH_3-BI		
			50 ppm	100 ppm	200 ppm
140 °C	30 °C	10	22.5	27.5	47.5
		20	25.0	40.4	50.0
		30	19.1	31.0	39.7
	35 °C	10	26.3	36.8	52.6
		20	25.8	34.8	48.5
		30	22.1	36.4	44.2
	40 °C	10	44.1	53.8	58.2
		20	47.9	58.1	60.5
		30	31.7	55.8	60.0
	45 °C	10	43.4	51.6	54.1
		20	45.6	53.0	57.7
		30	36.8	49.7	54.6
	50 °C	10	56.8	63.1	68.9
		20	52.6	61.4	68.1
		30	37.5	53.0	61.4
180 °C	30 °C	10	19.3	28.1	35.1
		20	19.3	25.8	32.3
		30	20.6	26.5	33.8
	35 °C	10	11.7	18.3	25.0
		20	13.5	19.0	25.7
		30	17.4	20.9	29.1
	40 °C	10	24.1	29.6	35.2
		20	32.2	40.4	46.6
		30	28.3	31.6	44.4
	45 °C	10	16.3	24.8	31.2
		20	28.7	33.9	40.8
		30	30.5	39.5	41.1
	50 °C	10	30.6	34.1	46.9
		20	30.7	35.8	41.3
		30	31.4	34.8	42.7
220 °C	30 °C	10	18.8	25.0	37.5
		20	20.5	30.1	43.6
		30	11.6	30.2	41.9
	35 °C	10	13.1	40.7	55.6
		20	24.2	37.1	54.8
		30	24.7	38.4	49.3
	40 °C	10	51.8	56.5	62.3
		20	46.7	59.8	62.6
		30	39.7	57.4	60.3
	45 °C	10	46.1	51.3	54.8
		20	45.7	53.6	57.2
		30	33.8	46.4	53.1
	50 °C	10	55.2	61.7	68.8
		20	50.2	61.5	66.7
		30	39.4	52.6	60.6

Table 5.7: % Inhibition efficiency (IE) of 2-SH-BI on under-aged samples

Under-aged at	Temperature	Acetic acid (vol %)	Inhibition Efficiency (%) of 2-SH-BI		
			50 ppm	100 ppm	200 ppm
140 °C	30 °C	10	31.1	42.2	53.3
		20	35.1	42.1	57.9
		30	27.4	35.5	50.0
	35 °C	10	26.7	40.0	51.7
		20	33.3	41.7	54.2
		30	25.0	35.7	50.0
	40 °C	10	42.2	53.9	57.8
		20	52.7	63.3	66.6
		30	44.4	51.1	56.2
	45 °C	10	53.1	58.5	61.2
		20	52.8	56.7	65.2
		30	39.7	45.6	57.1
	50 °C	10	56.0	65.1	71.8
		20	53.5	59.7	68.5
		30	45.1	55.6	62.4
180 °C	30 °C	10	26.6	31.2	39.1
		20	22.4	26.9	35.8
		30	23.9	28.2	36.6
	35 °C	10	16.7	24.2	27.2
		20	16.2	21.2	32.5
		30	16.3	19.6	27.2
	40 °C	10	27.6	30.2	37.9
		20	35.2	37.7	41.5
		30	26.4	29.0	46.1
	45 °C	10	20.3	22.2	28.1
		20	35.5	38.6	42.6
		30	37.6	40.9	43.8
	50 °C	10	33.2	36.4	49.6
		20	34.7	36.9	43.1
		30	37.4	38.3	46.4
220 °C	30 °C	10	25.6	35.9	48.7
		20	26.2	35.7	50.0
		30	23.4	40.4	49.0
	35 °C	10	31.0	44.8	55.2
		20	25.8	40.9	56.1
		30	27.3	40.3	53.2
	40 °C	10	42.5	48.3	56.3
		20	57.0	63.4	67.6
		30	38.4	46.4	52.3
	45 °C	10	51.2	57.5	60.6
		20	50.6	55.7	63.3
		30	38.0	43.3	55.6
	50 °C	10	54.6	64.2	72.9
		20	51.4	57.6	67.5
		30	43.2	52.6	59.8

Table 5.8: % Inhibition efficiency (IE) of 2-SH-BI on peak-aged samples

Peak-aged at	Temperature	Acetic acid (vol %)	Inhibition Efficiency (%) of 2-SH-BI		
			50 ppm	100 ppm	200 ppm
140 °C	30 °C	10	41.4	48.3	56.9
		20	37.7	46.4	56.5
		30	34.2	40.8	52.6
	35 °C	10	30.4	43.5	47.9
		20	33.3	43.2	50.6
		30	33.1	38.3	51.1
	40 °C	10	46.5	58.1	63.6
		20	55.2	62.6	69.5
		30	45.5	50.3	57.5
	45 °C	10	54.9	60.1	63.0
		20	53.8	59.3	62.3
		30	45.6	52.2	60.6
	50 °C	10	40.6	53.8	65.8
		20	39.5	54.2	64.1
		30	40.7	54.7	61.6
180 °C	30 °C	10	32.1	37.2	46.2
		20	31.9	38.5	47.2
		30	33.6	39.2	46.7
	35 °C	10	32.6	38.0	43.5
		20	30.1	35.5	43.9
		30	33.1	37.9	42.7
	40 °C	10	34.3	37.9	42.3
		20	35.9	39.9	44.4
		30	31.2	38.1	51.1
	45 °C	10	27.1	30.9	33.5
		20	35.4	40.6	46.7
		30	31.8	37.1	45.3
	50 °C	10	36.2	40.8	54.0
		20	34.3	40.1	48.1
		30	36.2	42.7	47.8
220 °C	30 °C	10	37.7	43.4	54.7
		20	39.1	46.9	56.3
		30	32.9	41.4	52.9
	35 °C	10	26.9	41.3	47.6
		20	30.3	43.4	48.7
		30	31.5	39.3	51.7
	40 °C	10	37.6	49.5	59.4
		20	56.4	62.4	69.7
		30	45.1	51.6	56.6
	45 °C	10	52.4	56.5	59.9
		20	52.2	56.2	62.4
		30	45.7	49.2	57.4
	50 °C	10	50.2	60.9	68.9
		20	45.5	53.8	68.8
		30	39.7	53.8	60.9

Table 5.9: % Inhibition efficiency (IE) of 2-SH-BI on over-aged samples

Over-aged at	Temperature	Acetic acid (vol %)	Inhibition Efficiency (%) of 2-SH-BI		
			50 ppm	100 ppm	200 ppm
140 °C	30 °C	10	30.0	42.5	55.5
		20	34.6	46.2	59.6
		30	31.0	41.4	48.3
	35 °C	10	36.8	45.6	59.6
		20	36.4	44.0	56.1
		30	28.3	44.2	53.2
	40 °C	10	51.6	59.3	64.8
		20	55.5	64.7	68.1
		30	48.9	61.4	68.2
	45 °C	10	50.0	59.0	64.0
		20	50.3	59.1	63.1
		30	43.6	55.2	58.9
	50 °C	10	65.5	69.9	74.8
		20	62.3	67.5	72.9
		30	47.7	59.5	67.4
180 °C	30 °C	10	28.1	36.8	43.9
		20	25.8	32.3	38.7
		30	26.5	29.4	39.7
	35 °C	10	20.0	26.7	33.3
		20	17.6	23.1	33.8
		30	20.9	25.6	33.7
	40 °C	10	29.6	36.1	43.5
		20	38.4	41.1	48.6
		30	32.6	37.4	48.1
	45 °C	10	22.7	28.4	34.0
		20	32.8	37.4	42.5
		30	37.1	41.1	44.7
	50 °C	10	34.1	40.5	50.0
		20	36.2	40.6	44.1
		30	35.5	42.7	49.8
220 °C	30 °C	10	21.9	34.4	46.9
		20	25.6	35.9	48.7
		30	20.9	39.5	46.5
	35 °C	10	42.6	50.0	63.1
		20	37.1	46.8	58.1
		30	31.5	45.2	54.8
	40 °C	10	54.1	60.0	64.7
		20	53.3	61.7	64.5
		30	49.3	59.6	66.9
	45 °C	10	49.6	54.8	62.6
		20	52.9	55.0	63.0
		30	41.1	54.3	59.0
	50 °C	10	61.7	66.7	72.7
		20	61.5	65.7	69.5
		30	46.2	59.0	67.1

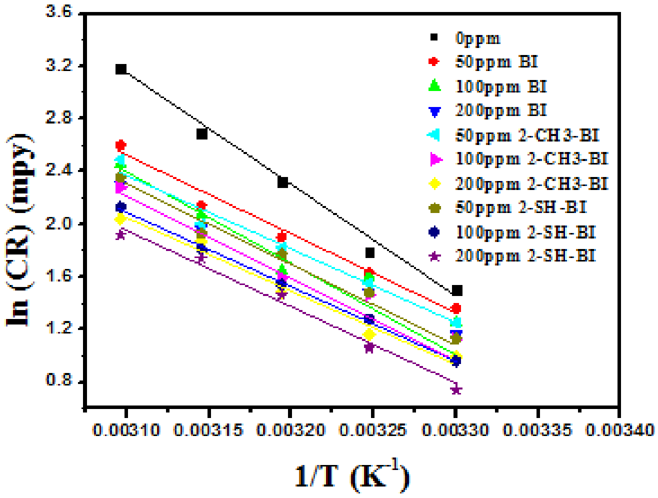

Fig.5.1: Arrhenius plots for under-aged (140 °C) samples in 10% acetic acid

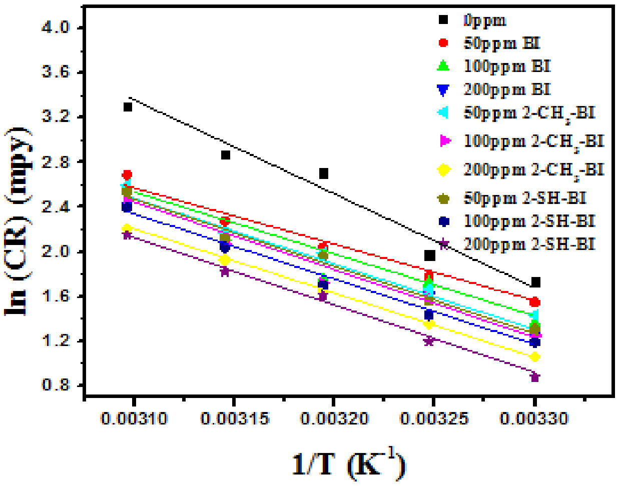

Fig.5.2: Arrhenius plots for under-aged (140 °C) sample in 20% acetic acid

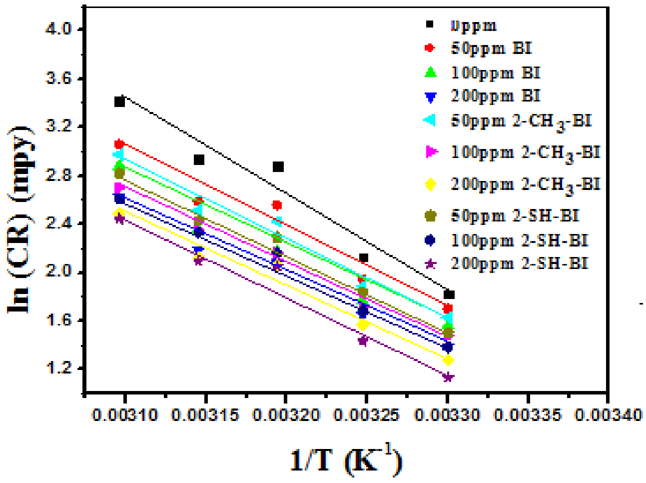

Fig.5.3: Arrhenius plots for under-aged (140 °C) sample in 30% acetic acid

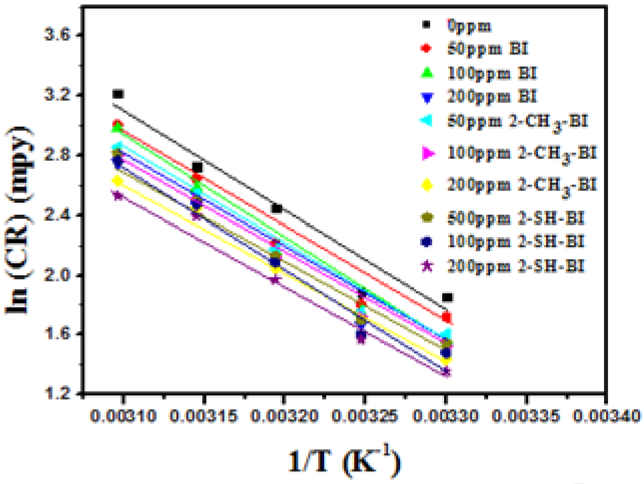

Fig.5.4: Arrhenius plots for under-aged (180 °C) sample in 10% acetic acid

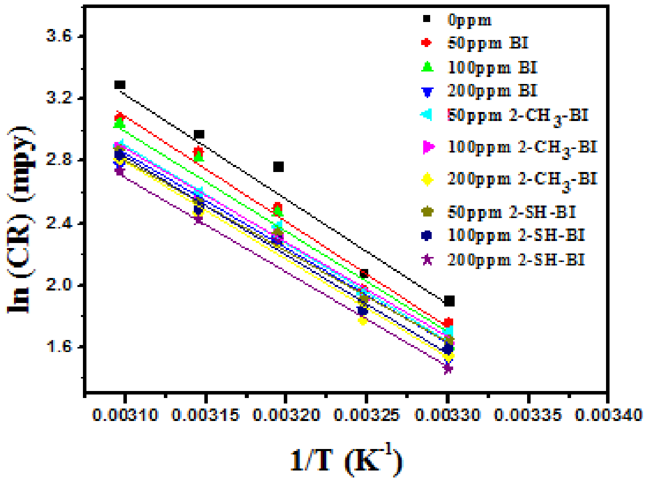

Fig.5.5: Arrhenius plots for under-aged (180 °C) sample in 20% acetic acid

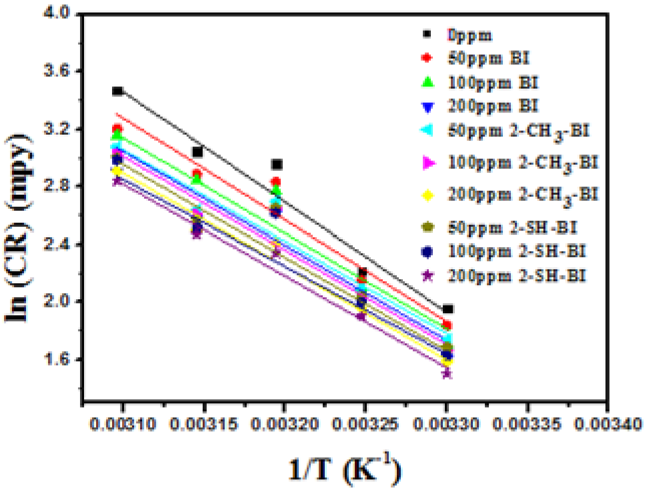

Fig.5.6: Arrhenius plots for under-aged (180 °C) sample in 30% acetic acid

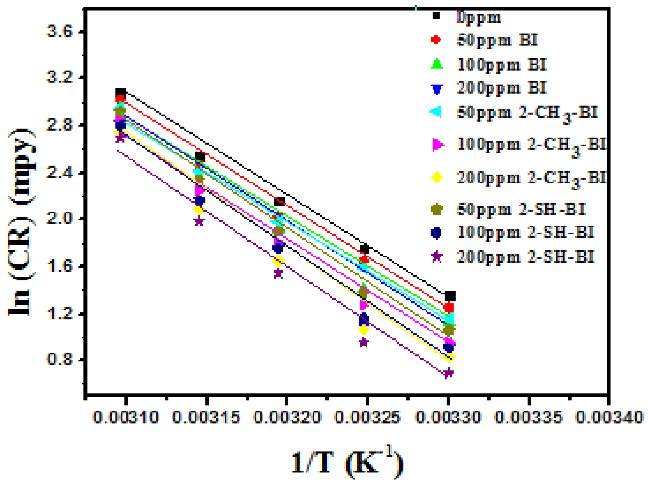

Fig.5.7: Arrhenius plots for under-aged (220 °C) sample in 10% acetic acid

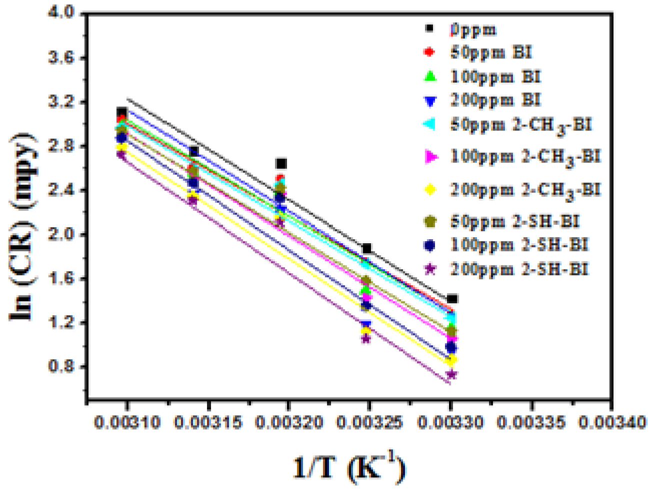

Fig.5.8: Arrhenius plots for under-aged (220 °C) sample in 20% acetic acid

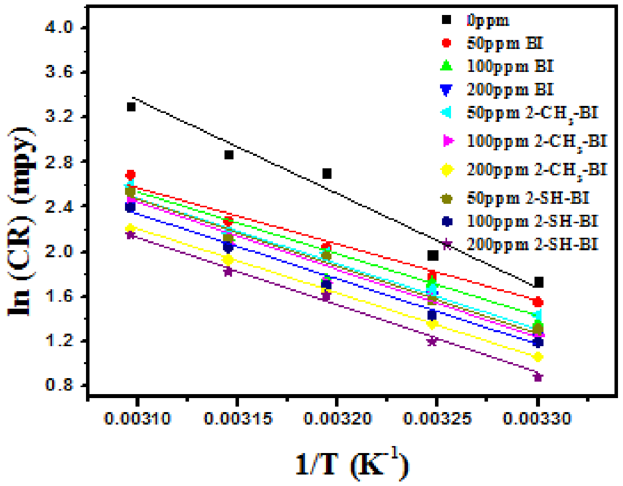

Fig.5.9: Arrhenius plots for under-aged (220 °C) sample in 30% acetic acid

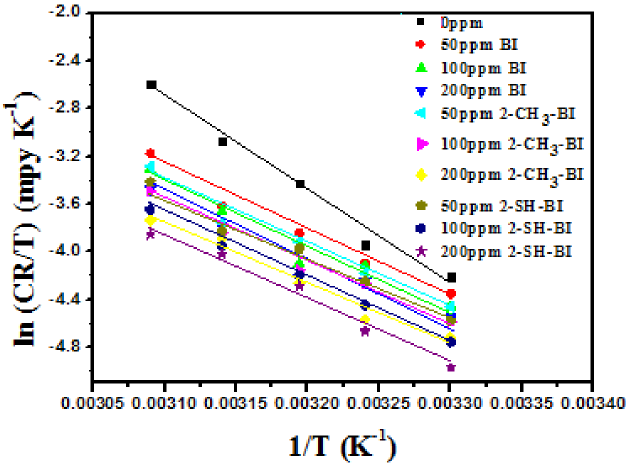

Fig.5.10: Plot of ln (CR/T) vs. (1/T) of under-aged (140 °C) sample in 10% acetic acid

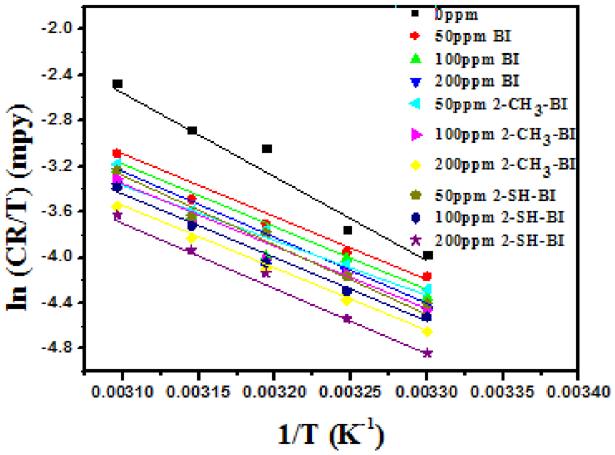

Fig.5.11: Plot of ln (CR/T) vs. (1/T) of under-aged (140 °C) sample in 20% acetic acid

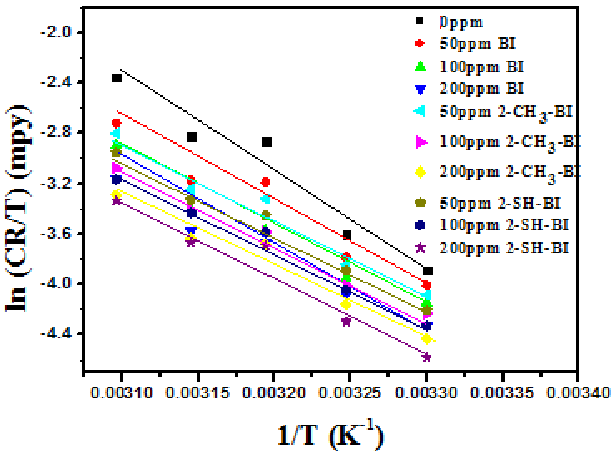

Fig.5.12: Plot of ln (CR/T) vs. (1/T) of under-aged (140 °C) sample in 30% acetic acid

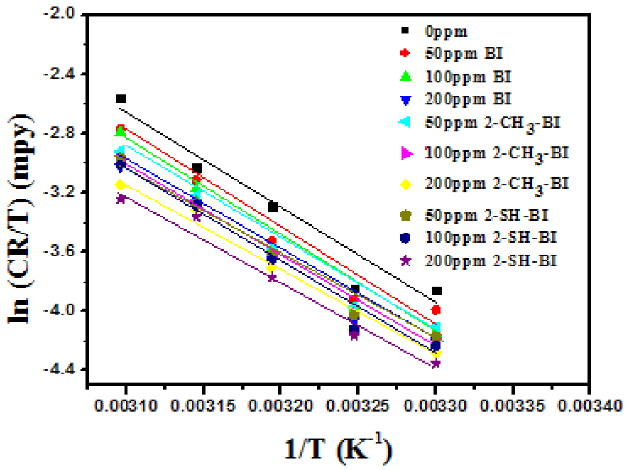

Fig.5.13: Plot of ln (CR/T) vs. (1/T) of under-aged (180 °C) sample in 10% acetic acid

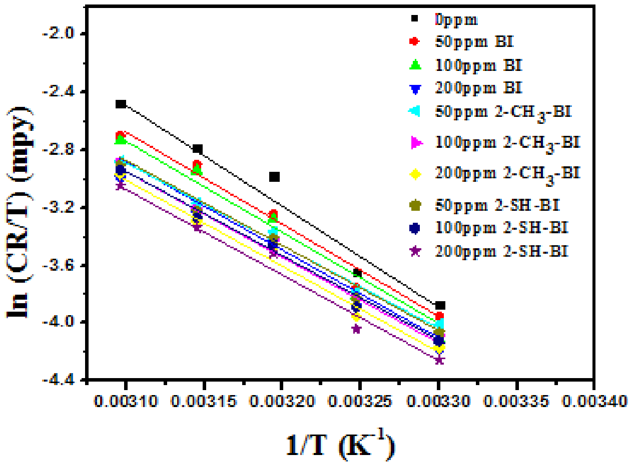

Fig.5.14: Plot of ln (CR/T) vs. (1/T) of under-aged (180 °C) sample in 20% acetic acid

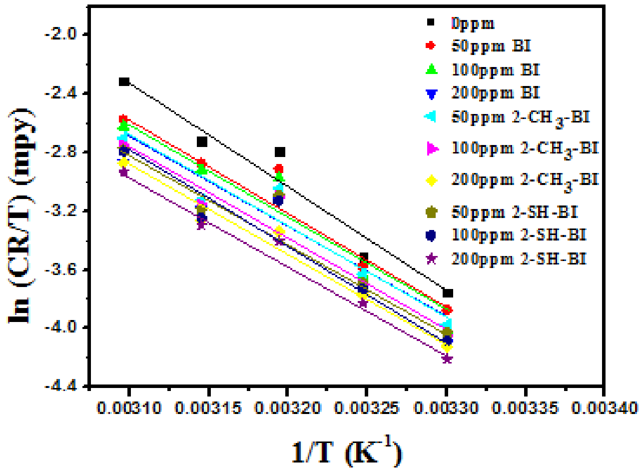

Fig.5.15: Plot of ln (CR/T) vs. (1/T) of under-aged (180 °C) sample in 30% acetic acid

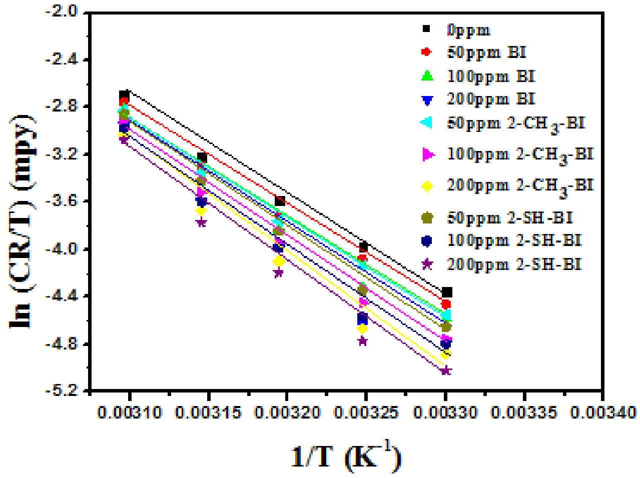

Fig.5.16: Plot of ln (CR/T) vs. (1/T) of under-aged (220 °C) sample in 10% acetic acid

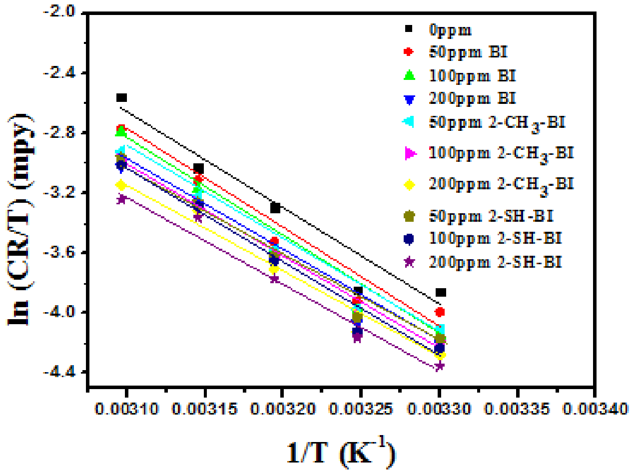

Fig.5.17: Plot of ln (CR/T) vs. (1/T) of under-aged (220 °C) sample in 20% acetic acid

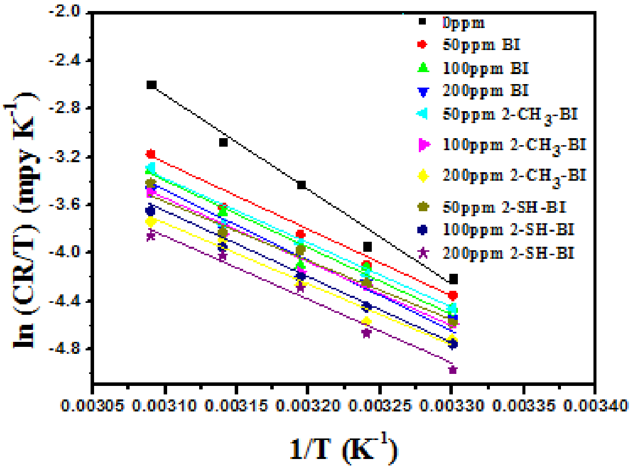

Fig.5.18: Plot of ln (CR/T) vs. (1/T) of under-aged (220 °C) sample in 30% acetic acid

Table 5.10: Activation parameters for the corrosion of under-aged (140 °C) samples in acetic acid

Inhibitor	Acetic acid (vol %)	Inhibitor Concentration (ppm)	Ea (kJ/mol)	ΔH# (kJ/mol)	ΔS# (J/mol)
BI	10 %	0	69.375	65.893	-63.045
		50	48.636	45.482	-131.319
		100	52.277	43.993	-137.038
		200	44.982	41.955	-144.565
	20 %	0	66.110	62.572	-71.767
		50	45.213	42.017	-141.249
		100	45.626	42.286	-141.712
		200	45.179	41.880	-143.881
	30 %	0	64.675	61.993	-72.646
		50	54.098	51.321	-108.971
		100	51.502	48.884	-118.582
		200	48.256	45.672	-130.242
2-CH_3-BI	10 %	0	69.375	65.893	-63.045
		50	47.681	44.462	-135.435
		100	44.882	41.781	-145.236
		200	45.761	42.729	-143.583
	20 %	0	66.110	62.572	-71.767
		50	46.223	42.843	-139.379
		100	47.630	44.352	-135.802
		200	46.459	43.517	-139.962
	30 %	0	64.675	61.993	-72.646
		50	53.595	51.245	-109.878
		100	49.477	46.872	-125.580
		200	47.749	45.281	-131.544
2-SH-BI	10 %	0	69.375	65.893	-63.045
		50	47.427	44.171	-137.097
		100	46.935	43.725	-140.070
		200	50.803	46.401	-132.895
	20 %	0	66.110	62.572	-71.774
		50	49.218	46.101	-129.555
		100	48.803	45.917	-131.366
		200	51.725	48.773	-124.096
	30 %	0	64.675	61.993	-72.646
		50	52.063	49.457	-116.527
		100	49.762	47.406	-124.269
		200	52.814	50.378	-116.476

Table 5.11: Activation parameters for the corrosion of peak-aged (140 °C) samples in acetic acid

Inhibitor	Acetic acid (vol %)	Inhibitor Concentration (ppm)	Ea (kJ/mol)	ΔH# (kJ/mol)	ΔS# (J/mol)
BI	10 %	0	63.813	61.318	-76.155
		50	61.514	58.913	-85.895
		100	56.750	54.323	-102.159
		200	50.360	47.743	-124.761
	20 %	0	61.951	59.450	-80.634
		50	61.009	57.977	-87.230
		100	54.705	51.963	-107.860
		200	50.672	48.030	-122.484
	30 %	0	62.904	60.278	-77.009
		50	59.504	56.816	-89.670
		100	56.536	53.842	-100.548
		200	53.592	51.555	-109.454
2-CH_3-BI	10 %	0	63.813	61.318	-76.155
		50	59.774	57.149	-92.964
		100	52.707	49.898	-117.899
		200	50.010	47.278	-127.303
	20 %	0	61.951	59.450	-80.634
		50	57.747	55.219	-97.611
		100	50.603	48.194	-121.887
		200	48.058	45.688	-131.075
	30 %	0	62.821	60.278	-77.009
		50	57.217	54.639	-98.143
		100	51.125	48.570	-118.956
		200	51.678	49.137	-118.481
2-SH-BI	10 %	0	63.813	61.318	-76.155
		50	56.978	54.371	-103.078
		100	54.006	51.800	-112.875
		200	50.598	48.321	-125.286
	20 %	0	61.951	59.450	-80.634
		50	54.538	52.104	-109.022
		100	50.988	48.707	-121.367
		200	50.855	48.768	-122.629
	30 %	0	62.904	60.278	-77.009
		50	55.778	53.360	-103.366
		100	50.288	47.525	-123.139
		200	52.552	49.946	-117.019

Table 5.12: Activation parameters for the corrosion of over-aged (140 °C) samples in acetic acid

Inhibitor	Acetic acid (vol %)	Inhibitor Concentration (ppm)	Ea (kJ/mol)	ΔH# (kJ/mol)	ΔS# (J/mol)
BI	10 %	0	64.995	62.410	-75.190
		50	44.051	41.335	-145.665
		100	40.222	37.822	-158.033
		200	40.452	38.066	-158.260
	20 %	0	60.756	58.193	-87.035
		50	41.804	39.212	151.018
		100	40.884	38.403	-155.027
		200	42.042	39.359	-153.002
	30 %	0	60.732	60.412	-78.890
		50	51.010	48.344	-119.318
		100	49.251	53.218	-106.108
		200	48.889	46.154	-129.594
2-CH_3-BI	10 %	0	64.995	62.410	-75.190
		50	42.074	39.442	-152.819
		100	39.114	36.393	-163.773
		200	48.077	45.313	-136.825
	20 %	0	60.757	58.193	-87.035
		50	40.890	38.314	-154.871
		100	41.467	38.941	-154.408
		200	43.375	40.828	-149.651
	30 %	0	60.732	60.412	-78.890
		50	48.876	46.489	-126.221
		100	44.456	42.011	-142.713
		200	43.300	40.591	-148.348
2-SH-BI	10 %	0	64.995	62.410	-75.190
		50	38.629	36.025	-167.482
		100	39.702	37.136	-162.860
		200	44.797	42.233	-148.221
	20 %	0	60.757	58.193	-87.035
		50	39.114	36.569	-161.718
		100	39.372	36.850	-162.316
		200	45.976	43.348	-143.042
	30 %	0	60.732	60.412	-78.890
		50	47.933	45.521	-130.694
		100	45.486	42.777	-141.412
		200	44.160	41.377	-147.223

Table 5.13: Activation parameters for the corrosion of under-aged (180 °C) samples in acetic acid

Inhibitor	Acetic acid (vol %)	Inhibitor Concentration (ppm)	Ea (kJ/mol)	ΔH# (kJ/mol)	ΔS# (J/mol)
BI	10 %	0	57.187	54.710	-97.668
		50	55.041	52.201	-106.896
		100	59.072	56.402	-94.052
		200	53.410	50.791	-112.928
	20 %	0	59.463	57.132	-88.453
		50	57.090	54.471	-98.377
		100	62.810	58.511	-85.988
		200	51.401	48.864	-118.299
	30 %	0	61.962	59.447	-80.013
		50	55.961	53.421	-100.491
		100	59.377	57.330	-88.654
		200	51.088	48.389	-118.563
2-CH_3-BI	10 %	0	57.187	54.710	-97.668
		50	52.853	50.249	-113.920
		100	53.864	51.167	-111.435
		200	52.068	49.737	-98.611
	20 %	0	59.463	57.132	-88.453
		50	49.040	46.495	124.934
		100	50.798	48.350	-119.408
		200	52.241	49.504	-116.400
	30 %	0	61.962	59.447	-80.013
		50	52.078	49.372	-114.540
		100	54.976	50.773	-110.511
		200	51.244	48.603	-118.470
2-SH-BI	10 %	0	57.187	54.710	-97.668
		50	53.831	51.137	-111.484
		100	55.819	52.861	-106.427
		200	51.150	48.817	-120.326
	20 %	0	59.463	57.132	-88.453
		50	49.663	47.235	-122.847
		100	66.934	48.245	-120.132
		200	52.795	50.544	-113.650
	30 %	0	61.962	59.447	-80.013
		50	50.797	48.381	-118.199
		100	52.217	49.457	-115.099
		200	52.432	49.807	-115.130

Table 5.14: Activation parameters for the corrosion of peak-aged (180 °C) samples in acetic acid

Inhibitor	Acetic acid (vol %)	Inhibitor Concentration (ppm)	Ea (kJ/mol)	ΔH# (kJ/mol)	ΔS# (J/mol)
BI	10 %	0	52.840	50.147	-110.582
		50	54.974	52.192	-105.441
		100	55.191	52.631	-105.152
		200	52.404	49.826	-115.192
	20 %	0	51.944	49.450	-111.334
		50	53.201	50.498	-109.153
		100	52.913	50.478	-110.387
		200	50.543	47.778	-120.266
	30 %	0	49.481	47.161	-117.370
		50	50.348	47.647	-117.091
		100	51.186	48.840	-114.320
		200	48.626	46.173	-124.357
2-CH_3-BI	10 %	0	52.840	50.147	-110.582
		50	50.196	47.832	-120.372
		100	52.791	50.416	-112.925
		200	47.966	45.357	-130.121
	20 %	0	51.944	49.450	-111.334
		50	49.253	46.935	-121.856
		100	49.499	46.736	-123.393
		200	48.065	52.778	-104.648
	30 %	0	49.481	47.161	-117.370
		50	47.389	44.975	-126.834
		100	49.671	47.094	-120.839
		200	46.286	43.902	-132.141
2-SH-BI	10 %	0	52.840	50.147	-110.582
		50	52.177	49.513	-115.877
		100	52.537	50.175	-114.339
		200	50.052	47.656	-123.451
	20 %	0	51.944	49.450	-111.334
		50	49.632	46.912	-122.837
		100	49.985	47.266	-122.412
		200	50.859	48.190	-120.498
	30 %	0	49.481	47.161	-117.370
		50	48.786	46.260	-123.603
		100	48.305	45.586	-126.518
		200	48.209	45.809	-126.936

Table 5.15: Activation parameters for the corrosion of over-aged (180 °C) samples in acetic acid

Inhibitor	Acetic acid (vol %)	Inhibitor Concentration (ppm)	Ea (kJ/mol)	ΔH# (kJ/mol)	ΔS# (J/mol)
BI	10 %	0	58.825	56.261	-93.441
		50	55.467	52.913	-105.305
		100	60.011	57.234	-92.219
		200	55.857	53.372	-105.679
	20 %	0	59.387	56.759	-90.356
		50	57.042	54.200	-115.662
		100	59.929	57.153	-91.032
		200	54.575	51.771	-109.722
	30 %	0	60.548	57.978	-85.204
		50	56.960	54.354	-97.923
		100	61.163	58.430	-85.649
		200	51.422	48.923	-117.465
2-CH_3-BI	10 %	0	58.825	56.261	-93.441
		50	53.192	50.717	-113.078
		100	54.920	52.272	-108.821
		200	51.206	48.649	-121.361
	20 %	0	59.387	56.759	-90.356
		50	51.254	48.660	-118.657
		100	51.071	48.685	-121.268
		200	51.043	48.380	-139.962
	30 %	0	60.548	57.978	-85.204
		50	52.931	50.461	-111.711
		100	53.583	51.014	-110.406
		200	52.916	50.302	-113.742
2-SH-BI	10 %	0	58.825	56.261	-93.441
		50	55.763	53.083	-106.219
		100	56.620	54.145	-103.643
		200	55.273	52.670	-109.343
	20 %	0	59.825	56.759	-90.356
		50	51.108	48.535	-119.667
		100	51.465	49.168	118.219
		200	53.673	51.427	-111.892
	30 %	0	60.548	57.978	-85.204
		50	52.569	50.001	-113.724
		100	52.916	47.457	-122.452
		200	51.877	49.151	-118.127

Table 5.16: Activation parameters for the corrosion of under-aged (220°C) samples in acetic acid

Inhibitor	Acetic acid (vol %)	Inhibitor Concentration (ppm)	Ea (kJ/mol)	ΔH# (kJ/mol)	ΔS# (J/mol)
BI	10 %	0	67.882	49.241	-115.533
		50	47.969	45.238	-132.629
		100	50.740	47.938	-125.302
		200	55.046	52.497	-112.310
	20 %	0	70.616	68.264	-54.715
		50	50.966	48.618	-120.920
		100	52.078	49.419	-119.949
		200	57.336	54.957	-103.656
	30 %	0	68.805	66.289	-60.197
		50	59.608	57.174	-90.957
		100	56.231	53.609	-104.286
		200	56.023	53.256	-107.069
2-CH_3-BI	10 %	0	67.882	49.241	-115.533
		50	47.089	44.433	-136.009
		100	49.004	46.505	-131.233
		200	47.110	44.412	-139.262
	20 %	0	70.616	68.264	-54.715
		50	46.603	44.036	-136.127
		100	51.787	49.408	-120.681
		200	52.180	49.800	-121.178
	30 %	0	68.805	66.289	-60.197
		50	59.484	57.117	-92.057
		100	58.324	55.839	-98.217
		200	56.341	53.535	-106.989
2-SH-BI	10 %	0	67.882	49.241	-115.533
		50	46.370	43.856	-138.940
		100	44.898	42.459	-144.823
		200	45.490	43.007	-144.660
	20 %	0	70.616	68.264	-54.715
		50	50.525	45.894	-130.762
		100	52.664	49.943	-119.304
		200	54.258	51.407	-116.508
	30 %	0	68.805	66.289	-60.197
		50	56.542	54.051	-102.819
		100	60.575	58.228	-90.895
		200	60.331	57.862	-93.601

Table 5.17: Activation parameters for the corrosion of peak-aged (220°C) samples in acetic acid

Inhibitor	Acetic acid (vol %)	Inhibitor Concentration (ppm)	Ea (kJ/mol)	ΔH# (kJ/mol)	ΔS# (J/mol)
BI	10 %	0	61.595	58.955	-84.895
		50	52.539	49.825	-115.947
		100	53.882	51.333	-112.830
		200	54.232	51.304	-114.527
	20 %	0	60.889	58.623	-81.665
		50	54.428	51.870	-107.855
		100	51.033	48.423	-120.414
		200	51.861	49.512	-118.426
	30 %	0	60.151	57.712	-85.927
		50	56.048	53.504	-101.153
		100	52.100	49.431	-115.814
		200	52.892	50.246	-114.381
2-CH_3-BI	10 %	0	61.595	58.955	-84.895
		50	53.571	51.101	-112.980
		100	46.541	43.960	-137.842
		200	49.986	47.717	-127.033
	20 %	0	60.889	58.623	-81.665
		50	52.566	50.208	-114.390
		100	48.494	46.107	-129.296
		200	43.306	41.056	-146.525
	30 %	0	60.151	57.712	-85.927
		50	54.265	51.658	-108.427
		100	49.643	47.304	-123.963
		200	47.426	44.744	-133.201
2-SH-BI	10 %	0	61.595	58.955	-84.895
		50	49.986	44.773	-134.696
		100	44.893	42.280	-144.086
		200	45.204	42.733	-144.080
	20 %	0	60.889	58.623	-81.665
		50	51.055	48.583	-121.031
		100	52.400	49.790	-118.415
		200	45.091	42.739	-142.696
	30 %	0	60.151	60.151	-85.927
		50	52.675	50.278	-113.825
		100	49.836	47.214	-124.818
		200	52.300	49.649	-118.522

Table 5.18: Activation parameters for the corrosion of over-aged (220°C) samples in acetic acid

Inhibitor	Acetic acid (vol %)	Inhibitor Concentration (ppm)	Ea (kJ/mol)	ΔH# (kJ/mol)	ΔS# (J/mol)
BI	10 %	0	68.852	65.850	-65.065
		50	45.839	43.305	-140.070
		100	48.226	45.887	-133.013
		200	50.541	47.914	-128.056
	20 %	0	67.770	65.129	-65.874
		50	50.557	47.904	-123.789
		100	48.350	45.675	-132.566
		200	57.654	55.089	-103.941
	30 %	0	68.083	65.821	-62.418
		50	56.819	54.297	-101.200
		100	50.841	48.413	-121.865
		200	57.210	54.558	-103.735
2-CH_3-BI	10 %	0	68.852	65.850	-65.065
		50	43.644	41.484	-147.344
		100	44.778	40.973	-150.083
		200	57.667	43.834	-142.429
	20 %	0	67.770	65.129	-65.874
		50	46.377	44.536	-135.736
		100	43.862	41.225	-148.019
		200	43.862	47.361	-129.799
	30 %	0	68.083	65.821	-62.418
		50	53.803	51.479	-111.281
		100	53.961	51.010	-114.844
		200	54.399	52.045	-112.875
2-SH-BI	10 %	0	68.852	65.850	-65.065
		50	43.424	40.770	-150.571
		100	45.254	42.486	-146.248
		200	47.401	44.713	-140.832
	20 %	0	67.770	65.129	-65.874
		50	41.809	39.058	-154.540
		100	44.762	42.243	-145.498
		200	48.949	46.380	-133.691
	30 %	0	68.083	65.821	-62.418
		50	53.470	50.874	-114.239
		100	52.526	50.260	-118.273
		200	51.172	48.644	-124.834

Table 5.19: Standard free energy (ΔG#) values for under-aged (140 °C) samples

Inhibitor	Acetic acid (vol %)	Inhibitor Concentration (ppm)	Standard free energy (ΔG#) (kJ/mol)				
			30 °C	35 °C	40 °C	45 °C	50 °C
BI	10 %	0	84.995	85.310	85.626	85.941	86.256
		50	85.271	85.928	86.584	87.241	87.898
		100	85.515	86.200	86.885	87.571	88.256
		200	85.758	86.521	87.243	87.966	88.649
	20 %	0	84.317	84.676	85.035	85.393	85.752
		50	84.815	85.521	86.227	86.934	87.640
		100	85.224	85.933	86.641	88.058	88.058
		200	85.475	86.195	86.914	87.634	88.353
	30 %	0	84.004	84.367	84.731	85.094	85.457
		50	84.339	84.884	85.428	85.973	86.518
		100	84.814	85.407	86.000	86.593	87.185
		200	85.135	85.786	86.437	87.088	87.740
2-CH_3-BI	10 %	0	84.995	85.310	85.626	85.941	86.256
		50	85.498	86.175	86.852	87.529	88.206
		100	85.787	86.513	87.230	87.965	88.691
		200	86.234	86.952	87.670	88.388	89.106
	20 %	0	84.317	84.676	85.035	85.393	85.752
		50	85.074	85.771	86.468	87.165	87.862
		100	85.500	86.179	86.858	87.537	88.216
		200	85.925	86.625	87.325	88.025	88.725
	30 %	0	84.004	84.367	84.731	85.094	85/457
		50	84.538	85.087	85.636	86.185	86.734
		100	84.922	85.550	86.178	86.806	87.434
		200	85.138	85.796	86.454	87.112	87.770
2-SH-BI	10 %	0	84.995	85.310	85.626	85.941	86.256
		50	85.711	86.396	87.081	87.766	88.451
		100	86.166	86.866	87.566	88.266	88.966
		200	86.668	87.332	87.996	88.660	89.324
	20 %	0	84.317	84.676	85.035	85.393	85.752
		50	85.356	86.003	86.650	87.297	87.94
		100	85.720	86.377	87.034	87.691	88.348
		200	86.374	86.994	87.614	88.234	88.854
	30 %	0	84.004	84.367	84.731	85.094	85.457
		50	84.764	85.347	85.930	86.513	87.197
		100	85.059	85.680	86.301	86.922	87.543
		200	85.670	86.252	86.834	87.416	87.998

Table 5.20: Standard free energy (ΔG#) values for peak-aged (140 °C) samples

Inhibitor	Acetic acid (vol %)	Inhibitor Concentration (ppm)	Standard free energy (ΔG#) (kJ/mol)				
			30 °C	35 °C	40 °C	45 °C	50 °C
BI	10 %	0	84.392	84.773	85.154	85.535	85.916
		50	84.939	85.368	85.797	86.226	86.655
		100	85.277	85.787	86.297	86.807	87.317
		200	85.545	86.169	86.793	87.417	88.041
	20 %	0	83.882	84.285	84.688	85.091	85.494
		50	84.407	84.843	85.279	85.715	86.151
		100	84.644	85.183	85.722	86.261	86.800
		200	85.142	85.755	86.368	86.981	87.594
	30 %	0	83.611	83.996	84.381	84.766	85.151
		50	83.986	84.434	84.882	85.330	85.778
		100	84.308	84.810	85.312	85.814	86.316
		200	84.719	85.266	85.813	86.360	86.907
2-CH$_3$-BI	10 %	0	84.392	84.773	85.154	85.535	85.916
		50	85.317	85.781	86.245	86.709	87.173
		100	85.621	86.210	86.799	87.388	87.977
		200	85.850	86.487	87.124	87.761	88.398
	20 %	0	83.882	84.285	84.688	85.091	85.494
		50	84.795	85.283	85.771	86.259	86.747
		100	85.125	85.735	86.345	86.955	87.565
		200	85.403	86.059	86.715	87.371	88.027
	30 %	0	83.611	83.996	84.381	84.766	85.151
		50	84.376	84.867	85.358	85.849	86.340
		100	84.613	85.208	85.803	86.398	86.993
		200	85.036	85.629	86.222	86.815	87.408
2-SH-BI	10 %	0	84.392	84.773	85.111	85.492	85.873
		50	85.603	86.119	86.635	87.151	87.667
		100	86.001	86.565	87.129	87.693	88.257
		200	86.282	86.909	87.536	88.163	88.163
	20 %	0	83.882	84.285	84.688	85.091	85.494
		50	85.137	85.682	86.227	86.772	87.318
		100	85.481	86.088	86.694	87.301	87.908
		200	85.924	86.537	87.150	87.764	88.377
	30 %	0	83.611	83.996	84.381	84.766	85.151
		50	84.679	85.196	85.713	86.230	86.747
		100	84.836	85.451	86.067	86.683	87.298
		200	85.402	85.987	86.572	87.158	87.743

Table 5.21: Standard free energy (ΔG#) values for over-aged (140 °C) samples

Inhibitor	Acetic acid (vol %)	Inhibitor Concentration (ppm)	Standard free energy (ΔG#) (kJ/mol)				
			30 °C	35 °C	40 °C	45 °C	50 °C
BI	10 %	0	85.192	85.568	85.944	86.320	86.696
		50	85.471	86.199	86.928	87.656	88.384
		100	85.705	86.496	87.286	88.076	88.866
		200	86.018	86.810	87.601	88.392	89.183
	20 %	0	84.564	84.999	85.434	85.870	86.305
		50	84.970	85.725	86.480	87.235	87.990
		100	85.376	86.151	86.926	87.701	88.476
		200	85.718	86.483	87.248	88.013	88.778
	30 %	0	84.315	84.710	85.104	85.499	85.893
		50	84.497	85.093	85.690	86.287	86.883
		100	85.368	85.899	86.429	86.960	87.490
		200	85.420	86.068	86.716	87.364	88.012
2-CH_3-BI	10 %	0	85.192	85.568	85.944	86.320	86.696
		50	85.746	86.510	87.274	88.038	88.802
		100	86.562	87.381	88.199	89.018	89.837
		200	86.770	87.455	88.139	88.823	89.507
	20 %	0	84.564	84.999	85.434	85.870	86.305
		50	85.239	86.014	86.788	87.562	88.337
		100	85.726	86.498	87.270	88.042	88.814
		200	86.172	86.920	87.668	88.417	89.165
	30 %	0	84.315	84.710	85.104	85.499	85.893
		50	84.733	85.365	85.996	86.627	87.258
		100	85.253	85.966	86.680	87.393	88.107
		200	85.540	86.282	87.023	87.765	88.507
2-SH-BI	10 %	0	85.192	85.568	85.944	86.320	86.696
		50	86.772	87.609	88.446	89.284	90.121
		100	86.482	87.296	88.111	88.925	89.739
		200	87.143	87.885	88.626	89.367	90.108
	20 %	0	84.564	84.999	85.434	85.870	86.605
		50	85.569	86.378	87.186	87.995	88.803
		100	86.031	86.843	87.654	88.466	89.278
		200	86.689	87.404	88.120	88.835	89.550
	30 %	0	84.315	84.710	85.104	85.499	85.893
		50	85.121	85.774	86.428	87.081	87.735
		100	85.624	86.331	87.038	87.746	88.453
		200	85.985	86.721	87.457	88.193	88.930

Table 5.22: Standard free energy (ΔG#) values for under-aged (180 °C) samples

Inhibitor	Acetic acid (vol %)	Inhibitor Concentration (ppm)	Standard free energy (ΔG#) (kJ/mol)				
			30 °C	35 °C	40 °C	45 °C	50 °C
BI	10 %	0	84.303	84.791	85.280	85.768	86.256
		50	84.590	85.124	85.659	86.193	86.728
		100	84.899	85.370	85.840	86.310	86.780
		200	85.008	85.572	86.137	86.702	87.266
	20 %	0	83.933	84.375	84.817	85.260	85.702
		50	84.279	84.771	85.263	85.754	86.246
		100	84.565	84.995	85.425	85.855	86.285
		200	84.708	85.300	85.891	86.483	87.074
	30 %	0	83.690	84.091	84.491	84.891	85.291
		50	83.869	84.372	84.874	85.377	85.879
		100	84.192	84.635	85.078	85.521	85.965
		200	84.313	84.906	85.499	86.092	86.684
2-CH_3-BI	10 %	0	84.303	84.710	85.280	85.768	86.256
		50	84.766	85.336	85.905	86.475	87.045
		100	84.931	85.488	86.046	86.603	87.160
		200	79.616	80.109	80.602	81.095	81.588
	20 %	0	83.933	84.375	84.817	85.260	85.702
		50	84.350	84.974	85.599	86.224	86.848
		100	84.530	85.127	85.724	86.321	86.918
		200	84.773	85.355	85.937	86.519	87.101
	30 %	0	83.690	84.091	84.491	84.891	85.291
		50	84.077	84.650	85.223	85.795	86.368
		100	84.257	84.810	85.362	85.915	86.468
		200	84.499	85.091	85.684	86.276	86.868
2-SH-BI	10 %	0	84.303	84.791	85.280	85.768	86.256
		50	84.916	85.474	86.031	86.588	87.146
		100	85.108	85.640	86.172	86.704	87.236
		200	85.275	85.877	86.479	87.080	87.682
	20 %	0	83.933	84.375	84.817	85.260	85.702
		50	84.457	85.071	85.686	86.300	86.914
		100	84.644	85.245	85.846	86.446	87.047
		200	84.979	85.548	86.116	86.684	87.252
	30 %	0	83.690	84.091	84.491	84.891	85.291
		50	84.195	84.786	85.377	85.968	86.559
		100	84.331	84.907	85.482	86.058	86.633
		200	84.691	85.267	85.842	86.418	86.993

Table 5.23: Standard free energy (ΔG#) values for peak-aged (180 °C) samples

Inhibitor	Acetic acid (vol %)	Inhibitor Concentration (ppm)	Standard free energy (ΔG#) (kJ/mol)				
			30 °C	35 °C	40 °C	45 °C	50 °C
BI	10 %	0	83.653	84.206	84.759	85.312	85.864
		50	84.140	84.667	85.195	85.722	86.249
		100	84.492	85.017	85.543	86.069	86.595
		200	84.729	85.305	85.881	86.457	87.033
	20 %	0	83.184	83.740	84.297	84.854	85.410
		50	83.571	84.117	84.662	85.208	85.754
		100	83.925	84.477	85.029	85.581	86.133
		200	84.218	84.819	85.421	86.022	86.623
	30 %	0	82.724	83.310	83.897	84.484	85.071
		50	83.125	83.711	84.296	84.881	85.467
		100	83.478	84.050	84.622	85.193	85.765
		200	83.853	84.474	85.096	85.718	86.340
2-CH_3-BI	10 %	0	83.653	84.206	84.759	85.312	85.864
		50	84.304	84.906	85.508	86.110	86.712
		100	84.632	85.196	85.761	86.326	86.890
		200	84.783	85.072	86.084	86.735	87.386
	20 %	0	83.184	83.740	84.297	84.254	85.410
		50	83.857	84.466	85.075	85.685	86.294
		100	84.124	84.741	85.358	85.974	86.591
		200	84.486	85.009	85.532	86.056	86.579
	30 %	0	82.724	83.310	83.897	84.484	85.071
		50	83.405	84.039	84.674	85.308	85.942
		100	83.708	84.312	84.916	85.520	86.124
		200	83.940	84.601	85.262	85.922	86.583
2-SH-BI	10 %	0	83.653	84.206	84.759	84.759	85.312
		50	84.623	85.203	85.782	86.361	86.941
		100	84.819	85.391	85.963	86.534	87.106
		200	85.061	85.678	86.296	86.913	87.530
	20 %	0	83.184	83.740	84.297	84.854	85.410
		50	84.131	84.745	85.359	85.974	86.588
		100	84.356	84.968	85.580	86.193	86.805
		200	84.700	85.303	85.905	86.508	87.110
	30 %	0	82.724	83.310	83.897	84.484	85.071
		50	83.711	84.329	84.947	85.565	86.183
		100	83.183	84.553	85.186	85.818	86.451
		200	84.270	84.905	85.539	86.174	86.809

Table 5.24: Standard free energy (ΔG#) values for over-aged (180 °C) samples

Inhibitor	Acetic acid (vol %)	Inhibitor Concentration (ppm)	Standard free energy (ΔG#) (kJ/mol)				
			30 °C	35 °C	40 °C	45 °C	50 °C
BI	10 %	0	84.573	85.040	85.508	85.975	86.442
		50	84.820	85.346	85.873	86.399	86.926
		100	85.176	85.637	86.098	86.559	87.020
		200	85.392	85.321	86.449	86.977	87.506
	20 %	0	84.136	84.588	85.040	85.492	85.943
		50	89.245	89.823	90.402	90.980	9.558
		100	84.735	85.190	85.646	86.101	87.921
		200	85.016	85.565	86.113	86.662	87.211
	30 %	0	83.794	84.220	84.646	85.072	85.498
		50	84.024	84.514	85.003	85.493	85.983
		100	84.381	84.809	85.238	85.666	86.094
		200	84.514	85.102	85.689	86.276	86.864
2-CH_3-BI	10 %	0	84.573	85.040	85.508	85.975	86.442
		50	84.979	85.545	86.110	86.675	87.241
		100	85.244	85.788	86.332	86.877	87.421
		200	85.421	86.028	86.634	87.241	87.848
	20 %	0	84.136	84.588	85.040	85.492	85.943
		50	84.613	85.206	85.799	86.392	86.986
		100	85.429	86.0355	86.641	87.248	87.854
		200	90.788	91.488	92.188	92.887	93.587
	30 %	0	83.794	84.220	84.646	85.072	85.498
		50	84.309	84.867	85.426	85.985	86.543
		100	84.467	85.019	85.571	86.123	86.675
		200	84.765	85.334	85.903	86.471	87.040
2-SH-BI	10 %	0	84.573	85.040	85.508	85.975	86.442
		50	85..267	85.798	86.329	86.860	87.391
		100	85.548	86.067	86.585	87.103	87.621
		200	85.800	86.347	86.894	87.441	87.987
	20 %	0	84.136	84.588	85.040	85.492	85.943
		50	84.794	85.392	85.990	86.589	87.187
		100	84.988	85.579	86.170	86.761	87.352
		200	85.330	85.889	86.449	87.008	87.568
	30 %	0	83.794	84.220	84.646	85.072	85.498
		50	84.459	85.027	85.596	86.165	86.733
		100	84.559	85.172	85.784	86.396	87.008
		200	84.943	85.534	86.124	86.715	87.306

Table 5.25: Standard free energy *(*ΔG#) values for under-aged (220 °C) samples

Inhibitor	Acetic acid (vol %)	Inhibitor Concentration (ppm)	Standard free energy (ΔG#) (kJ/mol)				
			30 °C	35 °C	40 °C	45 °C	50 °C
BI	10 %	0	84.247	84.825	85.402	85.980	86.558
		50	85.424	86.087	86.750	87.414	88.077
		100	85.904	86.531	87.157	87.784	88.410
		200	86.526	87.088	87.650	88.211	88.773
	20 %	0	84.842	85.116	85.389	85.663	85.936
		50	85.256	85.861	86.465	87.070	87.675
		100	85.763	86.363	86.963	87.562	88.162
		200	86.364	86.883	87.401	87.919	88.437
	30 %	0	84.528	84.829	85.130	85.431	85.732
		50	84.733	85.188	85.643	86.098	86.553
		100	85.207	85.729	86.250	86.771	87.293
		200	85.697	86.233	86.768	87.303	87.839
2-CH_3-BI	10 %	0	84.247	84.825	85.402	85.980	86.558
		50	85.643	86.323	87.003	87.683	88.363
		100	86.268	86.924	87.580	88.237	88.893
		200	86.608	87.304	88.001	88.697	89.393
	20 %	0	84.842	85.116	85.389	85.663	85.936
		50	85.282	85.963	86.643	87.324	88.005
		100	85.974	86.577	87.181	87.784	88.387
		200	86.516	87.122	87.728	88.334	88.940
	30 %	0	84.528	84.829	85.130	85.431	85.732
		50	85.010	85.470	85.930	86.391	86.851
		100	85.598	86.089	86.580	87.072	87.563
		200	85.952	86.487	87.022	87.557	88.092
2-SH-BI	10 %	0	84.247	84.825	85.402	85.980	86.558
		50	85.954	86.649	87.344	88.038	88.733
		100	86.340	87.064	87.88	88.512	89.236
		200	86.838	87.562	88.285	89.008	89.732
	20 %	0	84.842	85.116	85.389	85.663	85.936
		50	85.514	86.168	86.822	87.476	88.130
		100	86.092	86.688	87.285	87.881	88.478
		200	86.708	87.291	87.874	88.456	89.039
	30 %	0	84.528	84.829	85.130	85.431	85.732
		50	85.205	85.719	86.233	86.747	87.261
		100	85.769	86.223	86.678	87.132	87.587
		200	86.223	86.691	87.159	87.627	88.095

Table 5.26: Standard free energy (ΔG#) values for peak-aged (220 °C) samples

Inhibitor	Acetic acid (vol %)	Inhibitor Concentration (ppm)	Standard free energy (ΔG#) (kJ/mol)				
			30 °C	35 °C	40 °C	45 °C	50 °C
BI	10 %	0	84.678	85.102	85.527	85.951	86.376
		50	84.956	85.536	86.116	86.696	87.275
		100	85.520	86.084	86.648	87.212	87.777
		200	86.005	86.578	87.150	87.723	88.296
	20 %	0	83.367	83.775	84.184	84.592	85.000
		50	84.550	85.089	85.628	86.167	86.707
		100	84.908	85.510	86.112	86.714	87.316
		200	85.395	85.987	86.579	87.171	87.763
	30 %	0	83.747	84.177	84.607	85.036	85.466
		50	84.153	84.659	85.164	85.670	86.176
		100	84.522	85.101	85.680	86.259	86.838
		200	84.903	85.475	86.047	86.619	87.191
2-CH_3-BI	10 %	0	84.678	85.102	85.527	85.951	86.376
		50	85.333	85.898	86.463	87.028	87.593
		100	85.726	86.415	87.104	87.793	88.482
		200	86.207	86.843	87.478	88.113	88.748
	20 %	0	83.367	83.775	84.184	84.592	85.000
		50	84.868	85.440	86.012	86.584	87.155
		100	85.283	85.930	86.576	87.223	87.869
		200	85.453	86.185	86.918	87.650	88.383
	30 %	0	83.747	84.177	84.607	85.036	85.466
		50	84.511	85.053	85.595	86.137	86.679
		100	84.864	85.484	86.104	86.724	87.344
		200	85.103	85.769	86.435	87.101	87.767
2-SH-BI	10 %	0	84.678	85.102	85.527	85.951	86.376
		50	85.585	86.259	86.932	87.606	88.279
		100	85.938	86.658	87.378	88.099	88.819
		200	86.389	87.109	8.830	88.550	89.270
	20 %	0	83.367	83.775	84.184	84.592	85.000
		50	85.255	85.860	86.465	87.070	87.676
		100	85.669	86.261	86.853	87.445	88.038
		200	85.975	86.689	87.402	88.116	88.829
	30 %	0	86.186	86.616	87.046	87.475	87.905
		50	84.766	85.336	85.905	86.474	87.043
		100	85.033	85.657	86.282	86.906	87.530
		200	85.561	86.153	86.746	87.338	87.931

Table 5.27: Standard free energy (ΔG#) values for over-aged (220 °C) samples

Inhibitor	Acetic acid (vol %)	Inhibitor Concentration (ppm)	Standard free energy (ΔG#) (kJ/mol)				
			30 °C	35 °C	40 °C	45 °C	50 °C
BI	10 %	0	85.564	85.890	86.215	86.540	86.865
		50	85.746	86.446	87.146	87.847	88.547
		100	86.189	86.855	87.520	88.185	88.850
		200	86.714	87.355	87.995	88.635	89.276
	20 %	0	85.088	85.418	85.747	86.076	86.406
		50	85.412	86.031	86.649	87.268	87.887
		100	85.842	86.505	87.168	87.830	88.493
		200	86.583	87.102	87.622	88.142	88.661
	30 %	0	84.733	85.045	85.357	85.669	85.982
		50	84.960	85.466	85.972	86.478	86.984
		100	85.338	85.947	86.556	87.166	87.775
		200	85.989	86.508	87.027	87.545	88.064
2-CH_3-BI	10 %	0	85.564	85.890	86.215	86.540	86.865
		50	86.129	86.865	87.602	88.339	89.076
		100	86.448	87.198	87.948	88.699	89.449
		200	86.989	87.702	88.414	89.126	89.838
	20 %	0	85.088	85.418	85.747	86.076	86.406
		50	85.664	86.342	87.021	87.700	88.378
		100	86.074	86.814	87.554	88.295	89.035
		200	86.690	87.339	87.988	88.637	89.286
	30 %	0	84.733	85.045	85.357	85.669	85.982
		50	85.197	85.753	86.309	86.866	87.422
		100	85.807	86.381	86.956	87.530	88.104
		200	86.246	86.810	87.374	87.939	88.503
2-SH-BI	10 %	0	85.564	85.890	86.215	86.540	86.865
		50	86.393	87.145	87.898	88.651	89.404
		100	86.799	87.530	88.261	88.992	89.724
		200	87.385	88.089	88.793	89.497	90.201
	20 %	0	85.088	85.418	85.747	86.076	86.406
		50	85.883	86.656	87.429	88.201	88.974
		100	86.328	87.056	87.783	88.511	89.238
		200	86.888	87.556	88.225	88.893	89.562
	30 %	0	84.733	85.045	85.357	85.669	85.982
		50	85.488	86.059	86.630	87.202	87.773
		100	86.096	86.688	87.279	87.870	88.462
		200	86.468	87.092	87.717	88.341	88.965

Table 5.28: Free energy of adsorption (ΔG_{ads}) values of inhibitor BI on under-aged samples

Under-aged at	Temperature	Acetic acid (vol %)	Free energy of adsorption (ΔGads) (kJ/mol)		
			50 ppm	100 ppm	200 ppm
140 °C	30 °C	10	-24.963	-24.780	-23.914
		20	-25.779	-25.982	-25.014
		30	-24.495	-24.838	-24.690
	35 °C	10	-25.733	-24.285	-24.040
		20	-26.292	-25.189	-24.529
		30	-26.060	-26.206	-25.384
	40 °C	10	-28.974	-28.757	-27.581
		20	-30.530	-30.058	-28.635
		30	-28.142	-28.924	-27.591
	45 °C	10	-30.323	-28.856	-27.597
		20	-30.688	-29.619	-28.086
		30	-28.864	-28.674	-27.798
	50 °C	10	-30.986	-29.891	-28.845
		20	-31.225	-30.074	-28.934
		30	-29.420	-28.894	-28.484
180 °C	30 °C	10	-24.783	-25.171	-24.011
		20	-24.984	-25.225	-24.214
		30	-24.495	-24.571	-24.011
	35 °C	10	-23.778	-23.322	-23.028
		20	-24.577	-23.958	-23.280
		30	-23.348	-23.298	-22.829
	40 °C	10	-27.170	-26.002	-24.878
		20	-27.564	-26.112	-25.685
		30	-25.455	-24.734	-24.729
	45 °C	10	-29.332	-24.320	-24.175
		20	-25.681	-24.673	-26.095
		30	-26.421	-25.331	-26.152
	50 °C	10	-27.786	-26.193	-26.517
		20	-27.939	-26.462	-26.901
		30	-28.460	-27.085	-27.177
220 °C	30 °C	10	-24.233	-24.525	-24.734
		20	-25.174	-25.161	-24.972
		30	-22.885	-24.303	-24.993
	35 °C	10	-24.633	-26.144	-26.442
		20	-25.097	-26.446	-26.626
		30	-24.660	-25.546	-25.492
	40 °C	10	-28.583	-28.202	-27.121
		20	-30.592	-30.213	-28.738
		30	-27.447	-28.549	-26.955
	45 °C	10	-29.838	-28.523	-27.794
		20	-30.410	-29.259	-27.957
		30	-28.430	-28.545	-27.650
	50 °C	10	-30.745	-29.633	-28.669
		20	-30.731	-29.812	-28.642
		30	-28.214	-28.331	-28.332

Table 5.29: Free energy of adsorption (ΔG_{ads}) values of inhibitor BI on peak-aged samples

Peak-aged at	Temperature	Acetic acid (vol %)	Free energy of adsorption (ΔGads) (kJ/mol)		
			50 ppm	100 ppm	200 ppm
140 °C	30 °C	10	-26.302	-26.132	-25.141
		20	-26.783	-25.852	-25.236
		30	-25.709	-25.343	-24.690
	35 °C	10	-25.307	-25.335	-24.505
		20	-24.123	-24.818	-24.564
		30	-24.024	-25.053	-24.824
	40 °C	10	-28.194	-27.925	-27.507
		20	-28.351	-27.319	-28.027
		30	-27.491	-27.053	-27.142
	45 °C	10	-28.697	-28.360	-27.947
		20	-28.122	-28.032	-27.653
		30	-27.321	-27.674	-26.928
	50 °C	10	-27.645	-28.480	-28.009
		20	-27.364	-27.965	-27.862
		30	-27.972	-27.783	-27.291
180 °C	30 °C	10	-25.619	-25.421	-24.657
		20	-24.941	-24.895	-24.463
		30	-25.062	-24.885	-24.862
	35 °C	10	-25.773	-25.879	-25.019
		20	-25.624	-26.245	-24.853
		30	-25.935	-24.173	-25.274
	40 °C	10	-27.248	-26.828	-25.539
		20	-25.695	-25.960	-25.128
		30	-25.893	-25.635	-25.837
	45 °C	10	-25.316	-25.454	-25.085
		20	-26.244	-26.132	-25.947
		30	-25.845	-25.981	-25.829
	50 °C	10	-26.747	-26.890	-26.801
		20	-26.425	-26.634	-26.452
		30	-26.994	-26.873	-26.846
220 °C	30 °C	10	-26.016	-26.052	-25.719
		20	-26.367	-25.769	-25.624
		30	-25.451	-25.262	-24.712
	35 °C	10	-23.254	-25.189	-24.649
		20	-23.262	-24.986	-24.163
		30	-24.873	-25.368	-24.569
	40 °C	10	-25.919	-27.763	-26.902
		20	-29.479	-29.080	-28.245
		30	-27.916	-28.244	-27.288
	45 °C	10	-28.990	-28.414	-27.745
		20	-27.885	-28.117	-27.693
		30	-27.596	-28.034	-26.982
	50 °C	10	-29.227	-28.457	-27.859
		20	-29.428	-28.964	-27.765
		30	-28.070	-28.263	-27.236

Table 5.30: Free energy of adsorption (ΔG_{ads}) values of inhibitor BI on over-aged samples

Over-aged at	Temperature	Acetic acid (vol %)	Free energy of adsorption (ΔGads) (kJ/mol)		
			50 ppm	100 ppm	200 ppm
140 °C	30 °C	10	-24.783	-24.447	-24.060
		20	-25.394	-25.900	-25.215
		30	-24.690	-25.049	-24.961
	35 °C	10	-25.097	-25.532	-24.836
		20	-25.891	-25.489	-24.836
		30	-26.309	-26.243	-25.214
	40 °C	10	-29.324	-28.580	-27.340
		20	-29.739	-29.257	-27.909
		30	-27.386	-28.892	-27.676
	45 °C	10	-29.827	-28.802	-27.491
		20	-30.104	-28.993	-27.883
		30	-28.605	-28.371	-27.248
	50 °C	10	-31.333	-30.464	-29.249
		20	-31.128	-30.271	-29.128
		30	-29.266	-28.916	-28.213
180 °C	30 °C	10	-24.287	-24.867	-24.444
		20	-24.595	-24.843	-24.467
		30	-24.641	-25.171	-24.155
	35 °C	10	-23.431	-24.285	-23.575
		20	-24.403	-24.254	-23.717
		30	-24.389	-24.268	-23.218
	40 °C	10	-26.959	-26.002	-24.928
		20	-27.248	-26.233	-25.516
		30	-25.004	-25.037	-25.168
	45 °C	10	-25.517	-24.859	-24.458
		20	-24.986	-24.852	-25.924
		30	-25.976	-25.135	-26.135
	50 °C	10	-27.518	-26.241	-26.744
		20	-27.893	-26.568	-26.744
		30	-28.236	-26.614	-27.012
220 °C	30 °C	10	-24.783	-24.736	-24.202
		20	-24.795	-25.269	-25.014
		30	-23.169	-22.823	-24.985
	35 °C	10	-23.705	-25.943	-26.432
		20	-25.631	-26.493	-26.892
		30	-26.257	-26.531	-25.705
	40 °C	10	-29.347	-28.433	-27.486
		20	-29.014	-28.913	-28.028
		30	-27.264	-28.627	-27.547
	45 °C	10	-29.691	-28.631	-27.449
		20	-29.826	-28.973	-28.138
		30	-28.179	-28.217	-27.281
	50 °C	10	-31.376	-30.052	-29.023
		20	-30.545	-30.054	-28.408
		30	-29.633	-29.288	-28.203

Table 5.31: Free energy of adsorption (ΔG_{ads}) values of inhibitor 2-CH_3-BI on under-aged samples

Under-aged at	Temperature	Acetic acid (vol %)	Free energy of adsorption (ΔGads) (kJ/mol)		
			50 ppm	100 ppm	200 ppm
140 °C	30 °C	10	-26.807	-28.512	-25.453
		20	-27.371	-27.051	-26.383
		30	-26.095	-28.247	-25.864
	35 °C	10	-27.175	-26.305	-32.469
		20	-27.835	-27.281	-32.162
		30	-27.149	-27.743	-31.463
	40 °C	10	-29.813	-29.360	-28.071
		20	-31.091	-30.503	-28.993
		30	-29.437	-28.983	-27.914
	45 °C	10	-31.418	-30.009	-28.401
		20	-31.618	-30.391	-28.990
		30	-29.743	-29.023	-28.379
	50 °C	10	-31.912	-31.094	-30.246
		20	-31.976	-30.718	-29.991
		30	-30.388	-30.223	-29.400
180 °C	30 °C	10	-25.191	-25.854	-25.258
		20	-26.129	-25.303	-24.869
		30	-24.893	-25.658	-25.057
	35 °C	10	-25.383	-24.284	-23.987
		20	-25.397	-24.384	-24.169
		30	-25.376	-24.829	-23.728
	40 °C	10	-27.970	-26.745	-25.575
		20	-29.006	-27.632	-25.985
		30	-27.791	-26.613	-26.561
	45 °C	10	-27.276	-26.001	-24.766
		20	-29.469	-27.981	-26.724
		30	-29.034	-27.992	-26.947
	50 °C	10	-29.720	-28.302	-27.618
		20	-29.976	-28.031	-27.019
		30	-29.892	-28.417	-27.582
220 °C	30 °C	10	-26.129	-26.470	-25.557
		20	-25.067	-26.162	-25.618
		30	-25.792	-26.523	-25.591
	35 °C	10	-26.118	-27.421	-26.911
		20	-26.039	-27.269	-27.137
		30	-27.037	-27.092	-26.462
	40 °C	10	-29.670	-29.214	-28.007
		20	-31.174	-30.820	-29.516
		30	-29.106	-29.203	-27.972
	45 °C	10	-30.507	-29.818	-28.412
		20	-30.782	-29.994	-29.012
		30	-29.408	-28.840	-28.386
	50 °C	10	-31.546	-30.928	-30.172
		20	-31.769	-30.762	-29.976
		30	-29.771	-29.997	-29.077

Table 5.32: Free energy of adsorption (ΔG_{ads}) values of inhibitor 2-CH_3-BI on peak-aged samples

Peak-aged at	Temperature	Acetic acid (vol %)	Free energy of adsorption (ΔGads) (kJ/mol)		
			50 ppm	100 ppm	200 ppm
140 °C	30 °C	10	-28.160	-27.167	-25.948
		20	-28.037	-27.147	-25.738
		30	-27.371	-26.572	-25.731
	35 °C	10	-27.796	-27.235	-25.937
		20	-27.163	-27.081	-26.130
		30	-27.037	-26.744	-26.053
	40 °C	10	-29.593	-29.277	-34.449
		20	-29.997	-29.892	-34.981
		30	-29.651	-28.905	-34.011
	45 °C	10	-30.422	-30.255	-28.802
		20	-30.273	-30.243	-28.783
		30	-30.167	-29.522	-28.691
	50 °C	10	-30.139	-29.922	-28.913
		20	-30.113	-29.813	-28.872
		30	-29.964	-29.761	-28.761
180 °C	30 °C	10	-26.749	-26.181	-25.155
		20	-26.928	-26.289	-25.283
		30	-26.734	-26.181	-25.271
	35 °C	10	-27.495	-26.953	-25.776
		20	-27.316	-26.361	-25.893
		30	-27.947	-26.982	-25.682
	40 °C	10	-29.197	-27.981	-26.724
		20	-28.983	-27.990	-26.742
		30	-28.961	-27.893	-26.849
	45 °C	10	-28.205	-27.250	-25.924
		20	-29.631	-27.969	-27.061
		30	-29.497	-27.751	-26.824
	50 °C	10	-29.579	-28.314	-28.093
		20	-28.831	-28.368	-27.563
		30	-29.162	-28.016	-27.537
220 °C	30 °C	10	-27.856	-27.157	-26.565
		20	-27.791	-27.129	-25.999
		30	-27.653	-26.983	-25.961
	35 °C	10	-26.490	-26.907	-26.011
		20	-26.861	-26.993	-25.734
		30	-26.973	-27.001	-25.816
	40 °C	10	-28.459	-28.376	-27.608
		20	-30.549	-29.949	-29.016
		30	-29.737	-29.433	-28.209
	45 °C	10	-29.940	-25.932	-28.660
		20	-29.973	-25.794	-28.581
		30	-29.837	-29.374	-28.586
	50 °C	10	-30.618	-29.717	-29.210
		20	-30.834	-30.094	-29.364
		30	-30.175	-29.717	-28.771

Table 5.33: Free energy of adsorption (ΔG_{ads}) values of inhibitor 2-CH_3-BI on over-aged samples

Over-aged at	Temperature	Acetic acid (vol %)	Free energy of adsorption (ΔGads) (kJ/mol)		
			50 ppm	100 ppm	200 ppm
140 °C	30 °C	10	-26.851	-25.778	-26.222
		20	-26.969	-27.241	-26.642
		30	-26.734	-26.018	-25.421
	35 °C	10	-27.822	-27.301	-27.178
		20	-27.731	-27.037	-26.757
		30	-27.256	-27.294	-26.531
	40 °C	10	-30.338	-29.548	-28.209
		20	-30.737	-30.002	-28.462
		30	-28.958	-29.82	-28.431
	45 °C	10	-30.264	-29.318	-27.776
		20	-30.315	-29.492	-27.894
		30	-29.548	-29.219	-27.751
	50 °C	10	-32.679	-31.524	-30.358
		20	-32.224	-31.416	-30.349
		30	-30.573	-30.406	-29.468
180 °C	30 °C	10	-26.362	-25.854	-24.926
		20	-26.362	-25.692	-24.764
		30	-26.429	-25.761	-24.826
	35 °C	10	-25.279	-24.855	-24.098
		20	-25.391	-24.896	-24.108
		30	-26.472	-25.030	-24.345
	40 °C	10	-27.970	-26.897	-25.760
		20	-29.018	-28.140	-26.993
		30	-28.325	-27.142	-26.762
	45 °C	10	-27.124	-26.684	-25.694
		20	-29.044	-27.852	-26.801
		30	-29.138	-28.490	-26.893
	50 °C	10	-29.745	-28.314	-27.888
		20	-29.751	-28.691	-27.277
		30	-29.783	-28.368	-27.310
220 °C	30 °C	10	-26.281	-25.453	-25.187
		20	-26.327	-26.098	-25.826
		30	-24.850	-26.100	-25.623
	35 °C	10	-25.616	-27.720	-27.487
		20	-27.537	-27.360	-27.394
		30	-27.542	-27.417	-26.839
	40 °C	10	-31.143	-29.832	-28.655
		20	-30.611	-30.031	-28.662
		30	-29.868	-29.924	-28.604
	45 °C	10	-31.037	-29.755	-28.294
		20	-30.982	-29.792	-28.491
		30	-29.673	-29.236	-28.213
	50 °C	10	-32.505	-31.364	-30.345
		20	-31.966	-31.360	-30.087
		30	-30.788	-30.363	-29.378

Table 5.34: Free energy of adsorption (ΔG_{ads}) values of inhibitor 2-SH-BI on under-aged samples

Under-aged at	Temperature	Acetic acid (vol %)	Free energy of adsorption (ΔGads) (kJ/mol)		
			50 ppm	100 ppm	200 ppm
140 °C	30 °C	10	-28.287	-27.752	-27.132
		20	-28.742	-27.748	-27.491
		30	-27.836	-27.040	-27.037
	35 °C	10	-28.204	-27.977	-27.415
		20	-29.012	-27.993	-27.634
		30	-28.062	-27.508	-27.390
	40 °C	10	-30.472	-29.893	-28.502
		20	-31.572	-30.905	-29.479
		30	-30.581	-29.739	-28.471
	45 °C	10	-32.118	-30.865	-29.330
		20	-32.087	-30.738	-29.785
		30	-30.685	-29.491	-28.881
	50 °C	10	-32.938	-32.102	-30.725
		20	-32.816	-31.483	-30.654
		30	-31.762	-31.314	-30.314
180 °C	30 °C	10	-27.734	-26.552	-25.682
		20	-27.134	-26.139	-25.362
		30	-27.268	-26.301	-25.541
	35 °C	10	-26.675	-26.091	-24.720
		20	-26.661	-25.924	-25.369
		30	-26.664	-25.893	-24.720
	40 °C	10	-28.781	-26.870	-25.976
		20	-29.228	-27.729	-26.029
		30	-28.715	-26.870	-26.841
	45 °C	10	-28.174	-26.642	-25.641
		20	-30.211	-28.730	-27.337
		30	-30.354	-28.964	-27.561
	50 °C	10	-30.412	-28.930	-28.525
		20	-30.593	-28.946	-28.061
		30	-30.795	-29.094	-28.327
220 °C	30 °C	10	-27.603	-27.084	-26.668
		20	-27.683	-27.073	-26.831
		30	-27.386	-27.565	-26.711
	35 °C	10	-28.742	-28.481	-27.775
		20	-28.372	-28.316	-27.821
		30	-28.468	-28.283	-27.653
	40 °C	10	-30.504	-29.304	-28.342
		20	-32.024	-30.916	-29.597
		30	-30.427	-29.214	-28.183
	45 °C	10	-31.917	-30.756	-29.264
		20	-31.852	-30.634	-29.349
		30	-30.496	-29.244	-28.720
	50 °C	10	-32.785	-31.997	-31.225
		20	-32.516	-31.251	-30.530
		30	-31.555	-30.702	-29.634

Table 5.35: Free energy of adsorption (ΔG_{ads}) values of inhibitor 2-SH-BI on peak-aged samples

Peak-aged at	Temperature	Acetic acid (vol %)	Free energy of adsorption (ΔGads) (kJ/mol)		
			50 ppm	100 ppm	200 ppm
140 °C	30 °C	10	-29.415	-28.373	-27.498
		20	-29.025	-28.168	-27.492
		30	-28.896	-27.606	-27.216
	35 °C	10	-28.669	-28.345	-27.026
		20	-28.938	-28.338	-27.237
		30	-28.925	-27.794	-27.371
	40 °C	10	-30.925	-30.337	-29.135
		20	-31.833	-30.469	-29.826
		30	-30.837	-29.517	-28.470
	45 °C	10	-32.310	-31.040	-29.532
		20	-32.273	-31.011	-29.479
		30	-31.324	-30.190	-29.361
	50 °C	10	-31.268	-30.837	-30.325
		20	-31.210	-30.964	-30.241
		30	-31.271	-30.984	-30.103
180 °C	30 °C	10	-28.403	-27.225	-26.415
		20	-28.395	-27.291	-26.507
		30	-28.472	-27.326	-26.431
	35 °C	10	-28.930	-27.761	-26.571
		20	-28.793	-27.417	-26.598
		30	-29.002	-27.593	-26.503
	40 °C	10	-29.599	-28.201	-26.875
		20	-29.673	-28.392	-27.031
		30	-29.094	-28.283	-27.798
	45 °C	10	-29.174	-27.829	-26.313
		20	-30.200	-28.081	-27.776
		30	-29.238	-27.911	-27.664
	50 °C	10	-30.768	-29.429	-28.998
		20	-30.543	-29.413	-28.363
		30	-30.768	-29.511	-28.304
220 °C	30 °C	10	-29.025	-27.875	-27.274
		20	-29.133	-27.992	-27.346
		30	-28.495	-27.769	-27.169
	35 °C	10	-28.230	-28.115	-27.087
		20	-28.497	-28.271	-27.108
		30	-28.527	-28.095	-27.268
	40 °C	10	-29.972	-29.434	-28.673
		20	-31.960	-30.804	-29.853
		30	-30.779	-29.496	-28.571
	45 °C	10	-32.044	-30.643	-29.186
		20	-32.037	-30.639	-29.241
		30	-31.334	-29.873	-29.137
	50 °C	10	-32.311	-31.618	-30.704
		20	-31.805	-30.837	-30.702
		30	-31.168	-30.837	-29.821

Table 5.36: Free energy of adsorption (ΔG_{ads}) values of inhibitor 2-SH-BI on over-aged samples

Over-aged at	Temperature	Acetic acid (vol %)	Free energy of adsorption (ΔGads) (kJ/mol)		
			50 ppm	100 ppm	200 ppm
140 °C	30 °C	10	-28.156	-27.783	-27.355
		20	-28.364	-27.976	-27.491
		30	-28.243	-27.704	-26.627
	35 °C	10	-29.406	-28.563	-28.034
		20	-29.392	-28.483	-27.869
		30	-28.410	-28.487	-27.804
	40 °C	10	-31.457	-30.467	-29.271
		20	-31.641	-30.920	-29.914
		30	-31.378	-30.694	-29.917
	45 °C	10	-31.790	-30.919	-29.637
		20	-31.793	-30.923	-29.544
		30	-31.110	-30.793	-29.315
	50 °C	10	-34.012	-32.691	-31.342
		20	-33.927	-32.607	-31.225
		30	-32.043	-31.461	-29.952
180 °C	30 °C	10	-27.976	-26.976	-25.994
		20	-27.683	-26.680	-25.721
		30	-27.721	-26.476	-25.746
	35 °C	10	-27.201	-26.407	-25.451
		20	-26.993	-25.893	-25.492
		30	-27.294	-26.287	-25.487
	40 °C	10	-29.036	-28.072	-27.003
		20	-30.060	-28.418	-27.971
		30	-29.267	-28.146	-27.967
	45 °C	10	-28.551	-27.512	-26.372
		20	-29.894	-28.595	-27.326
		30	-30.394	-28.861	-27.435
	50 °C	10	-30.586	-29.401	-28.568
		20	-30.781	-29.406	-27.931
		30	-30.686	-29.974	-28.563
220 °C	30 °C	10	-27.087	-27.007	-26.486
		20	-27.758	-27.084	-26.891
		30	-26.989	-27.384	-26.481
	35 °C	10	-30.027	-28.996	-34.348
		20	-29.927	-28.687	-34.089
		30	-28.801	-28.437	-33.781
	40 °C	10	-31.861	-30.541	-29.237
		20	-31.634	-30.614	-29.231
		30	-31.243	-30.492	-29.397
	45 °C	10	-31.748	-27.188	-29.487
		20	-31.998	-27.204	-29.768
		30	-30.845	-27.164	-29.231
	50 °C	10	-33.570	-32.294	-30.957
		20	-33.568	-32.162	-30.779
		30	-31.881	-31.406	-30.648

The values of thermodynamic parameters for the adsorption of inhibitors can offer valuable evidence about the mechanism of corrosion inhibition. From Tables 5.10–5.18, it is evident that values for ΔH# are positive irrespective of experimental conditions. This suggests endothermic nature of matrix dissolution process [Zarrouk et al. 2011]. An endothermic adsorption (ΔH# > 0) is attributed unequivocally to chemisorption, and an exothermic adsorption (ΔH# < 0) may involve physisorption, chemisorption or a mixture of both. Also, the negative values of ΔS# indicate that the disorderness is smaller on going from reactant to product [Kairi 2013 and Aljourani et al. 2009]].

Ea values obtained for inhibited solutions are smaller than that obtained in the uninhibited solution as can be seen in Tables 5.10–5.18. In general, inhibitors are classified into three groups according to the temperature effects:

1. Inhibitors whose IE decreases with temperature increase. The value of the apparent activation energy Ea found is greater than that in the uninhibited solution.
2. Inhibitors whose IE does not change with temperature variation. The apparent activation energy does not change with the presence or absence of inhibitors.
3. Inhibitors in whose presence the IE increases with temperature increase, while the value of Ea for the corrosion process is smaller than that obtained in the uninhibited solution.

Studies also indicate that the corrosion process taking place in the presence of powerful inhibitors is characterized by an activation energy whose value is smaller than that of the uninhibited process. The point that IE increases with temperature is explained by the likely specific interaction between the composite surface and the inhibitor. But in certain experiments, it was observed that IE decreases with temperature. The rise in temperature might have suppressed the adsorption and accelerated the corrosion process. The lower value of the activation energy of the process in an inhibitor’s presence, when compared to that in its absence, is attributed to its chemisorption, while the opposite is the case with physical adsorption. It is considered that the increase of IE with temperature increase, is owing to the change in the nature of adsorptions. To be exact, the inhibitor is adsorbed physically at lower temperatures, while chemisorption is favoured as temperature increases. The same phenomenon is also described as, due to increase in the surface coverage by an inhibitor. Thus, at a high degree of coverage, the diffusion through the surface layer containing the inhibitor and corrosion products becomes the rate determining step of the metal dissolution process [Popova et al. 2003].

Tables 5.28-5.36 signifies ΔG_{ads} values for inhibition process involving different inhibitors. The negative sign of ΔG_{ads} indicates that the inhibitors are spontaneously adsorbed on the metal surface. The values come in between -23 KJ/mol to -34 KJ/mol. It has been reported that the ΔGads value up to -20 KJ/mol or lower indicates a physical adsorption, while that more negative than -40 KJ/mol involves sharing or transfer of electron from the inhibitor molecules to the metal surface to form a coordinate type bond (chemisorption) [Xiumei et al. 2011 and Aljourani et al. 2010]. Values of ΔG_{ads} between this range indicates that adsorption may involve mixed interactions, i.e. chemical and physical adsorption. Recently, studies have attributed values of ΔG_{ads} between -27.10 to -32.41 KJ/mol to chemisorption which involves direct adsorption in the presence of lone pairs of electrons and π-electrons. Thus, in the present work inhibitors are mixed type where chemisorption is prominent [Obot 2010]. Figure 5.19 shows the inhibitor layer on the corroded surface of the sample.

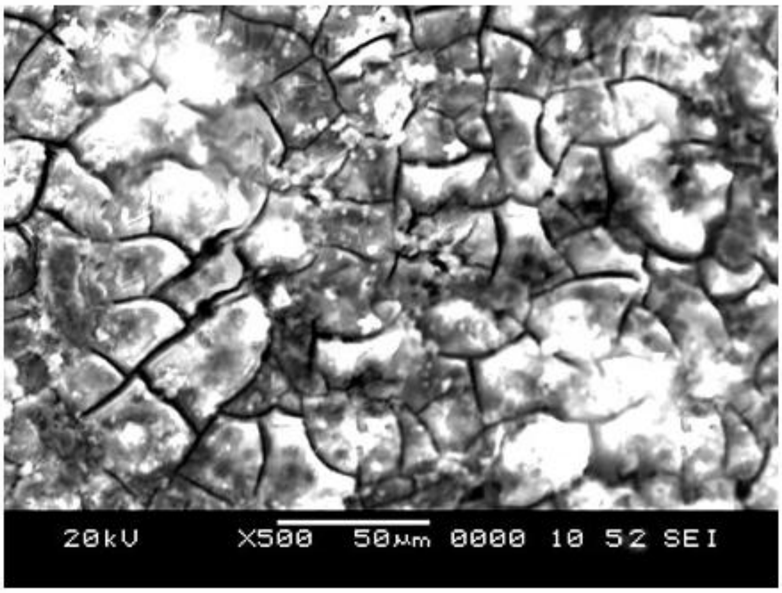

Fig.5.19: SEM micrograph of corroded over-aged Al-SiC sample at 50 °C in 10 vol% acetic acid in the presence of 200 ppm 2-SH-BI.

Basic information on the interaction between inhibitors and sample surface can be provided using the adsorption isotherms. It is known that the adsorption isotherm is an effective way to explain the adsorption mechanism of the inhibitors. The surface coverage (θ) data are very useful for discussing the adsorption characteristics. When the fraction of the surface covered is determined as a function of concentration at a constant temperature, adsorption isotherm could be evaluated at equilibrium condition. In order to determine the best fit for surface coverage (θ) to various isotherms, several adsorption isotherms were considered which are listed in table 5.37

Table 5.37 Adsorption isotherms

SI. No	Name	Verification plot
1	Langmuir	C/ θ vs c
2	Frumkin	θ vs log C
3	Bockris-Swinkels	θ/(1- θ) vs log C
4	Temkin	θ vs log C
5	Virial Parson	θ vs log (θ/C)
6	Flory-Huggins	log (θ/C) vs log (1- θ)
7	El-Awady	log [θ/(1- θ)] vs log C
8	Freundlich	log θ vs log C

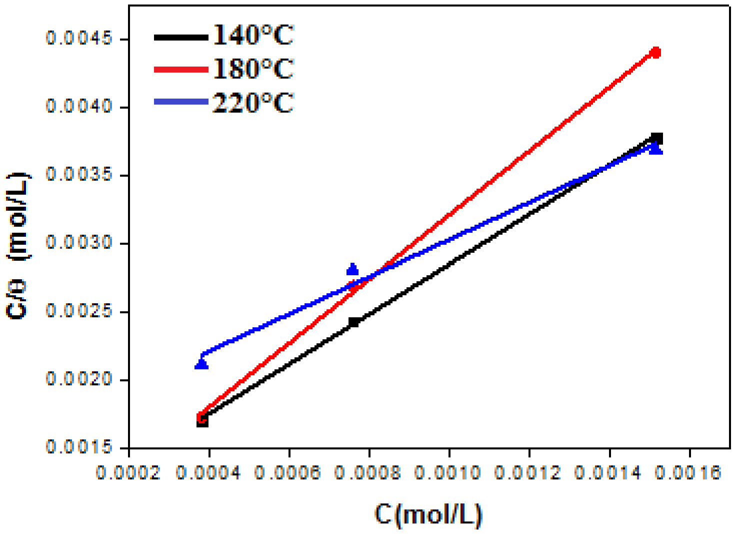

Fig.5.20: Langmuir adsorption isotherm of BI for under-aged samples in 10% acetic acid at 30°C.

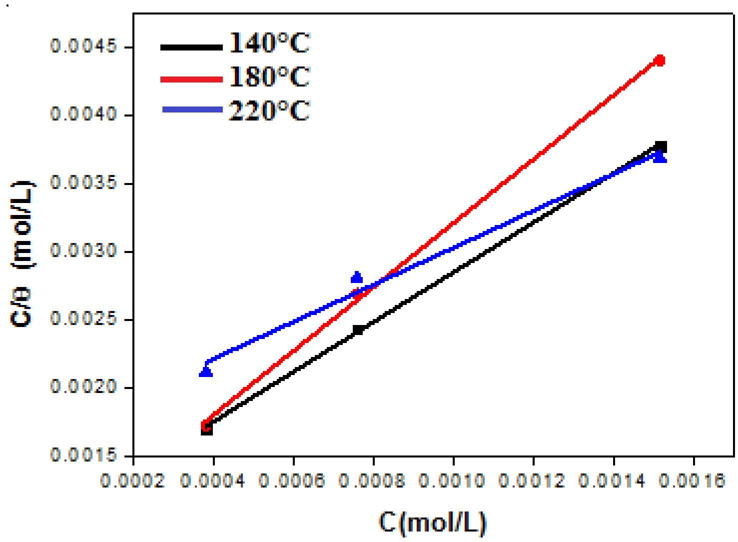

Fig.5.21: Langmuir adsorption isotherm of 2-CH_3-BI for under-aged samples in 10% acetic acid at 30°C.

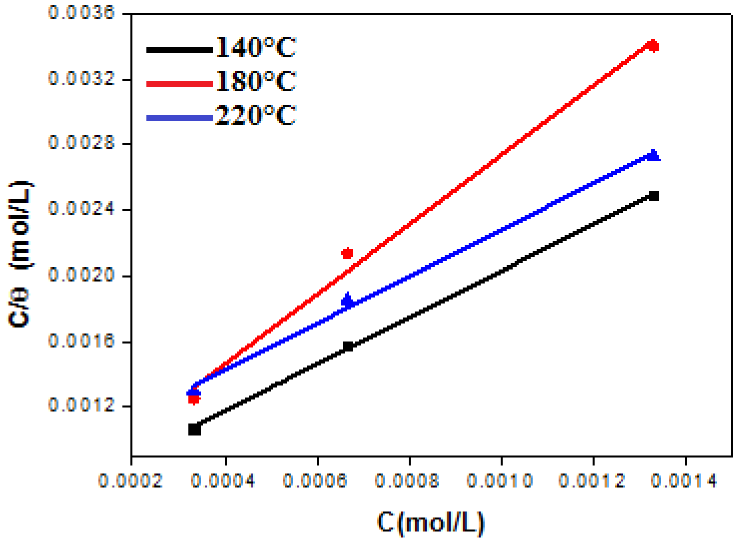

Fig.5.22: Langmuir adsorption isotherm of 2-SH-BI for under-aged samples in 10% acetic acid at 30°C.

Results reveal that Langmuir adsorption isotherm provides the best description of adsorption behaviour. In figures 5.20-5.22 three fitted lines are in good agreement and the linear correlation coefficients (R) of C/θ vs. C is more than 0.98. Same is the case with other samples too. This isotherm assumes that the adsorbed molecules occupy only one site and there are no interactions between adsorbed species, that is, it exhibit single layer adsorption isotherm [Zarrouk et al. 2011, Aljourani et al. 2010 and Lichao et al. 2010].

Molecules that contain nitrogen and sulphur in their structure like benzimidazole, 2-methylbenzimidazole and 2-mercaptobenzimidazole are of particular importance, since these provide an excellent inhibition. Benzimidazole and its derivatives show two anchoring sites suitable for surface bonding: the nitrogen atom with its lonely sp^2 electron pair and the aromatic rings. It is a general assumption that the adsorption of the organic inhibitors at the sample surface interface is the first step in the mechanism of inhibitor action. Organic molecules could be adsorbed on the metal surface by one of the following mechanisms:

1. Electrostatic interaction between charged surface of the metal and the charge of inhibitor.
2. Interaction of unshared electron pairs in the inhibitor molecule with the metal.
3. Interaction of π-electron with metal.
4. A combination of all the above types [Aljourani et al. 2009].

In general, the proceeding of physical adsorption requires the presence of both electrically charged surface of the metal and charged species in the bulk of the solution. Chemisorption process involves charge sharing or charge transfer from the inhibitor molecules to the metal surface to form a coordinate type of a bond. This is possible in case of a positive as well as a negative charge of the surface [Popova et al. 2003]

The effect of the molecular structure of BI, 2-CH_3-BI and 2-SH-BI on their protective properties as inhibitors of Al-SiC composite corrosion in acetic acid will be considered in the following aspects: (i) effect of the electronic structure, which determines the electronic density of the molecule’s reaction centre. From the point of view of inhibition process, it presents this part of the molecule through which it adsorbs. It will be designated as ‘‘adsorption centre of the molecule’’ (ii) effect of the chemical structure, which includes structural characteristics of the molecule like volume, surface area, and three-dimensional disposition of the substituents.

BI is a 5-membered N-containing heterocycle (imidazole), attached to a benzyl nucleus. It is very stable towards oxidation and reductive agents. It contains two nitrogen hetero-atoms: N1 or ‘pyrrolic’ nitrogen atom at the 1-position in the molecule, whose unshared electron pair participates in imidazole π-electron sextet and N3 or ‘pyridyne’ nitrogen atom at the 3-position in the molecule, whose unshared electron pair is free and facilitates the reaction with acids to give salts. It is evident from what stated above that the ‘pyridine’ N3 is a donor of electrons in BI molecule.

However, the inhibitors under study are organic bases which protonize in an acid medium, predominantly affecting the nitrogen atom (N3) in the imidazole ring. The protonation of the unshared electron pairs in some of the substituents, like $–CH_3$ and –SH, cannot be excluded as well because it would have improved the cation adsorption. Thus, they become cations. On the other hand, the presence of acetate ions ($CH_3CO_2^-$) in the solution should be mentioned. They are characterized with strong adsorbability on the metal surface which brings about a negative charge favouring the adsorption of cation type inhibitors [Popova 2004].

It is clear from Tables 5.7-5.9 that, inhibition efficiency of 2-SH-BI is higher than 2-CH_3-BI and BI. The higher inhibition properties of 2-SH-BI may be credited to the presence of S and N atoms in the molecular structure. Organic inhibitors which have reactional functional groups are locations of the adsorption process. The strength of adsorption bond depends on the electron density of donor atom. The inhibition efficiency of organic compounds containing different donor atoms is in the sequence $S > N > O$. The introduction of mercapto (SH) group can vary the orbital energy configurations of electrons, thus enhancing the inhibition properties of 2-SH-BI. Also, the greater inhibition efficiency of 2-CH_3-BI when compared to BI is due to the existence of methyl group (CH_3). Methyl groups are electron donors and it increases electron density of 2-CH_3-BI [Obot 2010]. This supports the experimental results.

5.3. Conclusions

- The highest percentage of efficiency achieved is 74.8% for 2-SH-BI for an over-aged sample at 50°C in 10 vol % of acetic acid.
- As the acid concentration got increased to 30 vol %, inhibition efficiency was reduced.
- Values for ΔH# are positive which suggests an endothermic dissolution.
- ΔG_{ads} values came in between -23 KJ/mol to -34 KJ/mol which attributed chemisorption.
- Langmuir adsorption isotherm provided the best description of adsorption behaviour.
- Benzimidazole, 2-methylbenzimidazole, and 2-mercaptobenzimidazole provided an excellent inhibition.
- 2-SH-BI provided maximum inhibition while BI presented the least efficiency.

CHAPTER 6

CONCLUSION

- The peak hardness in T4 treatment is 90 HRB which was obtained at 720 hours of aging at room temperature.
- In T6 treatments, the temperatures for under-aging, peak-aging and over-aging was determined using aging curves.
- The composite was under-aged at 140 and 160°C, peak-aged at 180°C and over-aged at 200 and 220°C.
- Maximum peak hardness value of 98 HRB was obtained when the composite was aged at 180°C for 3 hours.
- The peak-aging time was decreased from 4 hours to 2 hours when the aging temperature was increased.
- A rapid increase in the corrosion rate with increase in the concentration of acetic acid was observed till it reached a maximum at 30%. Further increase in the concentration of acetic acid resulted in the reduction of the corrosion rate.
- Corrosion rate of the 6061 Al-SiC composite increased with increase in temperature.
- During corrosion of the composite, the interfacial attack was prominent and likelihood of IGC was ruled out.
- Peak-aged samples were more corrosion prone while over-aged samples were minimally corroded.
- Corrosion rates of the samples peak-aged at 140 and 220°C was way lesser than the samples under-aged and over-aged at 180°C in almost all experimental conditions.
- The addition of inhibitors showed a marked reduction in corrosion rates.

- The highest percentage of efficiency achieved is 74.8% for 2-SH-BI for a sample over-aged at 140°C in 10 vol% of acetic acid tested at 50°C.
- As the acid concentration got increased to 30 vol%, inhibition efficiency was reduced.
- Values for enthalpy of activation are positive which suggests an endothermic dissolution.
- Free energy of adsorption values are in between -23 KJ/mol and -34 KJ/mol which attributed chemisorption.
- Langmuir adsorption isotherm provided the best description of adsorption behaviour.

SCOPE FOR FUTURE WORK

1. Corrosion studies on 6061 Al-SiC composite can be studied in different acid media and different heat treating atmosphere.
2. Same studies can be done using other inhibitors.
3. Benzimidazole and its derivatives being anti-microbial, it can be used to study the inhibition effects on microbial corrosion of the same composite.

REFERENCES

- Ahmad, Z. and Abdul, A. B. J. (1996). “Effect of Temper on Seawater Corrosion of an Aluminium- Silicon Carbide Composite Alloy.” *Corrosion Science*, 52 (11), 857-865.

- Ahn, H. K. and Yu, C. H. (2001). “Effect of SiC Volume Fraction on the Age-Hardening Behavior in SiC Particulate-Reinforced 6061 Aluminium Alloy Composite.” *Metals and Materials International,* 7, 1-7.

- Aljourani, J., Raeissi, K. and Golozar, M. A. (2009). “Benzimidazole and its Derivatives as Corrosion Inhibitors for Mild Steel in 1M HCl Solution.” *Corrosion Science*, 51, 1836-1843.
- Appendino, P., Badini, C., Marino, F. and Tomasi, A. (1991). “6061 Aluminium alloy- SiC particulate composite: a comparison between aging behavior in T4 and T6 treatments.” *Materials Science and Engineering,* A 135, 275-279.
- Arsenault, R. J. (1991) in “Metal Matrix Composites; Mechanism and Properties”, Academic Press, New York, 79-80.
- ASM Handbook, (2005). *Volume 13B, Corrosion: Materials,* ASM International, Ohio.
- Berg, L.K., Gjonnes, J., Hansen, V., Li, X. Z., Wedel, M. K., Waterloo, G., Schryvers, D. and Wallenberg, L. R. (2001). “GP- Zones in Al-Zn-Mg Alloys and Their Role in Artificial Aging.” *Acta Mater,* 49, 3443-3451.

- Bhat, M. S. N., Surappa, M. K. and Nayak, H. V. S. (1991). “Corrosion Behavior of Silicon Carbide Particle reinforced 6061/Al alloy composites.” *J. Mater. Sci.*, 26, 4991-4996.

- Borrego, A. and Gonzalez, G. (2003). “On the Stability With Temperature of The Dislocation Structure in 6061 Al-15 vol% SiC Composite as Studied by Hardness and Differential Scanning Calorimetry.” *Journal of Materials Science,* 38, 2761-2765.

- Burleigh, T.D., Rennick, R.C. and Bovard, F.S. (1993). "Corrosion Potentials for Aluminum Alloys Measured by ASTM G69." *Corrosion*, 49 (8), 683-685.

- Candan, S. (2004). "Effect of SiC particle size on corrosion behavior of pressure infiltrated Al matrix composites in a NaCl solution." *Materials Letters,* 58, 3601-3605.
- Candan, S. and Bilgic, E. (2004). "Corrosion behavior of Al-60 vol. % SiCp composites in NaCl solution." *Materials Letters,* 58, 2787-2790.
- Chawla, K. K. (1998). *Composite Materials- Science and Engineering,* Springer, Newyork.
- Christman, T. and Suresh, S. (1988). “Microstructural Development in An Aluminium Alloy- SiC Whisker Composite.” *Acta Metall*., 36, 1691-1704.
- Davis, J. R. (1993). *Aluminium and Aluminium Alloys*. ASM International, Ohio.
- El-Menshawy, K., El-Sayed, A. W. A., El-Bedawy, M. E., Ahmed, H. A. and El-Raghy, S. M. (2012). “Effect of Aging Time at Low Aging Temperatures on the Corrosion of Aluminium alloy 6061.” *Corrosion Science*, 54, 167-173.
- Fischer, H. (1972). “The Inhibition Of Vapor-Phase Corrosion.” Werkst. Korros., 23, 445–465.
- Fontanna, M. G. and Greene, N. D. (1978). *Corrosion Engineering*, McGraw Hill, USA.
- Gece, G. (2011). “Drugs: A review of promising novel corrosion inhibitors.” *Corrosion Science*, 53, 3873-3898.
- Ghali, E. (2010). *Corrosion Resistance of Aluminum and Magnesium Alloys Understanding, Performance and Testing*, John Wiley & Sons, Inc., Publication, New Jersey.
- Guillaumin, V. and Mankowski, G. (2000). “Localized Corrosion of 6056 T6 Aluminium Alloy in Chloride Media.” *Corrosion Science,* 42, 105-125.
- Hausler, R.H. (1983). paper 19*, International Conference on Corrosion Inhibition. National Association of Corrosion Engineers, National Association of Corrosion Engineers* Dallas, paper 19.
- Hollingsworth, E. H. and Hunsicker, H. Y. (1987). *Metals Hand Book, Vol.13*, 9th Edition, 583-609, ASM International, Metals Park, Ohio.

- Hsin-Hsiung Huang. (2016). "The Eh-pH Diagram and Its Advances." *Metals,* 6, 23, 1-30.
- Kairi, N. I. and Kassim, J. (2013). "The Effect of Temperature on the Corrosion Inhibition of Mild Steel in 1 M HCl Solution by Curcuma Longa Extract." *Int. J. Electrochem. Sci*., 8, 7138 – 7155.
- Lifka, B. W. (2005*). Corrosion Tests and Standards, Application and Interpretation*, 2nd edition, ASM International, Materials Park, Ohio.
- Lloyd, D. J. (1994). "Particle Reinforced Aluminium and Magnesium Matrix Composites" *International Metals Review,* 39(1), 1-3.
- Lorenz, W.J. and Mansfield, F. (1983). paper 2, *International Conference on Corrosion Inhibition. National Association of Corrosion Engineers*, Dallas.
- Marioara, C. D., Anderson, S. J., Stene, T. N., Hasting, H., Walmsley, J., Vanhelvoort, A. T. J. and Holmestad, R. (2007). "The Effect of Cu Precipitation in Al-Mg-Si Alloys." *Philosophical Magazine*, 87, 3385-3413.
- McCafferty, E., Hubler, G. K. and Natishan, P. P. M. (1987). "Naval Research Laboratory Surface Modification Program: Ion Beam and Laser Processing of Metal Surfaces for Improved Corrosion Resistance." *Mat. Sc. Eng.*, 87, 1-10.
- Min, Z., Gaohui, W. and Lonhtao, J. (2005). "Aging Behavior and Precipitation Kinetics of SiCp/6061 Al Composites." *Journal of Materials Science,* 39, 1759-1763.
- Mukherjee, A. K., Singh, S. K. and Singh, M. M. (2008). "Influence of formic Acid on Addition on the Electrochemical Behaviour of Mild Steel in Glacial Acetic Acid." *Indian Journal of Chemical Technology,* 15, 68-71.
- Nayak, J. and Hebbar, K. R. (2008). "Corrosion Inhibition Of T-6 Treated 6061 Al–SiC(p) Composite In Hydrochloric Acid." *Trans. Indian Inst. Met*, 61 (2-3), 221-224.
- Nikseresht, Z., Karimzadeh, F., golozar, M. A. And Heidarbeigy, M. (2010). "Effect of Heat Treatment on Microstructure and Corrosion Behaviour of Al6061 Alooy Weldment." *Materials and Design*, 31, 2643-2648.

- Nowotnik, G. M. and Sieniawski, J. (2005). "Influence of Heat Treament on the Microstructure and Mechanical Properties of 6005 and 6082 Aluminium Alloys." *Journal of Material Processing Technology,* 162, 367-372.
- Obot, I. B. and Obi-Egbedi, N. O. (2010). "Theoretical Study of Benzimidazole and its Derivatives and Their Potential Activity as Corrosion Inhibitors." *Corrosion Science*, 52, 657-660.
- Ovat, F. A., David, F. O. and Anyandi, A. J. (2012). "Corrosion Behaviour of Al (6063) Alloy (As-Cast and Age Hardened) in H2SO4 Solution." *Journal of Materials Science Research,* 1 (4), 35-40.
- Ozturk, F., Sisman, A., Toros, S., Kilic, S. and Picu, R. C. (2010). " Infleunce of Aging Treatment on Mechanical Properties of 6061 Aluminium Alloy." *Materials and Design*, 31, 972-975.
- Paciej, R. C. and Agarwala, V. S. (1986). "Metallurgical Variables Influencing the Corrosion Susceptibility of a Powder Metallurgy SiCw/ Al Composite." *Corrosion*, 42, 718-728.
- Philip, A. S. (2007). *Corrosion of Linings and Coatings- Cathodic and Inhibitor Protection and Corrosion Monitoring,* Taylor and Francis Group, USA
- Popova, A., Sokolova, E., Raicheva, S. and Christov, M. (2003). " AC and DC Study of the Temperature Effect on Mild Steel Corrosion in Acid Media in the Presence of Benzimidazole Derivatives." *Corrosion Science*, 45, 33-58.
- Popova, A., Sokolova, E., Raicheva, S. and Christov, M. (2004). "Adsorption and Inhibitive Properties of Benzimidazole Derivatives in Acid Mild Steel Corrosion." Corrosion science, 46, 1333-1350.
- Quraishi, M. A. and Sharma, H. K. (2004). "Inhibition of Mild Steel Corrosion in Formic and Acetic Acid Solutions." *Indian Journal of Chemical Technology,* 11, 331-336.
- Rafiquee, M. Z. A., Khan, S., Saxena, N and Quraishi, M. A. (2007). "Influence of Some Thiadiazole Derivatives on Corrosion Inhibition of Mild Steel in Formic and Acetic Acid Media." *Portugaliae Electrochimica Acta,* 25, 419-434.

- Rajasekaran, S., Udayasankar, N. K. and Nayak, J. (2012). “T4 and T6 Treatment of 6061 Al-15 vol % SiCp Composite” *ISRN Materials Science*, 2012, ID 374719.
- Roberge, P. R. (2000). *Handbook of Corrosion Engineering*, McGraw-Hill, USA.
- Sagalowicz, L., Lapasset, G. and Hug, G. (1996). “ Transmission Electron Microscopy Study of a Precipitate Which Forms in the Al-Mg-Si System.”*Philosophical Magazine*, 74, 57-66.
- Sankarap, S., Apavinasam, F., Pushpanaden, M. and Ahmed, F. (1991). “Piperidine, Piperidones and Tetrahydrothiopyrones as Inhibitors for the Corrosion of Copper in H_2SO_4.” *Corrosion Science*, 32, 193-203.
- Schwartz, M. M., (1997). “*Composite Material Processing Fabrication and Applications*” Prentice Hall, USA.
- Shimizu, T., Chen, R. and Iwabuchi, A. (2000). “The effect of a T6 heat treatment on the fretting wear of a SiC particle-reinforced A356 aluminum alloy matrix composite.” *Wear*, 238 (2), 110–119.
- Shimizu, Y., Nishimura, T. and Matsushima, I. (1995). “Corrosion resistance of Al-based metal matrix composites.” *Materials Science and Engineering A*, 198, 113-118.
- Singh, M. M. and Gupta, A. (1996). “Corrosion Behaviour of Mild Steel in Formic Acid Solutions.” *Materials Chemistry and Physics*, 46, 15-22.
- Singh, M. M. and Gupta, A. (2000). “Corrosion Behaviour of Mild Steel in Acetic Acid Solutions.” *Corrosion*, 56, 4, 371-379.
- Singh, S. K. and Mukherjee, A. K. (2010). “Kinetics of Mild Steel Corrosion in Aqueous Acetic Acid Solutions.” *J. Mater. Sci. Technol.*, 26(3), 264-269.
- Singh, S. K., Mukherjee, A. K. and Singh, M. M. (2011). “Corrosion Behaviour of Mild Steel in Aqueous Acetic Acid Solutions Containing Different Amounts of Formic Acid.” *Indian Journal of Chemical Technology*, 18, 291-300.
- Singh, V. B. and Singh, R. N. (1995). “Corrosion and Inhibition Studies of Copper in Aqueous Solutions of Formic Acid and Acetic Acid.” *Corrosion Science*, 37 (9), 1399-1410.

- Stansbury, E. E. and Buchana, R.A. (2000). *Fundamentals of Electrochemical Corrosio*n, ASM International, Ohio.
- Sun, H., Koo, E. Y. and Wheat, H. G. (1991). "Corrosion behavior of SiCp/6061 Al metal matrix composites." *Corrosion*, 47, 741-753.

- Sun, H., Koo, E. Y. and Wheat, H. G. (1991). "Corrosion behavior of SiCp/6061 Al metal matrix composites." *Corrosion,*47, 741-753.

- Trzaskoma, P.P., McCafferty, E., Crowe,. C.R. (1983). "Corrosion behavior of SiC/Al metal matrix composites." *Electrochem Soc. J, 130, 1804*-1809.
- Uhlig, H. H. and Revie, R.W. (2008). *Corrosion and Corrosion Control,* John Wiley & Sons, Inc., Publication, New Jersey.
- Viswanathan, S. S. (2010). "A Review on Recent Patents in Corrosion Inhibitors." *Recent Patents on Corrosion Science,* 2, 6-12.
- Wang, H. L., Fan, H. B. and Zheng, J. S. (2002). "Corrosion Inhibition of Mild Steel in Hydrochloric Acid Solution by a Mercapto-Triazole Compound." *Mater. Chem. Phys.*, 77, 655-661.
- Winkler, S.L. and Flower, H. M. (2004). "Stress corrosion cracking of cast 7XXX aluminium fibre reinforced composites." *Corrosion Science*., 46, 903–915.
- Winkler, S.L., Ryan, M.P. and Flower, H. M. (2004). "Pitting corrosion in cast 7XXX aluminium alloys and fibre reinforced MMCs." *Corrosion Science*., 46, 893–902.
- Winston, R. R. (2011). "Metal Matrix Composites." *Uhligs Corrosion Handbook,* 3rd ed. John Wiley &Sons Publications, New Jersey, 481-490.
- Xiumei, W., Huaiyu, Y. and Fuhui, W. (2011). "An Investigation of Benzimidazole Derivative as Corrosion Inhibitor for Mild Steel in Different Concentration HCl Solution." *Corrosion Science*, 53, 113-121.
- Yu, D. and Chandra, T. (1993). " Age Hardening in 6061 Al Alloy and Al_2O_3/ 6061 Al Composite." *Materials Transactions,*34, 1184-1190.
- Zaki, A. (2006). *Principles of Corrosion Engineering and Corrosion Control*, Elseveir, UK.

- Zarrouk, A., Hammouti, B., Zarrok, H., Al-Deyab, S. S. and Messali, M. (2011). "Temperature Effect, Activation Energies and Thermodynamic Adsorption Studies of L-Cysteine Methyl Ester Hydrochloride as Copper Corrosion Inhibitor in Nitric Acid 2M." *Int. J. Electrochem. Sci.*, 6, 6261-6274.

List of publications based on Ph.D. research work

Sl No.	Title of the paper	Authors	Name of the journal/conference, Vol, No, Pages	Year of publication	Category
1	Aging behavior of 6061 Al-15 vol% SiC Composite in T4 and T6 treatments	M. Chacko, J. Nayak	ICMSEM 2014: International Science Conference Proceedings.	2014	3
2	Benzimidazole as corrosion inhibitor for heat treated 6061 Al-SiCp composite in acetic acid	M. Chacko, J. Nayak	Journal of Physics: Conference Series DOI: 10.1088/1742-6596/622/1/012035	2015	1
3	Corrosion inhibition using 2-mercaptobenzimidazole on T6 treated 6061 Al-SiCp composite in acetic acid	M. Chacko, J. Nayak	Materials Today: Proceedings Vol: 2, Issue: 4-5, 2728.	2015	1

Category:
1. Journal paper, full paper reviewed
2. Journal paper, abstract reviewed
3. Conference/symposium paper, full reviewed
4. Conference/symposium paper, abstract reviewed
5. Others (papers in workshops, NITK research bulletin, short notes, etc.)

Melby Chacko	**Prof. Jagannatha Nayak**
Research Scholar	Research guide
(Signature with date)	(Signature with date)

BIO-DATA

MELBY CHACKO

Permanent address:

Pottamplackal House
Mandapam
Kasargod - 671326
Kerala, India

Contact Details:

Email 🖂: melbychacko@gmail.com
Phone ☏: +91-8050489047

Academic Qualifications:

Bachelor of Science, Physics (2007), Nehru Arts & Science College, Kannur University, Kerala, India.

Master of Science, Materials Science (2009), Department of Materials Science, Mangalore University, Karnataka, India.

Master of Technology in Materials Engineering (2011), Department of Metallurgical and Materials Engineering from National Institute of Technology Karnataka, Surathkal, India.

Research publications:

Articles in International Journals: 03
Articles in Conference Proceedings: 02